NASA Technical Memorandum 4437

Space Shuttle Solid Rocket Booster Main Parachute Damage Reduction Team Report

G. Watts
George C. Marshall Space Flight Center
Marshall Space Flight Center, Alabama

Three main parachutes decelerate a solid rocket booster for water impact.

TABLE OF CONTENTS

iii

TABLE OF CONTENTS (Continued)

LIST OF ILLUSTRATIONS

ABBREVIATIONS AND ACRONYMS

ARF	assembly and refurbishment facility
CG	center of gravity
DFI	development flight instrumentation
DTV	drop test vehicle
EMPSS	external MPSS
ft/s	feet per second
GSE	ground support equipment
KSC	Kennedy Space Center
LH	left hand
MSFC	Marshall Space Flight Center
MPDRT	main parachute damage reduction team
MPSS	main parachute support structure
lb/ft^2	pounds per square foot
PRF	parachute refurbishment facility
Qmax	maximum dynamic pressure
RH	right hand
SRB	solid rocket booster

TECHNICAL MEMORANDUM

SPACE SHUTTLE SOLID ROCKET BOOSTER MAIN PARACHUTE DAMAGE REDUCTION TEAM REPORT

1.0 INTRODUCTION

This report gives the findings of the solid rocket booster (SRB) main parachute damage reduction team (MPDRT). The MPDRT was formed at the request[1] of the SRB Chief Engineer at Marshall Space Flight Center (MSFC) following the main parachute failure that occurred on STS-30R, May 1989. The team was chartered to review the history of previous failures, investigate methods of eliminating or substantially reducing main parachute deployment damage, provide government-estimated costs for any recommended changes, and, specifically, to reassess the STS-30R failure mechanism.

Personnel from MSFC and the SRB prime contractor, United Space Boosters, Inc. (USBI), comprised the majority of the MPDRT. The organization and membership of the team is shown in figure 1. R. Runkle, of the SRB Chief Engineer's Office, served as team coordinator. D. Bacchus and J. Burnum headed the MSFC and USBI efforts, respectively. D. Wolf, from Sandia National Laboratories, and B. Woodis and F. Tallentire, from the Martin Marietta Corporation, served as parachute system consultants. J. Butler of Rockwell International, Huntsville Operations, provided technical writing assistance.
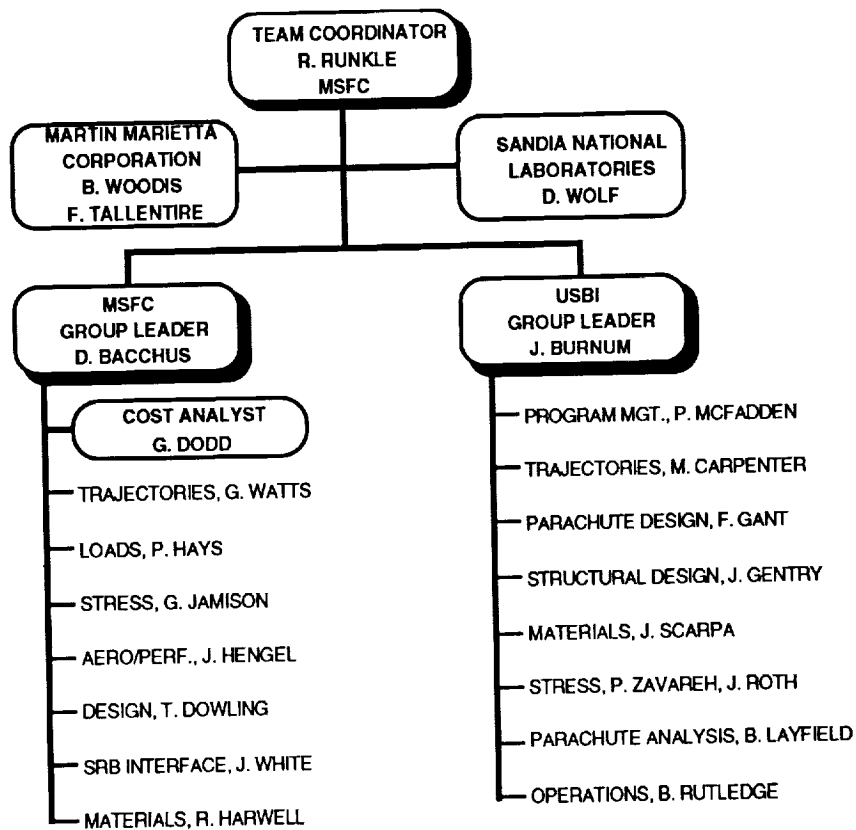
Figure 1. SRB main parachute damage reduction team.

The team held its first meeting June 23, 1989. After a series of planning sessions, MSFC and USBI personnel met separately for several weeks to allow the two groups to formulate independent ideas addressing main parachute deployment damage. The ideas were later combined in joint meetings. The team developed 23 damage reduction concepts, listed in figure 2. Each concept and its evaluation by the team are discussed in appendix A. The team also discussed various main parachute enhancements, which are discussed in section 6.0. The team's recommendations are discussed briefly in paragraph 1.4 and are listed formally in section 8.0.

In October 1989, the team presented the results of its investigation to MSFC management.[2] During the subsequent compilation of this report, MSFC decided to implement several of the team's recommendations. Section 9.0 provides a discussion of the implementation activities. The publication of this report is considered the completion of the team's entire assignment.

CONCEPT NUMBER	CONCEPT NAME
1	Shorten Isogrid
2	Delete Isogrid
3	Pilot Chute-Deployed Soft Pack
3A	Pilot Chute-Deployed Soft Pack (Frustum Mounted)
4	Soft Pack With Delayed Release From Frustum
4A	Soft Pack With Energy Absorber (Frustum Mounted)
5	External MPSS
6	Banana Bag
7	Longer Drogue Suspension Lines
8	Clustered Drogue
9	Larger Drogue
10	Increase Time on Drogue
11	Optimize Ties for Vent Cap and Canopy
12	Soft Pack With Mortar-Type Deployment
13	MPSS Fairing to Frustum Exit
14	Split Isogrid
15	Separation Plane Moved Forward
16	Lower Main Chute Pack in Frustum
17	Frustum Fairing
18	Individual Rigid Containers
19	Jettison Nozzle Extension at Apogee
20	Bridle-Deployed Soft Pack on Dome
21	Energy Absorber-Deployed Soft Pack on Dome

Figure 2. Damage reduction concepts.

1.1 General Description of SRB Recovery System

The SRB recovery system is contained within the nose cone (fig. 3) and consists primarily of a pilot parachute, drogue parachute, and three main parachutes. The main parachute packs are supported and separated by the main parachute support structure (MPSS) which is attached to the frustum. The MPSS consists of a forward ring, isogrid, and six bipod struts as shown in figure 4. The isogrid is composed of three machined panels joined at the center and held in a 120° spacing by the forward ring. The parachute packs are secured to the MPSS by circumferential and longitudinal straps. The MPSS absorbs nearly all the parachute inertial loads and transfers these loads to the frustum through the forward ring and the bipod struts. The small remaining inertial loads are handled by 24 lateral restraint straps attached to cinch fittings around the circumference of the frustum.
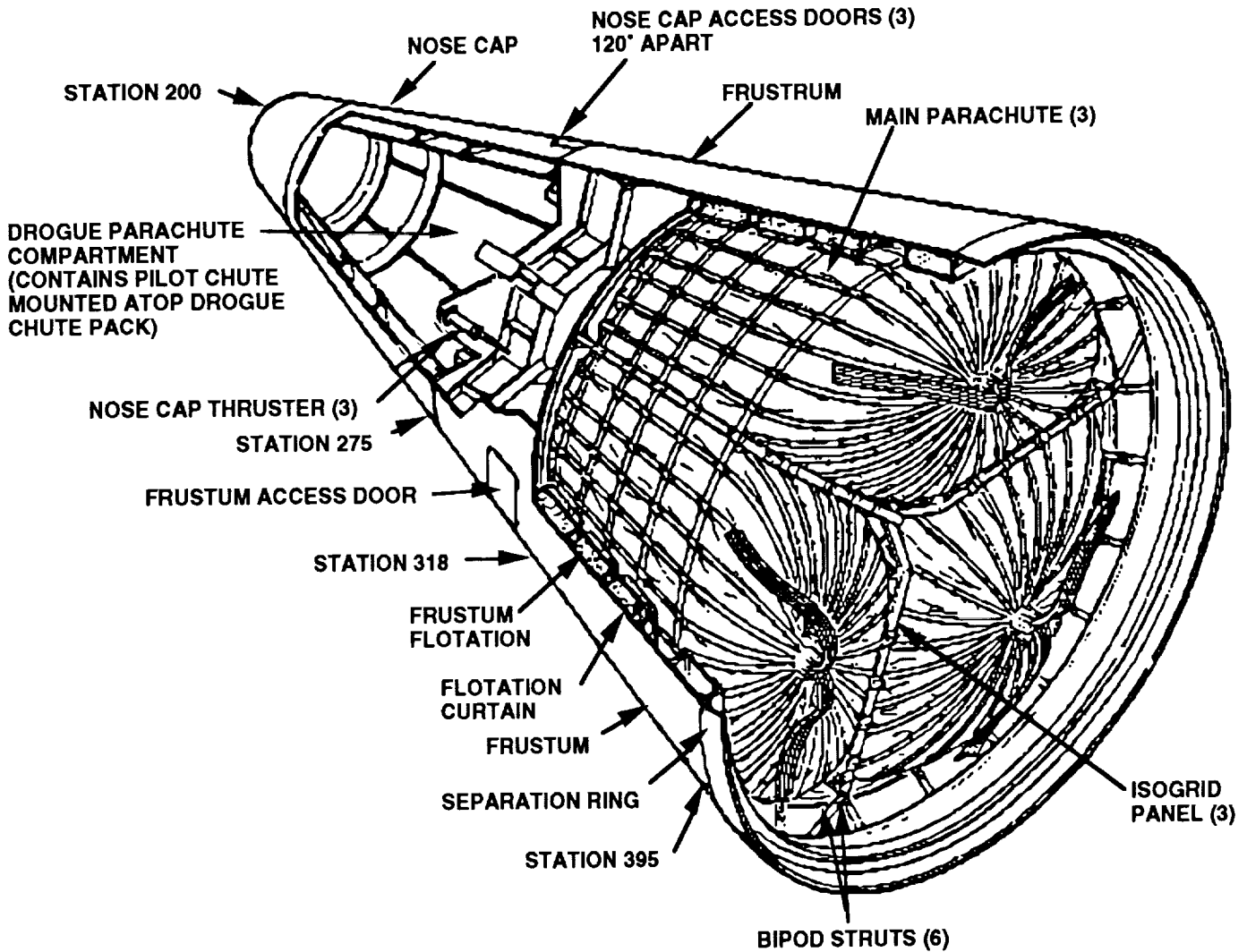
Figure 3. SRB nose cone assembly.

3

ISOGRID PANEL

GUSSET (3)

RING
SEGMENT (3)

STRAP (3)

RING SPLICE FITTING (3)

FORWARD RING
(82-inch dia)

BIPOD
STRUTS (6)

ISOGRID
PANEL (3)
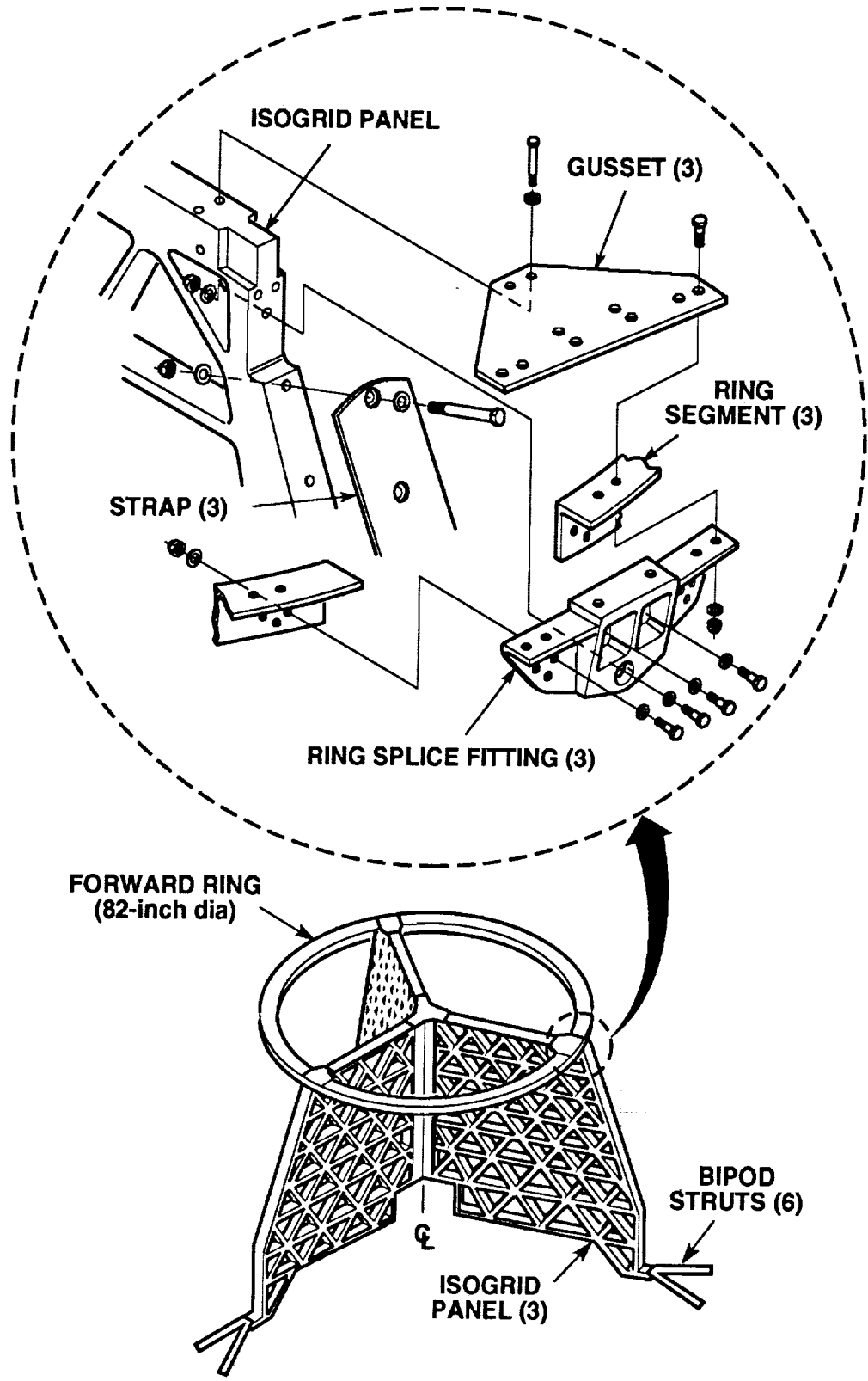
Figure 4. Main parachute support structure with detail of forward ring attachment.

The recovery sequence, shown in figures 5a and 5b, begins with separation of the nose cap at an altitude of approximately 15,000 ft. As the nose cap separates, it deploys the pilot parachute which, in turn, deploys the drogue parachute. The primary purpose of the drogue parachute is to orient the SRB in a tail-first attitude suitable for deployment of the three main parachutes. At an altitude of approximately 6,000 ft, the frustum, which contains the main parachute deployment bags, is severed from the SRB forward skirt. The drogue then deploys the main parachutes by decelerating the frustum away from the SRB. The main parachutes decelerate the SRB for water impact.

Originally, the SRB recovery system used 115-ft diameter main parachutes. These parachutes, now called small main parachutes, produced a nominal water impact velocity of 89 ft/s. To reduce the damage caused by water impact, 136-ft diameter large main parachutes were developed, bringing nominal water impact velocity down to 75 ft/s. The large mains were first flown on the right hand (RH) SRB on STS-41D in August 1984. They were next used two flights later on both STS-51A SRB's, followed by STS-51C, the last flight with small mains. Beginning with STS-51D, the large mains have been used exclusively.

1.2 Primary Damage Sources and Previous Corrective Measures

Throughout the history of SRB flights, the main parachutes have frequently been damaged during the deployment process. On several occasions, this damage has resulted in a complete failure (collapse) of the canopy. Appendix B contains a comprehensive parachute damage history and cause assessment for the first 29 shuttle flights and an analysis of the correlation of the damage with various parameters.

The team found two primary causes of significant deployment damage: vent entanglement and contact of the parachutes with components of the MPSS, namely, the isogrid and bipod struts. MPSS contact is, by far, the most frequent of all damage sources. The potential for contact and damage is increased when the frustum tilts during canopy deployment. Damage potential is further increased by the high bag stripping velocities inherent in the current system, which utilizes the drogue parachute to deploy the mains.

Following early incidents of parachute damage or failure, steps were taken to reduce the potential for damage. These included removing the frustum location aid, repositioning the main chute floats, placing foam around the bipod struts and lower section of the frustum, and eliminating the sharp corner of the isogrid near the SRB centerline. In addition, several changes were made to the main parachute packing procedure.

Despite these improvements, damage and failures still frequently occurred. A change was, therefore, implemented to make the main chutes more tolerant to localized damage. Beginning with STS-33R in November 1989, circumferential reinforcements, called ripstops, were installed on a trial basis on one main parachute on each SRB. The intended function of the ripstops is to prevent the propagation of chute tears along any gore during inflation. This modification, however, does not eliminate the causes of the damage.

The ripstops are 4,000-lb nylon horizontal ribbons that are sewn on top of the existing ribbons at six locations in the upper, highly loaded portion of the canopy (fig. 6). After several trial flights, this modification proved successful, and the decision was made to fully implement the ripstops on a permanent basis. Beginning with the first flight in 1991, all three main parachutes on each SRB have had ripstops installed.

NOSE CAP

NOSE CAP
SEPARATION
T = 0.0 s
Alt = 15,820 ft
Q̄ = 205 lb/ft²
V = 536 ft/s

PILOT
PARACHUTE

NOSE CAP
DEPLOYS
PILOT PARACHUTE
T = 0.6 s
Alt = 15,532 ft

PILOT PARACHUTE
DEPLOYS
DROGUE PARACHUTE
T = 1.8 s
Alt = 14,941 ft

DROGUE PARACHUTE INFLATES
TO 1ST REEFED CONDITION (60%)
T = 2.7 s
Alt = 14,510 ft

DROGUE PARACHUTE INFLATES
TO 2ND REEFED CONDITION (80%)
T = 8.8 s
Alt = 11,662 ft

DROGUE PARACHUTE DISREEFS
TO FULL INFLATION
T = 13.3 s
Alt = 9,697 ft
Q̄ = 158 lb/ft²
V = 428 ft/s

Figure 5a. SRB recovery sequence (drogue parachute phase).

6

DROGUE PARACHUTE
DEPLOYS MAIN
PARACHUTES
T = 21.7 s.
Alt = 6,450 ft
$\bar{Q}$ = 127 lb/ft^2
V = 365 ft/s

MAIN PARACHUTES
INFLATE TO 1ST
REEFED CONDITION
(15%)
T = 25.8 s
Alt = 4,873 ft
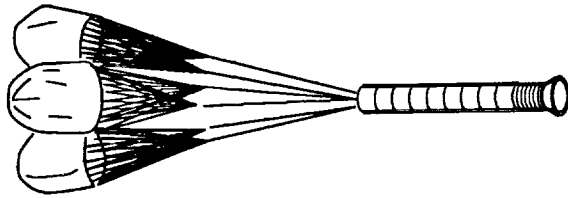
MAIN PARACHUTES
DISREEF TO 2ND
REEFED CONDITION
(37%)
T = 33.1 s
Alt = 3,060 ft
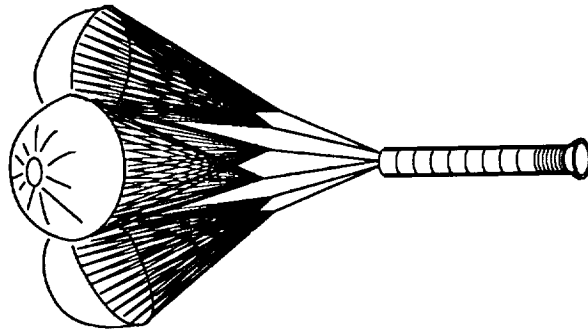
MAIN PARACHUTES
DISREEF
TO FULL INFLATION
T = 39.0 s
Alt = 2,125 ft
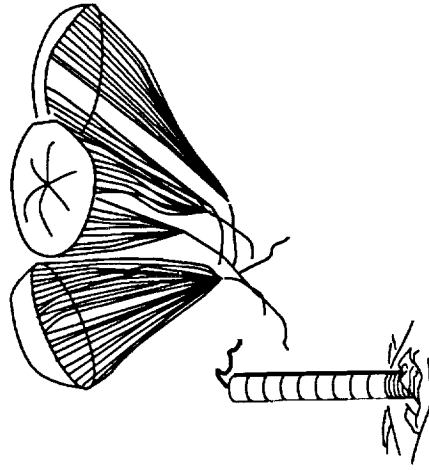
SRB WATER IMPACT
(DETACH PARACHUTES AT IMPACT)
T = 64.8 s
V = 75 ft/s

Figure 5*b*. SRB recovery sequence (main parachute phase).

7

HORIZONAL RIPSTOP RIBBONS AT SIX LOCATIONS
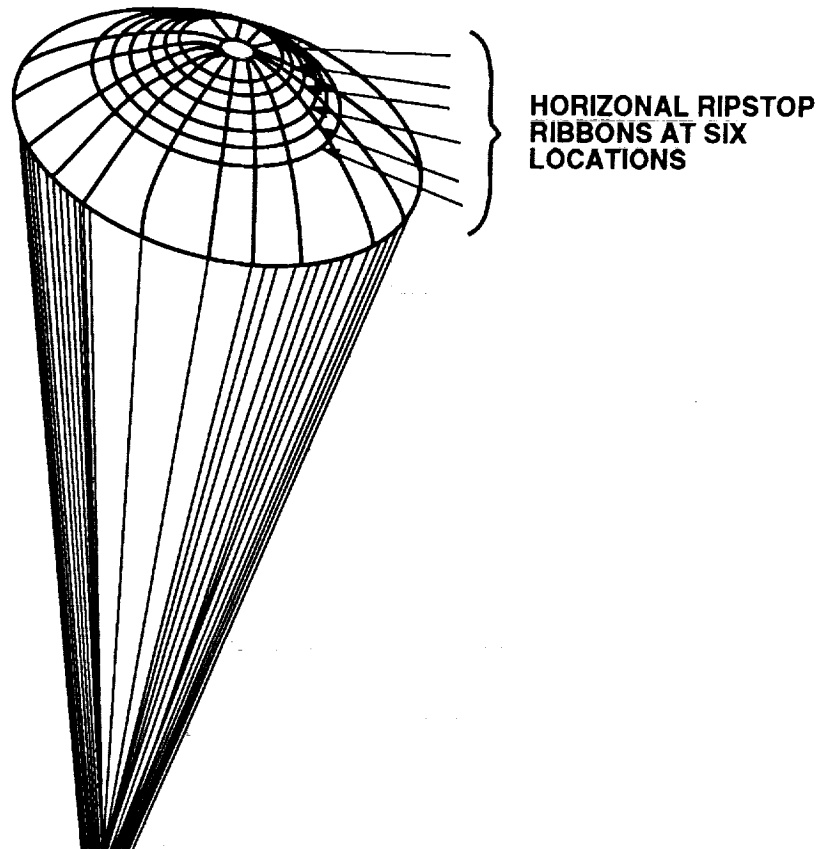
Figure 6. Main parachute ripstops.

1.3 Vent Entanglement (STS-30R Failure)

So far in the shuttle program there has not been a failure of more than one main parachute on the same booster. However, on the STS-30R left-hand (LH) SRB, a serious situation arose when the failure of one main parachute was coupled with delayed inflation of another. The resulting loss in drag caused the third parachute in the cluster to become highly overloaded to the point of near-failure. The fact that the third parachute had not sustained any damage during deployment is the only reason it did not fail. Failure would have resulted in loss of the LH SRB.

The team, as requested, closely examined the STS-30R failure to verify the postflight analyses by the SRB prime contractor (USBI)[3] and Dr. Wolf of Sandia National Laboratories.[4] The team examined essential photographic data from STS-30R and viewed a video-taped demonstration of the failure sequence performed by recovery personnel using the failed parachute. In addition, several team members had been previously involved in the postflight inspection of the failed parachute.

After reviewing the data from STS-30R and thoroughly discussing the sequence of events during deployment, the team agreed with the original conclusion that vent entanglement caused the STS-30R parachute failure. As would be expected, the team members did not agree totally on every detail. The

8

team did, however, agree that the vent entanglement was caused by absence of vent cap support combined with frustum tilt during deployment. The most likely sequence of events in the STS-30R failure is as follows:

> After frustum separation, the unsupported vent cap became inverted during frustum deceleration. The large frustum tilt angle resulted in vent cap lateral dynamics that caused the vent cap to become asymmetrical during deployment. This asymmetry prevented the proper exit of the vent cap from its inverted position, and a portion of the vent cap struck and protruded through another section of the vent cap. This entanglement then caused a foreshortening of the vent band and horizontal ribbons (fig. 7). The large radial loads normally transferred across the top of the canopy through the vent lines were redistributed as hoop tension loads in the horizontal members. This abnormal load distribution caused the canopy to fail.

Based on a reexamination of earlier failures, it now appears that the damage observed on STS-51B was also a result of vent entanglement. The STS-30R failure, therefore, was not a random occurrence but a clear indication of a deficiency in the vent packing procedure.

Vent entanglement caused foreshortening, which overloaded and failed the horizontal members.

VENT LINES

HORIZONTAL RIBBONS IN VENT CAP

RADIALS

VENT BAND
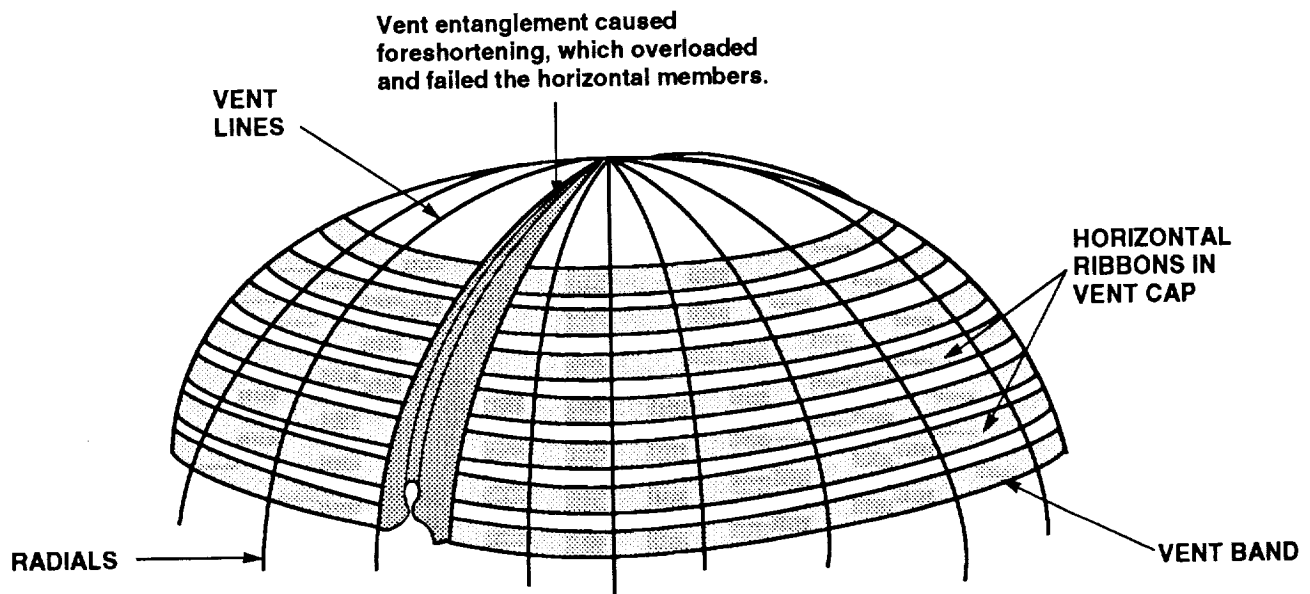
Figure 7. STS-30R main parachute failure mechanism.

1.4 Recommendations

The team recommends that the main parachute packing procedure be changed immediately by adding vent cap ties to support the vent cap as described in paragraph 6.1. The team also recommends implementation of a pilot chute-deployed soft pack (section 2.0). This conventional method of deploying parachutes eliminates all damage caused by contact with hard structure (MPSS and frustum). This concept is also the best method to reduce the current high bag stripping velocities. Three lower-cost alternative concepts (section 3.0) that eliminate contact with the MPSS, the most frequent source of significant damage, are also recommended.

2.0 RECOMMENDED CONCEPT: PILOT CHUTE-DEPLOYED SOFT PACK

A soft pack deployed by a pilot parachute (concept 3) is the approach recommended to provide the least probability of main parachute damage. This concept is similar to the system now used to deploy the drogue parachute, and has long been preferred by most parachute designers. The soft pack is so named because it has no structure to interfere with deployment of the canopies. This concept was investigated in some detail in 1984 and 1985 and documented in references 5 and 6.

2.1 Concept Description

The concept 3 configuration is shown in figure 8. The advantage of using a pilot parachute for main chute deployment is that it greatly reduces bag stripping velocities compared to the current system. This pilot chute will be called the cluster pilot chute to differentiate it from the existing pilot chute that deploys the drogue.
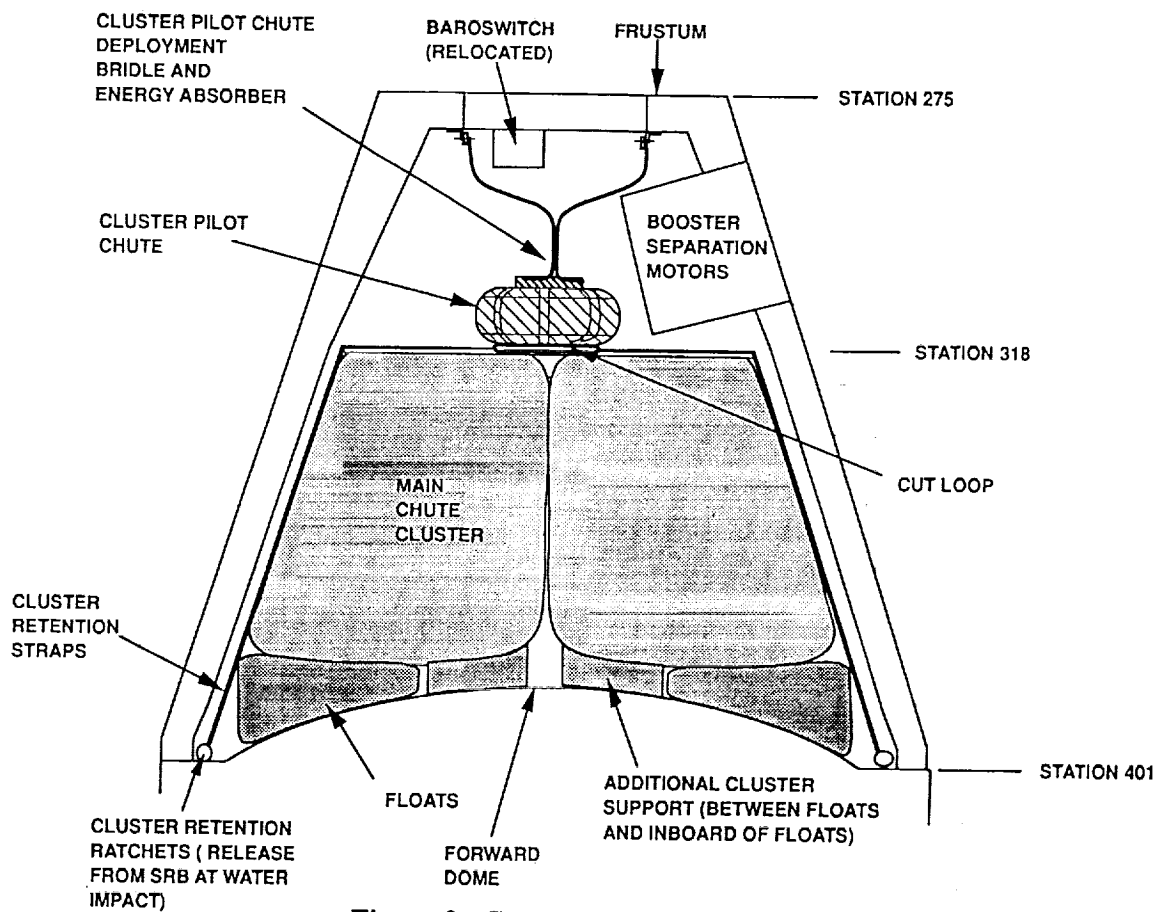
Figure 8. Concept 3 configuration.

In concept 3, the MPSS is eliminated, and the main parachute packs are mounted on the forward dome of the SRB forward skirt. The load of the main parachute packs must be distributed over the surface of the forward dome. This load distribution is achieved by contouring the upper and lower surfaces of the main parachute floats to fit the bottom of the cluster and the top of the dome. Additional foam support blocks are inserted to form nearly continuous top and bottom surfaces. Recesses in the foam support blocks allow space for the main chute risers.

10

The main parachute cluster is held in place by a retention strap arrangement similar to that of the current drogue. The top ends of the retention straps are secured by a cut loop. Severing the cut loop by means of cutters during cluster pilot deployment releases the cluster. The bottom ends of the retention straps are anchored to ratchets mounted around the circumference of the forward dome. The main chute cluster is thus cantilevered out from its mounting surface. After main chute deployment, the free ends of the cluster retention straps could entangle with the main chute floats and inhibit their release at water impact. Therefore, the ratchets will be released from the SRB at water impact by explosive bolts fired with the same signal that releases the main riser attach fittings.

The cluster pilot chute is mounted atop the center of the main parachute cluster, requiring relocation of the SRB baroswitch as shown in figure 8. A multilegged main bridle transfers extraction loads from the cluster pilot chute to the main chute bags. The bags must be rigidized to accept this load. The preferred method uses a rigid liner in the top of each main deployment bag, similar to the hardcover in the current drogue bag. The liner will prevent deformation of the top of the bag during main parachute deployment. For additional rigidity, the three main parachute bags are laced together at the top, down the outboard corners, and at the bottom where they meet in the center.

2.1.1 Deployment Sequence

The deployment sequence for concept 3 is shown in figure 9. The sequence through frustum separation is identical to the existing system. After the frustum moves approximately 7 ft from the SRB, the deployment bridle connecting the frustum to the cluster pilot parachute bag becomes taut, and the loads are transmitted through an energy absorber to the cluster pilot bag to pull it from the main parachute cluster. After the cluster pilot chute bag moves a predetermined distance, circular knives sever the cut loop to release the cluster retention straps. When the cluster pilot chute starts to inflate, the cluster is free to be deployed. After main parachute deployment, the cluster pilot chute, together with the main parachute deployment bags (which have built-in flotation), descend to the ocean surface and are retrieved for reuse.

2.1.2 Cluster Pilot Parachute Size

The team estimated that a cluster pilot chute 23 to 25 ft in diameter is required to deploy the main chute cluster. Analysis is required to trade cluster loads, bag stripping velocity, and suspension line sail before the final size is selected.

The cluster pilot chute weight for a nylon system is in the range of 100 to 150 lb depending on the size and deployment conditions. Use of Kevlar will result in a weight savings.

The energy absorber used for deployment of the cluster pilot chute is expected to have a transmitted force of less than 6,000 lb with a 10-ft stroke. Its weight is under 10 lb.

2.2 Assembly

Concept 3 requires considerable changes in assembly operations at Kennedy Space Center (KSC) in the parachute refurbishment facility (PRF) and assembly and refurbishment facility (ARF). In the current clustering procedure in the PRF, the MPSS is supported at the lower outboard corners of the isogrid

11

PILOT CHUTE

DROGUE BAG

DROGUE CHUTE

FRUSTUM

CLUSTER
PILOT CHUTE

MAIN CHUTE
BAGS

MAIN CHUTES

SRB
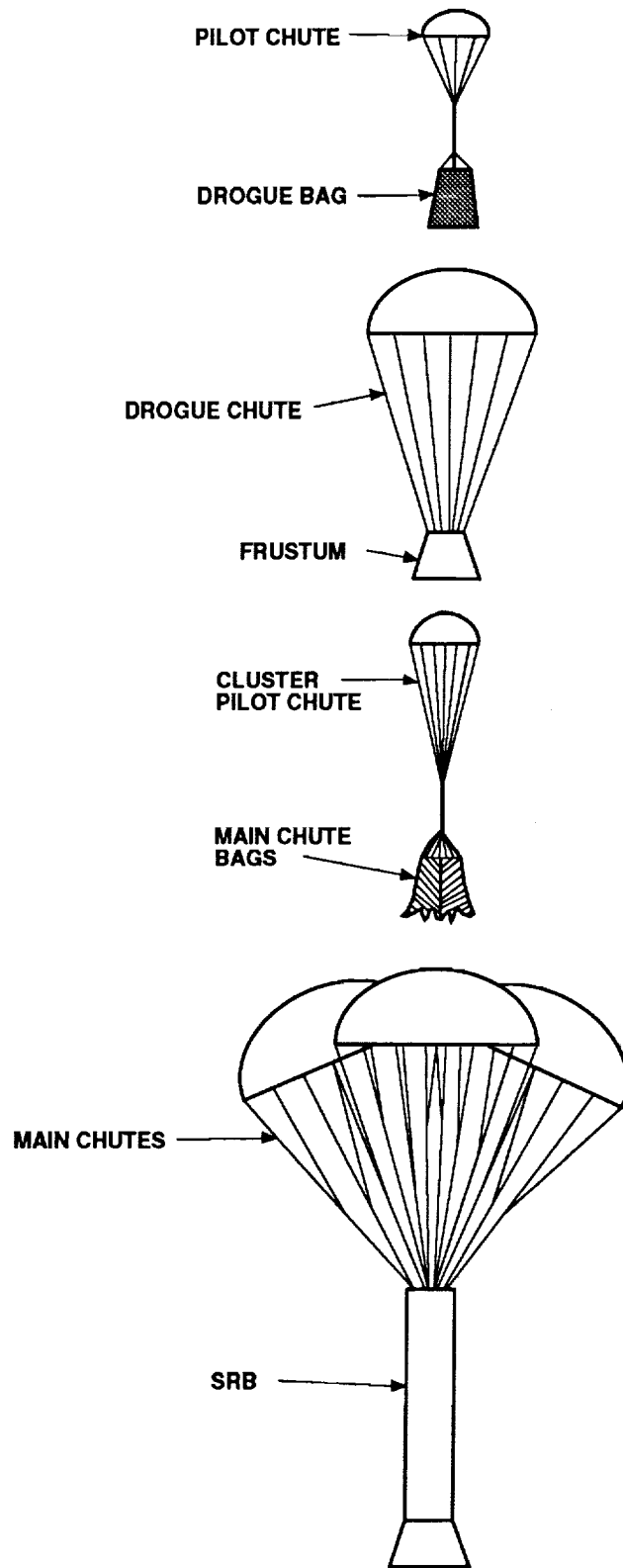
Figure 9. Concept 3 deployment sequence.

panels while the chute packs are being attached. Without an isogrid, the chute packs must be supported from underneath by a new clustering stand. The top surface of the new stand is a replica of the top surfaces of the parachute floats and additional foam supports, including recesses for main chute risers. Each main chute pack is placed on the stand and nested accurately on its support surface. The three chute bags are then laced together at the top and down their adjoining corners, and an access hole in the clustering stand permits the bags to be laced together at the bottom where all three bags meet. The cluster retention straps are put in place, and the cut loop is installed along with the cutters. The retention straps are passed down the sides of the packs and attached with temporary ties to retain them until later. As the cluster pilot chute is being mounted on top of the cluster, its main bridle legs are connected to the main chute bags, and the cutter lanyards are connected to the cluster pilot chute pack.

The new clustering stand will also serve as a transportation dolly for transfer of the cluster from the PRF to the ARF. A new clustering sling is required to lift the cluster from the dolly.

Integration of the recovery system and the SRB forward skirt in the ARF starts with installation of the floats, additional foam supports, and main riser attach fittings. The cluster is placed on the floats. The main risers are connected to the main riser attach fittings, the float risers are connected to the main risers, and the cluster retention straps are attached and tensioned. The frustum is then lowered into place and connected to the forward skirt. The cluster pilot chute deployment bridle is attached near the top of the frustum, after which the drogue, pilot chute, and nose cap are installed in the current manner.

2.3 Weight Delta

Concept 3 is expected to weigh 100 to 200 lb less than the current system. Elimination of the MPSS more than offsets the added weight of the cluster pilot chute, main chute bag flotation, and cluster retention hardware. No structural changes to the frustum or forward skirt are included in this estimate.

2.4 Development Description

2.4.1 Design

The team performed a preliminary analysis of the cluster retention loads on the forward skirt components. Results indicate that the forward skirt ring is capable of taking the retention strap loads since they would be less than the loads caused by the main riser attach fittings. The bulkhead stresses on the forward dome would be lowered by 11 to 30 percent with the exception of a 5-percent increase in localized bending stresses. The stress reduction is caused by the cluster load counteracting the internal pressure load occurring at high altitude.

A more detailed stress analysis is required to ensure that the forward skirt is qualified to sustain the loading. This analysis may indicate the need for a total redesign of the structure. If so, the team proposes that alternative recommended concepts be pursued (see section 3.0).

2.4.2 Testing

Because concept 3 is almost totally new, it requires more testing than the other recommended concepts. The new cluster pilot chute will undergo seam and joint tests, and its performance will be validated by rocket sled testing. The energy absorber for the cluster pilot chute will be tested, and the

deployment of the cluster pilot chute by the frustum will be verified by rocket sled test. Another rocket sled test will verify the ability of the cluster retention system to withstand the lateral load experienced during SRB reentry. A static pull test will be performed for the three main chutes. After all these tests are completed, a series of drop tests will be conducted to verify the ability of the cluster pilot chute to deploy the main chutes. See section 4.0 for a description of these tests.

In addition, a frustum water impact test will be conducted to assess the effect of MPSS removal. Structural requalification tests will be performed for the forward skirt and frustum.

2.5 Development Schedule

The concept 3 development schedule is shown in figure 10.

Event	Months											
	2	4	6	8	10	12	14	16	18	20	22	24
Preliminary Design	* *	* *	*									
Preliminary Design Review			*									
Detailed Design				* *	* *							
Test Equipment Design		* *	* *									
Test Equipment Fabrication/Refurb.				* *	* *	* *						
Test Item Fabrication						* *	* *	* *				
Tests							* *	* *	* *	* *	* *	
Critical Design Review												*

Figure 10. Concept 3 development schedule.

2.6 Costs

The estimated cost of implementing concept 3 is $9M. A significant portion of the cost is allocated to the test program to develop the new deployment method. Other one-time costs are associated with fabrication of the new cluster pilot parachutes and bags, replacing the current inventory of main parachute deployment bags, and any required frustum and forward dome modifications. The cost of new equipment at KSC to assemble the chute packs is not included in the $9M estimate.

Implementation of concept 3 increases operations costs approximately $20K per flight, attributable primarily to packing, retrieval, and refurbishment of the cluster pilot parachute. Cost and cost amortization comparisons with other recommended concepts are provided in section 5.0.

3.0 ALTERNATIVE RECOMMENDED CONCEPTS

This section presents three alternative concepts that provide a substantial reduction in deployment damage at lower total cost than the pilot chute-deployed soft pack. These concepts are recommended as viable alternatives because they eliminate the most frequent cause of significant damage, contact with the isogrid and bipod struts. All three concepts use the drogue parachute to deploy the mains, as does the current system.

3.1 Concept 2: Delete Isogrid

3.1.1 Concept Description

In concept 2, the isogrid and bipod struts are removed. The major drawback of this change is that it also removes the current means of supporting the main parachute packs under axial and lateral load conditions. In concept 2, axial support is achieved by a support structure at the top of the cluster. Lateral support is achieved by filling the present space between the chute packs and frustum with foam support blocks so that the cluster load passes directly to the frustum. The primary factor in the development of this concept is the extent to which the frustum can react the cluster lateral loads. Before this concept is adopted, a static lateral load test (described in paragraph 4.5) is required to establish the structural capability of the frustum. If testing proves this load condition to be undesirable, a more positive lateral restraint system would be required to maintain the parachute packs within a prescribed envelope. Paragraph 3.2 describes a recommended concept (external MPSS) which eliminates parachute pack contact with the frustum.

3.1.2 Assembly

Assembly of the main parachute packs without an isogrid requires a new clustering stand. The support surfaces of the new stand would be contoured to properly position the chute packs for attachment to the upper support structure. The three packs are then laced together at the outside corners, after which the circumferential straps are installed. The cluster is then ready for installation of the frustum and connection of the 24 lateral restraint straps, as in the current procedure.

3.1.3 Weight Delta

Implementation of concept 2 is expected to reduce system weight by approximately 350 lb, assuming no structural reinforcements are required.

3.1.4 Development Description

3.1.4.1 Design

The only significant new hardware required is the support structure at the top of the cluster, which provides axial restraint. This structure will use the upper bay of the current isogrid, most likely requiring some reinforcements. Other existing hardware will also be used, including ring segments, ring splice fittings, and the gussets and spacers mounted on the ring segments.

3.1.4.2 Testing

Cluster lateral load tests, both static and dynamic, must be performed to ensure that the frustum can withstand the lateral loads of the cluster during SRB reentry. A static pull test and a dynamic deployment test are required to determine the effects of large tilt angles during main chute deployment without the isogrid. See section 4.0 for a description of these tests. In addition, water impact and structural requalification tests are required for the frustum.

3.1.5 Development Schedule

The development schedule for concept 2, shown in figure 11, includes the static lateral load test required before proceeding with this concept.

Event	Months											
	2	4	6	8	10	12	14	16	18	20	22	24
Preliminary Design		* *	*									
Preliminary Design Review			*									
Detailed Design				* *								
Test Equipment Design	*		*									
Test Equipment Fabrication/Refurb.	*			* *								
Test Item Fabrication	*				* *							
Tests	*					* *	* *					
Critical Design Review								*				

Figure 11. Concept 2 (delete isogrid) development schedule.

3.1.6 Costs

The initial cost of implementing this change is approximately $2M, associated primarily with testing. The operations costs are reduced because refurbishment of the isogrid is eliminated.

3.2 Concept 5: External MPSS

3.2.1 Concept Description

In concept 5, the isogrid is eliminated, and the parachute packs are supported by an external MPSS (EMPSS). The EMPSS is a conical container externally reinforced with structural legs located 120° apart (fig. 12). The parachute packs bear directly on the EMPSS skin, which extends down to station 381. Below station 381, a separate frustum fairing is used to provide each parachute with a smooth, continuous exit from the frustum. The deployment sequence for the system remains unchanged.
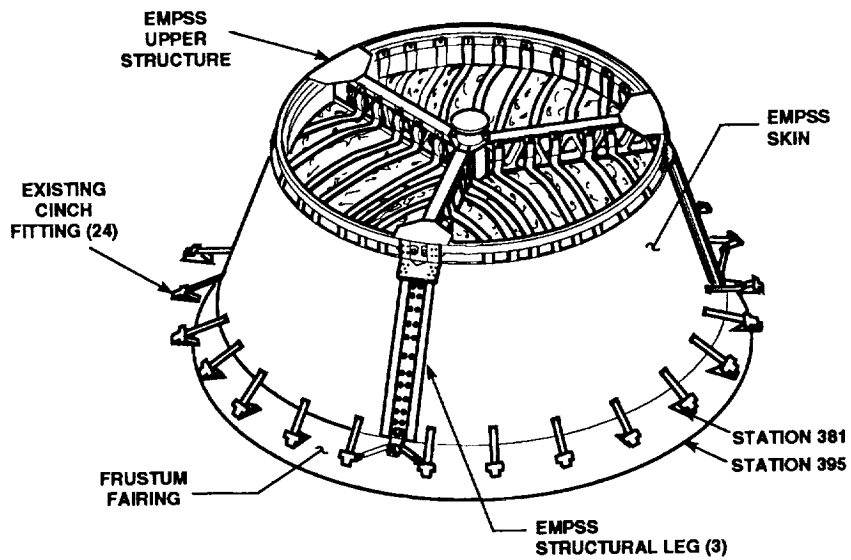
Figure 12. EMPSS configuration.

The EMPSS upper structure provides axial support and incorporates existing MPSS components where possible. These include ring segments, ring splice fittings, the gussets and spacers mounted on the ring segments, and the uppermost bay of the isogrid. A yoke fitting fastens to the existing ring splice fitting and serves as an upper attach point for the structural legs, as shown in figure 13. The yoke fitting will not interfere with assembly of the existing ring segments. The structural legs will probably consist
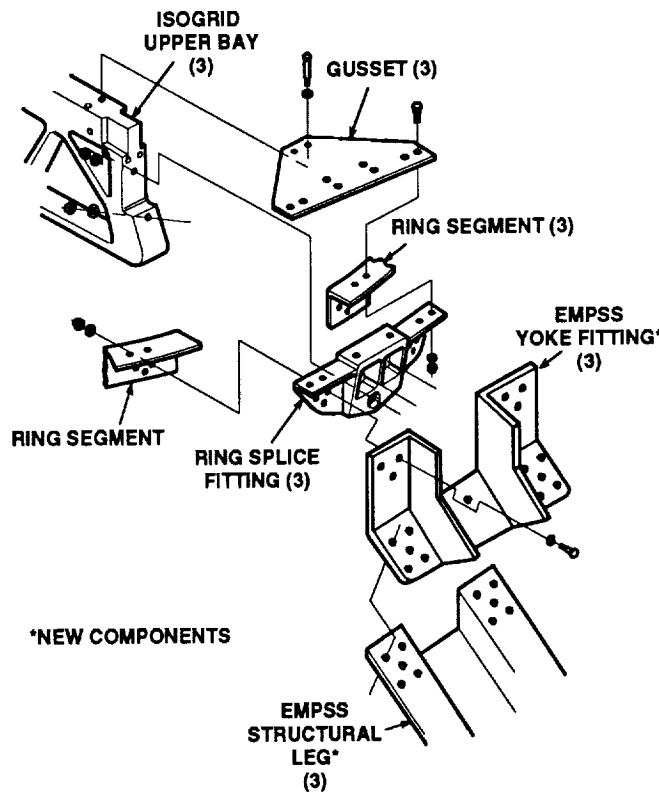
Figure 13. EMPSS upper structure.

of one hat-section per yoke fitting. EMPSS skin sections attach to the structural elements with flush fasteners. Additional stiffeners can be attached around the circumference of the EMPSS if stress analysis indicates they are necessary.

Bipod struts transmit cluster lateral loads to the frustum (fig. 14). Dual fittings are used to attach the EMPSS to the bipod struts and frustum fairing. The bipod struts, which are shorter than the current configuration, are attached at their outer ends to the existing cinch fittings.

*NEW COMPONENTS
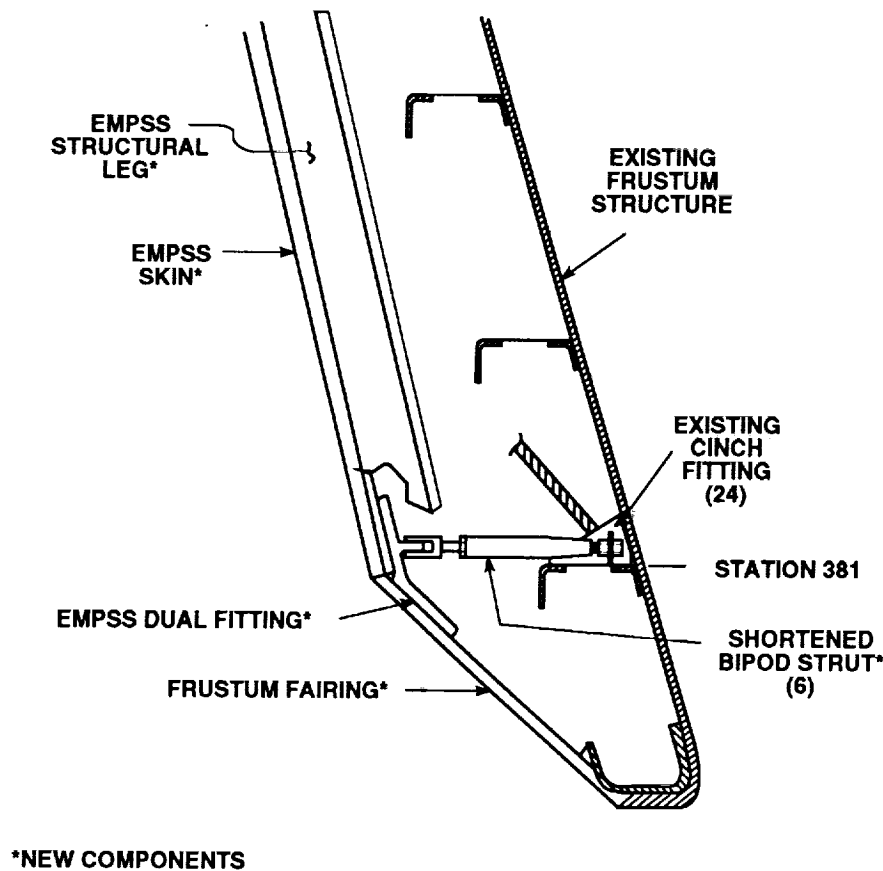
Figure 14. EMPSS lower structure.

3.2.2 Assembly

Because the isogrid is eliminated, a new clustering stand is required for assembly of the main parachute packs with the EMPSS. The support surfaces of the new stand would be contoured to properly position the chute packs to allow the EMPSS to be lowered onto them, aligned, and attached.

The assembled EMPSS with main parachutes installed is joined to the frustum in essentially the same manner as the current system. Attachment of the upper portion is identical. Attachment of the lower portion is nearly the same. After the bipod struts are installed, the main parachute bag lateral restraint straps are attached to the existing cinch fittings through slots around the perimeter of the EMPSS. The slots are oversized to prevent abrasion. The frustum fairing is then attached to the EMPSS dual fittings. No changes are anticipated for the attachment of the frustum to the forward skirt.

18

3.2.3 Weight Delta

The weight of the EMPSS is expected to be approximately 200 lb greater than the current MPSS, depending on the amount of structural stiffening required around the circumference.

3.2.4 Development Description

3.2.4.1 Design

Design of the EMPSS structure is expected to be relatively simple. Study items during this phase include material selection and manufacturing methods. The use of composites for the EMPSS skin could result in a weight savings compared to aluminum. The use of a fabric curtain for the frustum fairing should also be considered.

3.2.4.2 Testing

Testing of the EMPSS includes the cluster dynamic lateral load test, static pull test, and dynamic deployment test described in section 4.0. Structural requalification and water impact testing of the frustum with EMPSS are also required.

3.2.5 Development Schedule

The schedule for development of the EMPSS is shown in figure 15.

Event	Months											
	2	4	6	8	10	12	14	16	18	20	22	24
Preliminary Design	* *	*										
Preliminary Design Review		*										
Detailed Design			* *	*								
Test Equipment Design		*	*									
Test Equipment Fabrication/Refurb.			*	* *								
Test Item Fabrication				*	* *							
Tests						* *	* *					
Critical Design Review								*				

Figure 15. EMPSS development schedule.

3.2.6 Costs

The one-time cost associated with implementation of the EMPSS is approximately $3.5M, which includes all design, testing, and the MPSS inventory replacement cost. This cost is partially offset by a reduction in operations costs of approximately $10K per flight, resulting from the use of the frustum fairing in lieu of instafoam in the frustum lower bay. Both the installation and removal of the instafoam is a labor intensive process.

19

3.3 Concept 4A: Soft Pack With Energy Absorber (Frustum Mounted)

3.3.1 Concept Description

In concept 4A, energy absorbers are used to release the main chute cluster from the frustum prior to deployment of the canopies. The isogrid and bipod struts are eliminated to allow easy exit of the cluster. The drogue parachute provides the force to deploy the main parachutes. The energy absorbers serve the dual function of axially supporting the main chute cluster during flight and softening the release of the cluster from the frustum after frustum separation. The energy absorbers must be pretensioned to support the cluster, and experience has shown that pretensioning actually results in more predictable performance during release. Concept 4A is shown in figure 16.
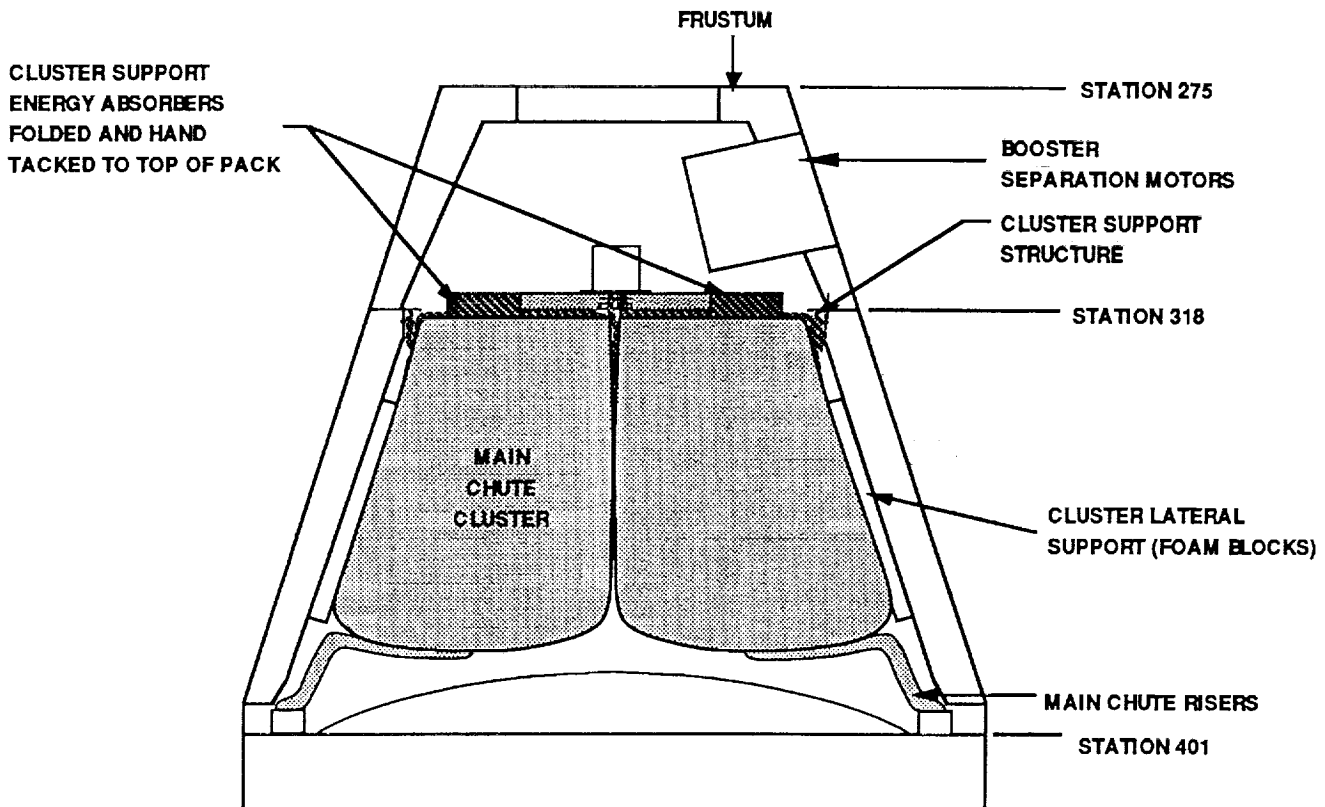
Figure 16. Concept 4A configuration.

Cluster support loads are transmitted to the frustum by the same method used in concept 2, i.e., axial loads are handled by a cluster support structure above the parachute packs, and lateral loads are passed directly to the frustum by foam support blocks. Ramifications of this cluster support method are discussed in paragraph 3.1.1.

3.3.1.1 Deployment Sequence

The deployment sequence is shown in figure 17. The energy absorbers allow the bags to drop from the frustum before the parachute canopies exit the bags. Since the bags remain attached to the frustum, the bag strip velocity is nearly the same as that of the current configuration.

20
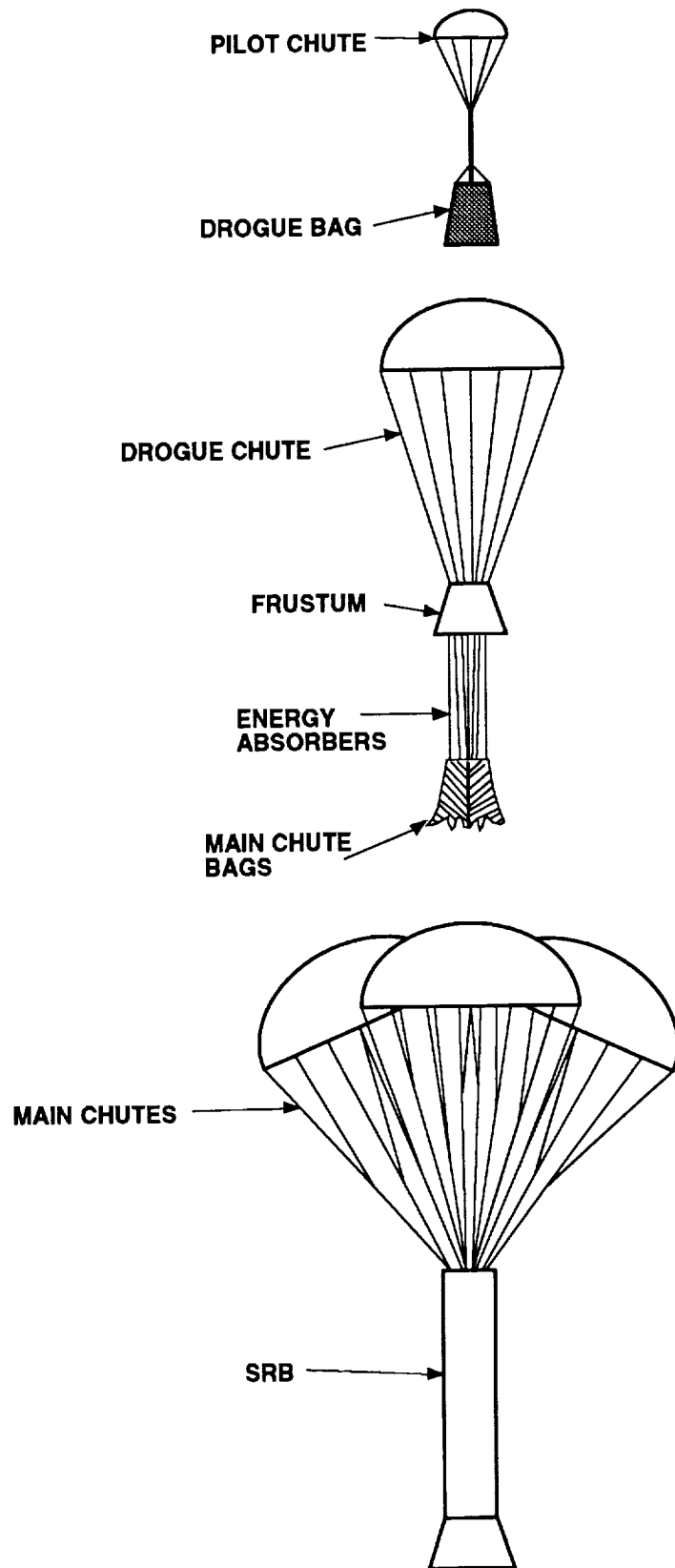
Figure 17. Concept 4A deployment sequence.

3.3.1.2 Energy Absorber Requirements

The team conducted a preliminary analysis of energy absorber requirements to demonstrate the feasibility of concept 4A. The energy absorbers must be strong enough to support the chute packs during SRB reentry (4.5 G's, rigid body) but still allow the packs to exit the frustum for deployment. The analysis showed that designing the energy absorbers to provide 9 G's to the parachute packs is close to optimum, and the calculations described in the following paragraphs are based on the 9-G value.

To simplify the energy absorber analysis, the frustum and drogue parachute were combined into a single rigid body weighing 6,200 lb. The cluster of three main parachute packs, which weighs 6,300 lb, was also considered to be a rigid body. The total energy absorber force required to decelerate the chute packs at 9 G's was 56,700 lb. In considering the design of the energy absorbers, mild (low dynamic pressure) frustum separation conditions are more critical than severe conditions. Mild conditions dictate a decrease in energy absorber strength, and thus provide less margin relative to the reentry G level. A mild dynamic pressure of 122 lb/ft^2, corresponding to an SRB descent velocity of 358 ft/s, was calculated for the time of frustum separation. A minimum drogue chute drag force of 181,000 lb was assumed for the dynamic pressure calculation. No other aerodynamic forces were considered.

The analysis begins at frustum separation, with the drogue chute providing the force to decelerate the frustum and the chute packs away from the SRB. The energy absorbers begin to stroke immediately, applying a constant 9-G deceleration to the chute packs. The initial deceleration of the frustum and drogue is 20 G's, taking into account the constant energy absorber force. After frustum separation, the frustum and drogue continue to decelerate, although the deceleration quickly decreases because of the rapid reduction in dynamic pressure. The chute packs continue to exit the frustum as the energy absorbers stroke with constant force. The energy absorbers must continue to stroke until the chute pack velocity matches frustum velocity. This condition occurs at approximately 0.45 s after frustum separation. At this time, the energy absorbers have stroked 9.4 ft, and the chute packs have completely cleared the frustum. Only 29 ft of riser length has been deployed by this time, and the bag stripping velocity is roughly 130 ft/s. From this point on, the drogue decelerates the frustum and chute packs together until the main parachutes are fully deployed. The parachute canopies do not deploy until well after the chute packs have exited the frustum.

Energy absorber length is determined by the highest expected dynamic pressure at frustum separation. The energy absorbers must have enough stroke to prevent snatching the bags during high dynamic pressure conditions. The estimated energy absorber weight is 90 lb based on the use of nylon webbing. This weight can be reduced by 50 percent if Kevlar is used for the energy absorber material.

3.3.2 Assembly

The concept 4A assembly procedure is similar to that of concept 2 (paragraph 3.1.2) except for attachment of the chute packs. Energy absorbers are used to attach the chute packs to the cluster support structure, and the 24 lateral restraint straps are omitted.

3.3.3 Weight Delta

Implementation of concept 4A is expected to result in a recovery system weight reduction of 200 to 250 lb. Elimination of the isogrid and bipod struts more than offsets any additions for energy absorbers or cluster support structure.

22

3.3.4 Development Description

3.3.4.1 Design

The primary design concern for concept 4A is to ensure that the energy absorbers can support the cluster during SRB reentry. The accelerations measured on flight SRB's must be carefully examined in terms of both rigid-body and flexible-body values. The energy absorbers are pretensioned and will probably release the cluster prematurely if exposed to high frequency accelerations that exceed the break-out strength. Such a release is unacceptable because the packs would be banged around inside the frustum by violent SRB motions during reentry.

3.3.4.2 Testing

Like the other two alternative recommendations, drop tests are not required for concept 4A. Adequate ground testing will be performed to certify the concept for flight. The energy absorbers will be developed by a series of laboratory tests. The complete energy absorber system and chute packs will then be installed in a frustum for rocket sled testing to ensure proper release of the cluster by the energy absorbers. This test cannot be used to simulate deployment of the main chutes from their bags because the bags drop down after exiting the frustum. The deployment of the mains will be certified by similarity to the current system, or by a specially designed rocket sled test. A static pull test also will be performed for the mains.

Because the isogrid is eliminated, the cluster lateral load tests, frustum water impact test, and structural requalification tests specified in paragraph 3.1.4.2 for concept 2 are required.

3.3.5 Development Schedule

Figure 18 gives the concept 4A development schedule. The schedule, like that for concept 2, includes the initial static lateral load test required before proceeding with concept 4A.

Event	Months											
	2	4	6	8	10	12	14	16	18	20	22	24
Preliminary Design		* *	*									
Preliminary Design Review			*									
Detailed Design				* *	*							
Test Equipment Design	*		*	*								
Test Equipment Fabrication/Refurb.	*			*	* *							
Test Item Fabrication	*				*	* *						
Tests	*						* *	* *	* *			
Critical Design Review										*		

Figure 18. Concept 4A development schedule.

3.3.6 Costs

The one-time cost associated with this concept is estimated to be $5M. This cost primarily includes testing of the energy absorbers, replacing the current inventory of main parachute deployment bags, and all required frustum testing.

Operations costs will increase by approximately $15K per flight due primarily to the energy absorbers. A comparison of these costs and cost amortization with other concepts is provided in section 5.0.

4.0 DEVELOPMENT TESTING

Parachute-related tests required to develop the recommended damage reduction concepts include material strength tests, cluster pilot parachute load tests, static pull tests, dynamic deployment tests, cluster lateral load tests, and drop tests. These tests are described below. In addition, structural requalification tests and water impact tests are needed. The tests required for each recommended concept are summarized in figure 19.

Recommended Concept	Tests Required
Delete Isogrid – Concept 2	Cluster static and dynamic lateral load tests; static pull test and dynamic deployment test for mains; water impact test and structural requalification for frustum.
EMPSS – Concept 5	Cluster dynamic lateral load test; static pull test and dynamic deployment test for mains; water impact test and structural requalification for frustum with EMPSS.
Soft Pack With Energy Absorber (Frustum Mounted) – Concept 4A	Cluster static and dynamic lateral load tests; static pull test for mains; energy absorber laboratory tests; rocket sled test to verify cluster release; water impact test and structural requalification for frustum.
Pilot Chute-Deployed Soft Pack – Concept 3	Seam and joint tests for cluster pilot; rocket sled tests for cluster pilot performance; laboratory tests for cluster pilot energy absorber; dynamic deployment test for cluster pilot using frustum; cluster dynamic lateral load test; static pull test for mains; drop tests to verify the ability of the cluster pilot to deploy the mains; water impact test for frustum; structural requalification for frustum and forward skirt.

Figure 19. Development test summary.

4.1 Material Strength Tests

Tests in this category include seam and joint tests for the new cluster pilot chute (concept 3). The strength of each seam and joint must be validated by a test or by similarity to existing seams and joints. It is anticipated that few tests of this type will be needed. Testing is performed in standard tensile testing machines such as the Tinius-Olsen machine in the PRF.

Also, in this category are laboratory tests for the development of the various energy absorbers and a rocket sled test for concept 4A to verify release of the cluster from the frustum by the energy absorbers. The rocket sled test will use the multiple sled arrangement described in paragraph 4.4. All rocket sled testing for the recommended concepts will be performed at Sandia National Laboratories in New Mexico.

4.2 Cluster Pilot Parachute Load Tests

The performance of the new cluster pilot chute will be validated by rocket sled testing like that used recently for the pilot chute that deploys the drogue (see paragraph 7.2). A prime objective of this test is to determine the opening shock factor. The test chute is installed in a test vehicle mounted on a pop-up sled. At the appropriate sled speed (25 percent over design dynamic pressure), the test vehicle is ejected upward to 150 to 200 ft and the test chute is deployed. Parachute loads and test vehicle accelerations are measured by instrumentation on the test vehicle. Laser tracking measures velocity and position, and onboard and track-side photography records chute deployment.

4.3 Static Pull Tests

Static pull tests will be performed on any new or modified main chute configuration. A cluster of three large main chutes is installed in the test rig to allow horizontal extraction. The frustum must be included if the configuration is not a soft pack. The cluster or the frustum is oriented at a base-up angle to simulate tilting during deployment. The ends of the risers are pulled horizontally away from the packs. As each increment of the parachute emerges from the pack, it is suspended from overhead tracks to minimize friction. Extraction loads are measured continuously to establish break-out loads for the bag flap, line, and canopy element release events. Video photography records the entire extraction, and still photography records specific events. This technique has been successfully used at the PRF.

4.4 Dynamic Deployment Tests

A rocket sled will be used to conduct dynamic deployment tests for concept 2 (delete isogrid) and concept 5 (EMPSS). For these two concepts, the parachute bags remain in the frustum. The system to be tested is mounted on two sleds that simulate the two major moving elements—the SRB and the frustum (fig. 20). The sleds are pushed in an "SRB nozzle first" direction by a third (propulsion) sled.
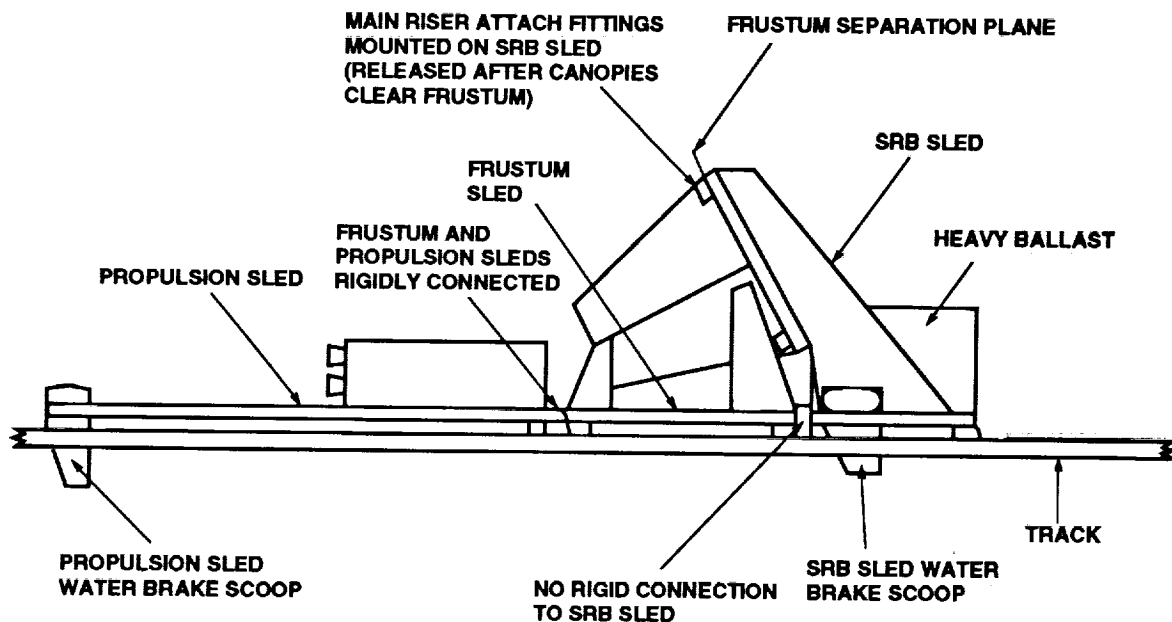
Figure 20. Dynamic deployment sled test configuration.

When the required speed is reached, the propulsion and frustum sleds are slowed by a water brake, and the heavily ballasted SRB sled coasts along the track to extract the main chutes from the frustum. In addition to simulating relative velocities of the SRB and frustum, this approach provides the correct direction for the "relative wind." Immediately after canopy deployment, the main chute risers are released from the SRB sled. This technique minimizes damage to the canopies caused by dragging along the track. The frustum sled will be rapidly decelerated to prevent it from running over the chutes. Instrumentation includes onboard and track-side photography of chute deployment and laser tracking, or the equivalent, to develop frustum and SRB velocities.

In addition to testing main parachutes, this sled arrangement can be used to verify the deployment of the cluster pilot chute for concept 3 (pilot chute-deployed soft pack). The cluster pilot chute bag would remain attached to the SRB sled until the frustum sled begins to decelerate. The bridle connecting the frustum to the cluster pilot bag would then snatch the bag away from the SRB sled and deploy the cluster pilot chute. No main chutes are used in this test.

4.5 Cluster Lateral Load Tests

Two types of lateral load tests are recommended: static tests that provide preliminary information on the effects of side forces into the frustum from a single parachute pack or from a pair of packs, and dynamic tests that determine the effects of interactions of the three chutes in a complete cluster.

The static test is a prerequisite to allowing the cluster to be supported directly by the frustum (concepts 2 and 4A). The frustum to be tested is mounted horizontally and attached to the test rig structure at station 395. As an option, the frustum can be supported at both ends. A single parachute pack, or a pair of packs, is placed on the foam support blocks on the lower arc of the frustum at the correct location. In the single-pack test (fig. 21), a V-shaped loading pad simulates the adjoining surfaces of the other two packs and rests on the two flat surfaces of the pack. In the two-pack test, the loading pad simulates the remaining single pack. The loading jacks pull down on the pack(s) with a force equal to the design lateral G's times the weight of the complete cluster without the pack(s). Instrumentation measures the load and strain on the frustum elements.
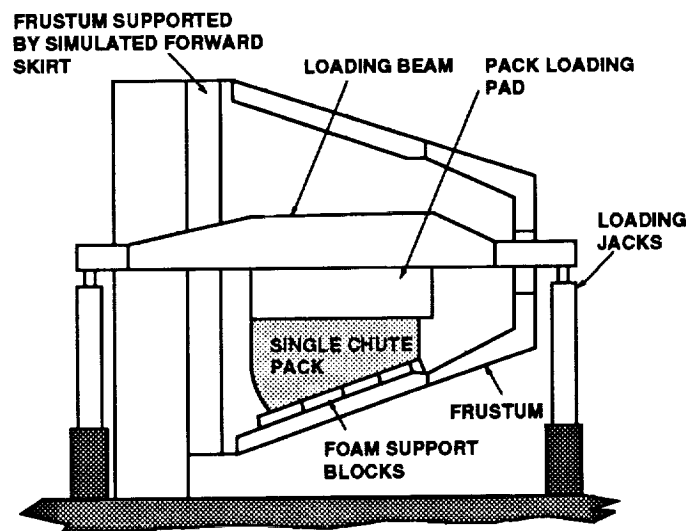
Figure 21. Cluster static lateral load test for concepts 2 and 4A.

Centrifuge testing is the customary method of testing the dynamic loads in the structure; however, there is no known centrifuge with the capacity to carry a complete frustum/cluster assembly. The proposed method is to mount the entire assembly on a rocket sled and accelerate it down the track (fig. 22). By controlling both acceleration and water brake deceleration, cluster side loads in opposite directions can be simulated in one run. If concept 3 (pilot chute-deployed soft pack) is tested, a portion of the SRB forward skirt is included because the cluster is mounted on the forward dome. Instrumentation for the concept 3 test will record cluster deflections and forward skirt loads. For the frustum-mounted configurations (concepts 2, 5, and 4A), instrumentation will measure the deflections in the surrounding structure. Acceleration will be measured for all configurations.
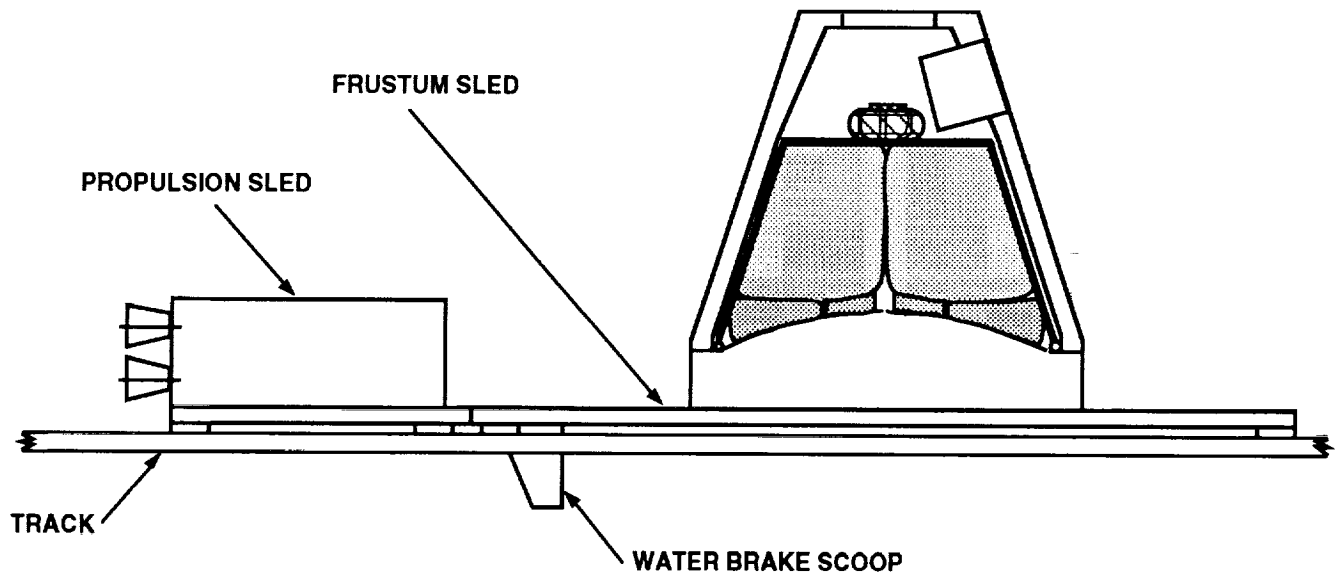
Figure 22. Cluster lateral load sled test configuration for concepts 3, 2, 5, and 4A (concept 3 shown).

4.6 Drop Tests

The team investigated the suitability of the SRB drop test vehicles (DTV's) for testing concept 3, and the availability of a B-52 aircraft to perform the tests. The objective of these tests is to study parachute deployment rather than demonstrate parachute strength. As a result, high altitude over-speed tests are not needed.

Two DTV's and associated support equipment have been in storage since 1984 at the Naval Weapons Center at China Lake, CA. DTV-1 may be in need of some structural repair after damage sustained during a 1984 drop test. DTV-2 is in satisfactory structural condition. Both DTV's have been stored outdoors and will require extensive refurbishment of their electrical wiring. The bomb loaders used in mating with a B-52 aircraft will also require refurbishment.

In preparation for tests of the large main parachutes in 1983, both DTV's were modified to meet new B-52 interface requirements. These requirements prevent the installation of a cluster of three main parachutes together with the SRB drogue and pilot chutes. However, since concept 3 does not require the SRB drogue and pilot chutes, the DTV's can accommodate the concept 3 configuration of three main chutes and a cluster pilot chute.

28

Figure 23 shows the proposed configuration for testing concept 3 in DTV-2. A contoured surface is incorporated into the DTV to simulate the tops of the floats and additional foam supports on which the cluster rests in the flight configuration. The cluster is secured to this surface by flight configuration retention straps. The cluster and cluster pilot chute are contained in a cluster cover which simulates the inside of an SRB frustum. The cluster cover is released by explosive nuts and deployed by an extraction chute in the same way that the nose cap was deployed in previous SRB recovery system drop tests. The DTV can be ballasted to produce a release weight less than in previous tests and a center of gravity (CG) inside the required envelope (fig. 24).
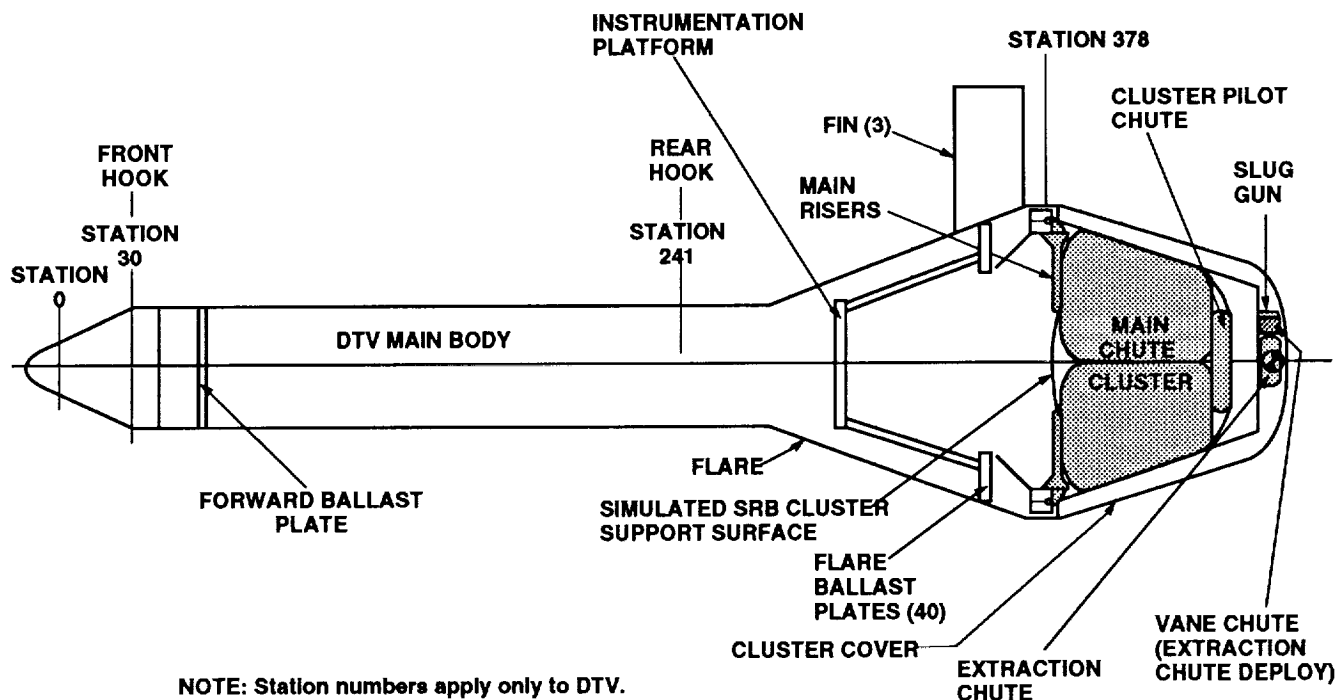
Figure 23. DTV-2 configuration for concept 3 drop test.

The team investigated the availability of the B-52, serial No. 008, maintained at Dryden Flight Research Facility in California. The 1989–1990 B-52 program included F-111 escape module tests, Pegasus launches, and shuttle braking chute tests. None of these activities affected the DTV/B-52 interface. Additional Pegasus launches and F-111 escape module tests are planned for 1991 and 1992, but there should be adequate time in the B-52 schedule to conduct the concept 3 drop tests beginning in late 1991. The team concluded that this aircraft is the best choice for the drop test program, and that the tests should be conducted at the Naval Weapons Center at China Lake, CA.

DESCRIPTION	WEIGHT (LB)	X - CG STATION (INCHES)
DTV MAIN BODY (NO BALLAST PLATES)	28,811.60	63.76
FLARE (INCLUDING INSTRUMENTATION PLATFORM)	7,405.30	339.09
AVIONICS	129.10	300.00
FINS	253.00	368.00
FORWARD BALLAST PLATE	1,458.00	55.90
FLARE BALLAST PLATES (41.60 LB/PLATE, 40 PLATES)	1,664.00	358.00
MAIN CHUTE CLUSTER AND ATTACH HARDWARE	6,549.00	412.00
CLUSTER PILOT CHUTE	150.00	447.00
CLUSTER COVER (FRUSTUM SIMULATOR)	1,500.00	427.00
EXTRACTION CHUTE	150.00	466.00
VANE CHUTE (EXTRACTION CHUTE DEPLOY)	5.00	466.00
SLUG GUN	5.00	466.00
TOTAL DTV	48,080.00	179.65

DTV X - CG ALLOWABLE RANGE	177.56 TO 182.86

Figure 24. DTV-2 mass properties for concept 3.

5.0 COST COMPARISON AND AMORITIZATION STUDY

The team assessed the costs of each major recommended damage reduction concept taking into account initial investment, changes in operations costs, and savings due to damage reduction. It was decided to calculate the number of shuttle flights it would take to pay back the initial investment given a specific lowered risk of SRB loss per flight. Thus, the initial investment was amortized over a calculated number of shuttle flights. Parachute ripstop is a damage reduction concept that has already been implemented, and all recommended concepts were evaluated with ripstop in place. Calculation of the payback period for ripstop itself is shown as an example.

5.1 Assumptions

1. If two or more chutes fail, complete SRB loss—$35,000,000.

2. If single chute fails—$400,000 loss—incremental water impact damage.

3. Chute failure incidence = 4 failures/15.5 flights = 0.258 per shuttle flight (based on the first 31 SRB's successfully recovered by large main parachutes without ripstops).

4. The failure rate of one chute in a two-chute cluster is 1.5 times the failure rate of one chute in a three-chute cluster.

5. Ripstop alleviates 75 percent of chute failures.

5.2 Nomenclature

PFR_3—Failure rate per chute for a three-chute cluster.

PFR_2—Failure rate per chute for a two-chute cluster.

5.3 Analysis

$PFR_3 = 0.258/6 = 0.043$ per chute use without ripstop.

$PFR_2 = 0.043 \times 1.5 = 0.0645$ — expected failure rate per parachute for a two-chute cluster without ripstop.

The likelihood of two chutes failing is the product of separate probabilities, shown below.

Probability of chutes 1 and 2 failing is:

$$PFR_3 \times PFR_2$$

However, we have three combinations: 1 and 2, 1 and 3, 2 and 3.

Probabilities of any two chutes failing is:

$$3 \times PFR_3 \times PFR_2 = 0.00832 \text{ per booster, or } 0.01664 \text{ per shuttle flight.}$$

Probability of two or three chutes failing is:

$$2 \times (3 \times PFR_3 \times PFR_2 + PFR_3 \times (PFR_2)^2) = 0.0170 \text{ per shuttle flight.}$$

Thus, we would expect to lose a booster every $(0.017)^{-1} = 58.8$ shuttle flights (without ripstops). (We would also expect to lose two or more chutes for every $0.258/0.017 = 15.2$ incidents of single chute failure.)

Continuing the example, the monetary risk per flight without ripstop is:

$$0.017 \times \$35,000,000 + 0.258 \times \$400,000 = \$595,000 + \$103,200 = \$698,200$$

With parachute ripstop fully incorporated, it is anticipated that the parachute failure incidence will be reduced by 75 percent. Therefore, the parachute failure incidence is 0.258/4, one-quarter the pre-ripstop rate. However, the incidence of two chutes failing is not one-quarter the pre-ripstop rate. It is one-sixteenth because the two-chute failure probability is the product of two separate probabilities.

With ripstop, PFR_3 becomes $0.043/4 = 0.01075$, and PFR_2 becomes $0.01075 \times 1.5 = 0.016123$

Probability of booster loss becomes:

$$2 \times (3 \times PFR_3 \times PFR_2 + PFR_3 \times (PFR_2)^2) = 0.001046 \text{ per shuttle flight.}$$

Thus, we would expect to lose a booster every $(0.001046)^{-1} = 956$ shuttle flights with ripstop installed.

Single chute failure would be expected to occur every $(0.258/4)^{-1} = 15.5$ shuttle flights.

Monetary risk with ripstop becomes:

$$0.001046 \times \$35,000,000 + (0.258/4) \times \$400,000 = \$36,610 + \$25,800$$

$$= \$62,410 \text{ per shuttle flight with ripstop.}$$

5.4 Amortization Equation

The payback period in number of flights for any modification is:

$$PBP \text{ (mod)} = TI(mod)/(MR(base) - MR(mod) - OPS \text{ Change(mod)})$$

where PBP (mod) is the payback period, TI(mod) is the total initial investment for the modification, MR(base) is the baseline monetary risk per flight before any new modification (\$698,200 before ripstop or \$62,410 after ripstop), MR(mod) is the new monetary risk per flight with the modification in

place, and OPS Change(mod) is the change in operations costs per flight with the modification in place (positive if operations costs increase and negative is operations costs decrease).

If the change in operations costs is a savings, it serves to pay back the investment sooner.

To calculate the payback period for ripstop in our example, the following parameters are used:

TI(mod)   = $780,000
MR(base)   = $698,200
MR(mod)   = $ 62,410
OPS Change (mod)   = $ 0

The payback period for ripstop thus becomes:

$$PBP = \$780,000/(\$698,200 - \$62,410 - \$0) = 1.2 \text{ shuttle flights.}$$

5.5 Results

The results of the amortization exercise are summarized in figure 25 for ripstop and the recommended concepts. The ripstop modification was assumed to be fully implemented when each recommended concept was evaluated. Ripstop greatly lowered the previously large monetary risk associated with each flight, and limits to some extent the degree of improvement available from future modifications. The vent cap ties concept is a relatively inexpensive change that will correct the vent entanglement problem. Because it was anticipated that this change would soon be incorporated, the four other recommended concepts in figure 25 were evaluated with the vent cap ties included.

MAIN CHUTE CONFIGURATION	CHANCE OF LOSING A CHUTE PER FLIGHT	CHANCE OF LOSING AN SRB PER FLIGHT	MONETARY RISK PER FLIGHT	INITIAL INVESTMENT	CHANGE IN OPERATIONS COSTS PER FLIGHT	NUMBER OF FLIGHTS FOR PAYBACK	PAYBACK* TIME (YRS)
BEFORE RIPSTOP	$\frac{1}{4}$	$\frac{1}{59}$	$700K	N/A	N/A	N/A	N/A
WITH RIPSTOP	$\frac{1}{16}$	$\frac{1}{956}$	$62K	$780K	0	1.2	0.1
VENT CAP TIES	$\frac{1}{24}$	$\frac{1}{2296}$	$32K	$200K	+$1K	7	0.6
DELETE ISOGRID	$\frac{1}{78}$	$\frac{1}{24,000}$	$6.6K	$2M	-$5K	33	2.8
EMPSS	$\frac{1}{78}$	$\frac{1}{24,000}$	$6.6K	$3.5M	-$10K	54	4.5
SOFT PACK WITH ENERGY ABSORBER (FRUSTUM MOUNTED)	$\frac{1}{78}$	$\frac{1}{24,000}$	$6.6K	$5M	+$15K	124	10.3
PILOT CHUTE - DEPLOYED SOFT PACK	0	$\frac{1**}{10,000}$	$3.5K	$9M	+$20K	234	19.5

* BASED ON 12 FLIGHTS PER YEAR
** FROM LOSS OF CLUSTER PILOT CHUTE

Figure 25. Cost amortization results.

6.0 MAIN PARACHUTE ENHANCEMENTS

The team identified a number of desirable improvements for the main parachute system and has grouped them under the general category of enhancements because of their ease of implementation and low cost. One of these enhancements, vent cap ties (paragraph 6.1), will solve the vent entanglement problem and is recommended for immediate implementation. Additional enhancements are described in paragraphs 6.2 through 6.10, and the team recommends that these be considered for implementation at a convenient time.

6.1 Vent Cap Ties

This change adds canopy bag ties to the vent cap to eliminate main parachute failures caused by vent entanglement. The current main parachute packing procedure allows the vent to sag into the lower portions of the canopy during deployment because the vent is not supported in the deployment bag. The vent cap ties would provide the necessary support and control for the vent during deployment.

6.2 Canopy Vent Apex Tie Lanyard Modification

The present apex tie lanyard does not stroke (i.e., fully extend) for approximately half of its usages. This modification alters the configuration of the apex lanyard so that it strokes every time, providing better control of main parachute vent deployment.

6.3 Optimize Canopy Ties

Presently, the canopy ties are 350-lb cotton at all of the canopy tie locations. It is speculated that using 350-lb cotton at the higher rows of canopy ties aggravates violent vent deployment. This problem can be alleviated by optimizing canopy tie strength for each row. Before this enhancement can be implemented, an analysis is required to determine the optimum strength of canopy ties for each row.

6.4 Relocation of Canopy Ties

The canopy tie loops of the present recovery system are located such that the main parachute canopies do not pull straight out of the pack. The present packing procedure requires the parachute canopy to be rotated eight gores relative to the position it attains at deployment. It is recommended that the canopy ties be relocated so that the chutes will deploy without having to rotate into position. This change should reduce some of the violent deployment dynamics.

6.5 Use of Filament Wound Case Bidirectional Canopy Tie Loops

A minor problem observed during refurbishment operations is that the canopy tie loops are pulled away from and off of the canopy radials. A modification that should correct this condition is to replace the present tie loops with the bidirectional tie loops designed for the filament-wound case drogue. When combined with some of the other changes described in this section (e.g., relocation of canopy ties), this change is easily implemented. It should also reduce tie loop repairs during refurbishment operations.

6.6 Alternate Vent Line Stacking

At present, the vent lines are stacked such that vent lines 1 and 80 are separated at the center of the vent by a stack of lines approximately 10 inches high. It is suspected that this separation causes a load concentration in the vent band. By stacking the vent lines in a different sequence, the vertical separation of any two adjacent vent lines can be minimized.

A stacking sequence has been devised by which vent line 80 is placed directly on top of vent line 1, then vent line 2 on vent line 80, vent line 79 on vent line 2, etc. This arrangement will result in a stacking separation between all vent lines equal to the thickness of one vent line. This method of vent line stacking is being considered for a patent application.

6.7 Mesh Top for Deployment Bag

This change replaces a section of the top of the main parachute bag with a mesh material, alleviating any pressure differential and resulting damage that may occur in the main parachute bag during deployment and water impact.

6.8 Reduce Number of Reefing Line and Suspension Line Tacks

SRB onboard cameras reveal a restriction to smooth main chute inflation which appears to be caused by reefing line tacks and suspension line tacks that do not break when required. A solution to this problem is to eliminate some of the tacks to reduce interference with chute deployment. Analysis is first required to determine the minimum number of tacks that could be used without negative effects.

6.9 Fabric Liner for Parachute Vent

Main parachutes frequently lag during inflation. It is believed that this condition is mainly caused by too much parachute vent area. This modification adds a fabric liner to the vent region of the main parachutes to reduce the effective vent area and thereby improve first stage inflation. Before implementation, an analysis is required to study the new load paths introduced into the vent region of the parachute.

6.10 Apply Friction Reducing Material During Refurbishment

The greatest increase of large main parachute friction burn damage occurs during the chutes' second and subsequent flight uses. It is assumed that the lubricant applied to the material during the weaving process of the nylon ribbons and webbings is washed out during normal retrieval, defoul, and wash operations. It is proposed that a lubricant be applied to the parachutes during the normal refurbishment procedure at the PRF to restore the original friction burn resistance to the parachutes. A preliminary study indicates that TL-403 is the best candidate for the friction reducing material. TL-403 has good abrasion reduction characteristics and a minimum of undesirable traits.

7.0 RELATED ISSUES

During MPDRT activities, several issues associated with the SRB recovery system were identified. While these issues may not be directly associated with reducing damage to the main parachutes, they affect SRB recovery probability and data collection. These issues are discussed in the following paragraphs.

7.1 SRB Center of Gravity

The most important related issue identified by the MPDRT is the longitudinal position of the SRB CG during reentry. The SRB has an aft CG location which produces its characteristic tail-first reentry at high Mach number. During a normal reentry, after the SRB Mach number decreases below 1.0, the trim angle changes to a more broadside orientation. This orientation increases the aerodynamic drag of the SRB, which provides adequate deceleration and favorable conditions for pilot chute deployment.

A problem arises when the CG has an extreme aft position. The SRB might not attain the broadside orientation as it passes through Mach 1.0, but would remain at a very high angle of attack. The resulting low aerodynamic drag would cause unacceptably severe deployment conditions, and the recovery system would fail. The SRB Monte Carlo trajectory simulation indicates vehicle station 1270 is the critical CG location for recovery. For a reentry CG location aft of station 1270, the possibility exists for a severe deployment condition.

Thiokol Corporation is considering for future use several motor configurations that would result in reentry CG locations aft of station 1270. This situation is caused by the need to use some heavyweight case segments in the aft motor segment to maintain production flow. The MPDRT recommends that this issue be given due attention.

7.2 Pilot Parachute Capability

The SRB pilot parachute that deploys the drogue was originally designed for a dynamic pressure of 250 lb/ft^2 at deployment. Because of cost and schedule constraints, the pilot chute load was never measured during the drop test program or rocket sled tests. As a result, the opening shock effects, which cause the peak load, were unknown. The capability of the pilot chute could therefore only be estimated.

The maximum predicted dynamic pressure to which the pilot chute could be subjected has increased since the beginning of the shuttle program because of an increase in SRB weight, an aft shift in CG location, and the retention of the nozzle extension until just before SRB water impact. Using the current range of SRB reentry parameters and excluding the extreme aft CG condition discussed in paragraph 7.1, there exists the possibility that the pilot chute could be deployed at a dynamic pressure of 400 lb/ft^2. Because of the concern for the loss of an SRB, the MPDRT, in late 1989, recommended a rocket sled program to determine the opening shock factor and capability of the pilot chute. In the summer of 1990, two rocket sled tests[7] were conducted for the pilot chute. Analysis of the test data indicated a rated capability of only 272 lb/ft^2. A design study was subsequently initiated to incorporate stronger components in certain critical areas of the pilot chute and to correct a design flaw discovered during the rocket sled tests. This effort led to a modified pilot chute design. In January 1991, the modified pilot chute underwent a successful rocket sled test program.[8] Test results indicated a rated

capability of 426 lb/ft^2, making the modified pilot chute adequate for use on the current SRB configuration. Concern for the loss of an SRB still exists, however, because the modified pilot chute is not planned for flight use until the summer of 1992.

7.3 Parachute Performance Data

The performance of the main chutes in decelerating the SRB's for water impact is one of the critical concerns for recovery. Practically every problem experienced with the recovery system has been associated with the main parachute system. The drogue and pilot chutes are also critical because the failure of one of them results in loss of an SRB.

Fortunately, measured flight data have been obtained to evaluate the various recovery system malfunctions thus far. The prime sources of this data have been parachute load cells, radar tracking ships, photo aircraft, and an onboard motion picture camera mounted on the forward dome of the SRB forward skirt. Data from these sources have often been used to develop a reconstruction of the entire recovery phase to evaluate parachute performance. Such an evaluation is absolutely necessary to solve recovery system problems and prevent the loss of an SRB. The reconstruction can also provide an estimate of water impact velocity, which is important in determining the reuse capability of certain SRB components.

Use of the parachute load cells and tracking ships has been discontinued, and budget constraints are currently preventing the use of photo aircraft. The only remaining system to provide parachute data is the SRB onboard motion picture camera. This camera has been useful in the past, but it is old and requires a lot of maintenance. In addition, it is useless for night launches, which occur regularly.

The MPDRT proposes two improved methods for obtaining parachute data: (1) Replace the SRB onboard motion picture camera system with a modern, self-contained video cassette camera and recorder. The new video system would be a regular production item and would provide data even in minimal lighting conditions. (2) Mount a self-contained instrumentation and data recorder package in the frustum or forward skirt. Such a system could be used on every flight to provide data such as accelerations, event times, and chute loads.

7.4 Prime Contractor Data Requirements

When Martin Marietta Corporation was originally under contract to NASA and later under contract to USBI, they were obligated to publish a recovery system report after every launch. This report stated the accuracy of load predictions, summarized parachute performance, and assessed parachute damage. This type of data is valuable in producing parachute damage trends and correlations. Currently, USBI is under contract for the recovery system and is not required to publish this report. This lack of data from STS-26R to present has hindered the collecting of an accurate parachute historical data base.

8.0 SUMMARY AND RECOMMENDATIONS

As part of its investigation, the MPDRT compiled a main parachute damage history for the first 29 shuttle flights (appendix B). After studying these data, the team concluded that there are two primary sources of significant main parachute damage during deployment. The most frequent source of damage is contact with the MPSS (isogrid and bipod struts). The other source is vent entanglement, which causes the overstressing of horizontal ribbons and leads to parachute failure. The team identified a relatively simple change to the parachute packing procedure (vent cap ties) that will prevent entanglement of the vent.

The team investigated data correlations to determine if main parachute damage is related to various parameters. Although a general lack of data hindered this study, some interesting results were noted. These results are summarized in appendix B, section B.4, and should be considered before any future changes are made to the SRB or recovery system.

The team selected the pilot chute-deployed soft pack as the most effective damage reduction concept. Several alternatives are recommended that would result in a major reduction in deployment damage at lower total cost than the pilot chute-deployed soft pack. The team also addressed issues related to main parachute inflation, SRB recovery probability, and parachute data collection.

Specific recommendations of the team are as follows:

1. Incorporate vent cap ties as soon as possible to eliminate vent entanglement (paragraph 6.1).

2. Proceed with implementation of one of the team's recommended concepts for eliminating damage from contact with the MPSS (sections 2.0 and 3.0).

3. Resolve the recovery system-related issues identified in section 7.0.

4. Incorporate, at a convenient time, the main parachute enhancements described in paragraphs 6.2 through 6.10.

9.0 CONCLUSION

The MPDRT made its recommendations to MSFC management in late 1989. MSFC has since decided to implement several of the team's recommendations. First flight for these changes and other recovery system improvements is scheduled for the summer of 1992 on STS-46.

One of the most significant changes to be implemented is the addition of vent cap ties to support the main parachute vent cap (paragraph 6.1). The team urgently recommended this modification to eliminate entanglement.

Main parachute changes described in paragraphs 6.3, 6.4, and 6.5 are also to be implemented. These involve reducing the canopy tie strength in the upper canopy area, relocating the canopy ties so that the parachutes deploy without having to rotate eight gores, and using bidirectional tie loops for the canopies.

The team recommended modifying the apex tie lanyard so it always strokes during main chute deployment (paragraph 6.2). The decision was made, instead, to simply eliminate the lanyard.

The main parachute riser tack configuration will be changed to obtain a more circular shape for the deployed canopies. This change was not included in the team's recommendations, but is scheduled to be implemented.

Improvements will also be implemented for recovery system elements other than the main parachutes. A stronger pilot chute will replace the current one, as the result of a team recommendation (paragraph 7.2). Other changes have been initiated since the team completed its investigation. The drogue parachute bag will be strengthened in several areas, and the attachment of the pilot chute to the bag will also be strengthened. Finally, stronger bolts will be used in the MPSS to attach the ring splice fittings to the isogrid panels (fig. 4). This change will allow the MPSS to meet the ultimate strength requirement for the high axial load that occurs after frustum separation.

The combined effect of these changes, when implemented on STS-46, will be to reduce the probability of main parachute deployment damage and increase the probability of successful SRB recovery. Even when a main parachute is damaged during deployment, the ripstops now used on all flights (paragraph 1.2) will help prevent total parachute failure. In fact, ripstops have already been credited with saving a main parachute from total failure on a 1991 flight.

REFERENCES

1. Smith, J.D.: SRB Main Parachute Damage Reduction Investigation Team, NASA Internal Memorandum EE11 (89-145), Marshall Space Flight Center, AL, June 19, 1989.

2. Bacchus, D.L.: SRB Main Parachute Damage Reduction Team Briefing, NASA Internal Presentation, Marshall Space Flight Center, AL, October 26, 1989.

3. "STS-30R Main Parachute Failure Investigation Report." USBI-ANAL-137-89, United Technologies/USBI Co., Huntsville, AL, June 1989.

4. Wolf, D.F.: "Failure Investigation Report for STS-30 Main Parachute S/N 8045." Memorandum to NASA-MSFC, Sandia National Laboratories, Albuquerque, NM, June 12, 1989.

5. "SRB 'Soft-Pack' Main Parachute Deployment Concept Study." Technical Report SD84-MSFC-2761, Teledyne Brown Engineering, Huntsville, AL, October 1984.

6. Brecheen, W., and Tallentire, F.: "Summary Final Report, Preliminary Design Study for Main Parachute Deployment From 'Soft' Container." Technical Note TN32122-67, Martin Marietta Corporation, Denver, CO, April 15, 1985.

7. "Solid Rocket Booster Pilot Parachute Rocket Sled Test Report." USBI-ANAL-174-90, United Technologies/USBI Co., Huntsville, AL, September 1990.

8. "Modified Pilot Parachute Rocket Sled Test Report." USBI-ANAL-195-91, United Technologies/USBI Co., Huntsville, AL, March 1991.

APPENDIX A

SUMMARY OF ALL DAMAGE REDUCTION CONCEPTS CONSIDERED

The main parachute damage reduction team (MPDRT) developed 23 concepts for reducing main parachute deployment damage. Team members independently derived pros and cons for each concept. The individual efforts were then collected and tabulated for open discussion by the entire team. The 23 concepts are presented below with the pros and cons for each concept. Following each concept is a brief summary of the team's evaluation.

Concept 1: Shorten Isogrid

This previously studied concept eliminates the lower bay of the isogrid and moves the bipod strut connection up 14 inches to station 367.

Pros: Reduces contact with isogrid and bipod strut. No extensive testing required. Previous engineering analysis available.

Cons: Parachutes will still contact frustum, isogrid, and bipod struts. Corners still exist. Possible structural problems associated with attaching isogrid to station 367. Improvements are uncertain.

The team concluded that this concept offers only marginal improvements at best and should not be pursued. The team also considered cutting off more of the isogrid but decided it would be more efficient to completely eliminate the isogrid. (See concept 2).

Concept 2: Delete Isogrid

This concept completely eliminates the isogrid and bipod struts. The cluster lateral load is transmitted directly to the frustum.

Pros: Eliminates most probable cause of damage (contact with the isogrid and bipod struts).

Cons: Possible frustum beef-up to withstand cluster lateral loads. Still deploying out of rigid container. Requires modification of GSE for clustering.

The team agreed that eliminating the isogrid would offer a significant improvement and selected it as an alternative recommended concept. However, questions about frustum structural capability would need to be addressed and resolved prior to proceeding with this concept.

Concept 3: Pilot Chute-Deployed Soft Pack

In this concept, the parachutes are mounted on the forward dome of the SRB forward skirt and deployed by a cluster pilot chute. The cluster pilot chute is deployed by a bridle attached to the frustum.

Pros: Eliminates damage due to contact with surrounding structure. Optimum bag strip veloci-
ties. Large pull-off angles accommodated. Traditional parachute deployment. Concept
has been studied extensively. Not sensitive to frustum dynamics.

Cons: Possible beef-up of forward skirt to support parachute packs. Requires extensive hard-
ware modification and system redesign. Requires drop tests. Requires new cluster pilot
chute development program. Longer time required to deploy main parachutes. Requires
additional flotation system and retrieval operation to recover deployment bags and cluster
pilot parachute. May increase first stage main parachute load. Requires new GSE.

The team concluded that this concept offers the best technical approach for solving the problem
of main parachute damage, and made it the top recommended concept.

Concept 3A: Pilot Chute-Deployed Soft Pack (Frustum Mounted)

This concept is similar to concept 3. Instead of being mounted on the dome, however, the system
is suspended within the frustum and uses an open-ended energy absorber to release the main chute
cluster.

Pros: Eliminates damage due to contact with surrounding structure. Optimum bag strip
velocities.

Cons: Requires extensive hardware modification and system redesign. Requires drop tests.
Requires new cluster pilot chute development program. Longer time required to deploy
main parachutes. Requires additional flotation system and retrieval operation to recover
deployment bags and cluster pilot parachute. May increase first stage main parachute
load. Requires GSE modification. Unpredictable parachute pack dynamics after release
from energy absorber.

The team concluded that although this concept is risky, it may be worth pursuing if costly
redesign and qualification testing of the dome prevents the development of concept 3.

Concept 4: Soft Pack With Delayed Release From Frustum

This concept keeps the cluster suspended in the frustum until just after frustum separation. The
cluster is released from the frustum on a bridle at approximately 0.6 seconds after frustum separation,
providing a soft-pack deployment. The delay allows the high deceleration at frustum separation (about
17 G's) to decay to about 5 G's before cluster release.

Pros: Eliminates damage due to contact with structure. Not very sensitive to frustum dynamics.

Cons: Extensive redesign required. Complex cluster release mechanism required. Drop testing
may be required. High bridle loads cause design problems. Requires GSE modification.

This concept received much consideration and was subsequently modified to include an energy
absorbing bridle. This modified concept then became alternative recommended concept 4A.

42

Concept 4A: Soft Pack With Energy Absorber (Frustum Mounted)

This concept upgrades concept 4 by using energy absorbers to soften the release of the cluster from the frustum. The energy absorbers support the cluster during ascent and reentry. At the time of frustum separation, the high deceleration imparted by the drogue causes the cluster to exit the frustum before parachute canopy deployment occurs. As in concept 4, the bags remain attached to the frustum by a bridle arrangement.

> Pros: Eliminates damage caused by contact with structure. Not very sensitive to frustum dynamics.

> Cons: Extensive redesign required. Energy absorber design requires much analysis. Requires GSE modification.

The team spent a good deal of time developing this concept. It has a much lower cost than the pilot chute-deployed soft pack, but is nearly as effective in reducing damage. The team selected concept 4A as one of its alternative recommended concepts.

Concept 5: External MPSS

The isogrid is eliminated and replaced with a smooth rigid-walled container to support the main chute cluster. This concept is further enhanced by fairing the lower portion of the frustum to provide a continuous smooth surface for parachute deployment.

> Pros: Eliminates most probable cause of damage (contact with the isogrid and bipod struts). Puts chutes in convenient transport container. Eliminates installation of aft bay instafoam.

> Cons: Still deploying out of rigid container. Requires GSE modification.

This concept received much consideration and was selected as an alternative recommended concept.

Concept 6: Banana Bag

The banana bag concept offers a soft deployment by using a double-walled deployment bag. The S-folded bag is pulled completely clear of the frustum before the parachute begins to come out of the bag. The outer bag then pulls at the edge of the inner bag to peel it, rather than strip it away from the parachute.

> Pros: Protects parachute during deployment (no sliding contact with structure or bag). Canopies deploy when clear of frustum, providing soft pack effect.

> Cons: Unknown dynamics involved. Much testing required. New bags required. Complicates packing procedure. Requires modification to GSE.

This approach is too unconventional to be considered at this time for SRB application.

Concept 7: Longer Drogue Suspension Lines

With this concept, the drogue is provided with longer suspension lines to reduce the effects of wake overtake on the drogue and frustum.

Pros: Should provide additional stability to drogue to reduce frustum tilt angle.

Cons: Does not eliminate structural interference. Increases drogue bag strip velocity. May require drogue modification. Improvements are uncertain. Nose cap volume is limited; may require redesign.

Frustum tilt angle may be a significant contributor to the problem of structural contact, but it is not certain that longer drogue suspension lines will alleviate the problem. The team concluded that this concept offers only marginal improvements at best, with some serious disadvantages, and should not be pursued.

Concept 8: Clustered Drogue

With this concept, the current drogue is replaced with a three-parachute cluster to increase stability and offset wake overtake effects, possibly reducing the frustum tilt angle.

Pros: Should provide more stability and reduce frustum tilt angle. Redundancy for drogue.

Cons: Does not eliminate structural interference. New drogues require major development program. Drop testing required. Nose cap volume limited; may require redesign. Introduces problems of nonuniform inflation, load sharing, and other problems associated with clustering. Improvements uncertain.

It is not certain that a clustered drogue would significantly reduce frustum tilt angle. The team concluded that this concept offers only marginal improvements at best and is far too complex and costly to be considered for SRB application.

Concept 9: Larger Drogue

This concept replaces the current drogue with a larger parachute in order to reduce the dynamic pressure at main parachute deployment.

Pros: Slightly lower main chute bag stripping velocity. Would allow more time on drogue for a given altitude margin, thus providing more effective damping of SRB oscillation and reducing frustum tilt angle. Lower frustum water impact velocity.

Cons: Does not eliminate structural interference. New drogue requires major development. Drop testing required. Drogue loads increase significantly (may require frustum beef-up). Nose cap volume is limited.

The team concluded that this concept represents a major change, would be costly to implement, and would not sufficiently reduce main parachute damage.

44

Concept 10: Increase Time on Drogue

This concept requires the baroswitch settings to be adjusted to allow more time for the drogue parachute phase.

Pros: Minimal cost. No testing required. Helps prevent frustum separation from occurring near drogue disreef (frustum high-G problem). Allows more time to dampen SRB oscillation.

Cons: Reduces altitude margin for main chutes. Does not eliminate structural interference. Adjustable range of switch may be insufficient.

The team agreed that the baroswitch settings should be optimized, but that this concept by itself would not significantly reduce main parachute damage.

Concept 11: Optimize Ties For Vent Cap and Canopy

This concept includes four important changes to the current main parachute tie arrangement. These four changes are described in paragraphs 6.1 through 6.4 under the category of enhancements. One change in particular, vent cap ties, is most urgently recommended by the team to prevent parachute failure caused by vent entanglement.

Pros: Low cost. Easy to implement. Minimal system impacts and testing.

Cons: Does not eliminate structural interference.

Because of the relative ease of implementation of these four changes, the team grouped them in section 6.0 with other recommended enhancements.

Concept 12: Soft Pack With Mortar-Type Deployment

This concept is similar to concept 4 except that the main parachute bags do not remain attached to the frustum after being dropped out. Deployment is similar to a mortar-deployed system except that the velocity relative to the SRB is generated by the drogue rather than a mortar.

Pros: Eliminates structural contact during deployment. Reduces bag strip velocity.

Cons: Proper bag strip not assured. Unconventional approach for large parachutes. Design of cluster release mechanism could be difficult. Separate flotation system and retrieval operations required for deployment bags. Drop test required.

The team concluded that this concept is not appropriate for SRB application because of unpredictable behavior of the main parachute packs after release from the frustum.

Concept 13: MPSS Fairing to Frustum Exit

This concept extends the current isogrid with a smooth fairing to the frustum exit. This new fairing has three compartments as does the current MPSS.

Pros: Eliminates contact with bipod struts. Eliminates need for aft bay instafoam.

Cons: Chutes still deployed from rigid container. Adds more length to isogrid for chutes to contact. Parachute deployment dynamics may be worse for large frustum tilt angles.

The team concluded that this concept might actually increase main parachute damage.

Concept 14: Split Isogrid

This concept splits the isogrid approximately in half with the lower half being attached to the SRB. The purpose is to retain lateral restraint until frustum separation at which time the lower half of the isogrid remains attached to the SRB where it will not interfere with parachute deployment.

Pros: Removes significant portion of the isogrid as a potential damage source during deployment.

Cons: Major redesign of MPSS and forward skirt. Lower portion of isogrid may damage parachute bags at frustum separation, and may interfere with main riser release, flotation deployment, and SRB retrieval. Still deploying from rigid container. Improvements uncertain. Requires GSE modification.

The team concluded that this concept should not be pursued because significant new problems and damage sources would be created.

Concept 15: Separation Plane Moved Forward

This concept moves the frustum separation plane forward (higher) so that the bottoms of the parachute bags are below the separation plane. Also, the isogrid is shortened.

Pros: Reduces probability of structural contact. Reduces frustum impact velocity.

Cons: Major redesign of frustum, MPSS, and forward skirt. Causes interference with main chute risers, riser release, and main chute float deployment. Could make SRB retrieval and towback more difficult. Still deploying from rigid container. Requires requalification of ordnance. Much testing required. Improvements uncertain, especially with high frustum tilt angles.

The team concluded that this concept should not be pursued because it represents a significant change in the SRB configuration, and has other serious disadvantages.

Concept 16: Lower Main Chute Pack in Frustum

In this concept, the forward dome of the SRB forward skirt is inverted, and the parachute packs are lowered in the frustum such that the bottoms of the packs are below the separation plane.

Pros: Reduces probability of structural contact. Allows more volume for parachute packs.

Cons: Extensive hardware redesign. Requires mods to parachute packs. May complicate SRB towback and increase towback loads on dome. Still deploying out of rigid container. Requires GSE modifications.

The team agreed that the additional volume might prove useful, but that overall improvements are not worth the high cost of implementation.

Concept 17: Frustum Fairing

A frustum fairing is added to the lower portion of the frustum.

Pros: Provides smoother exit from frustum. Eliminates need for aft bay instafoam. Inexpensive.

Cons: Does not eliminate structural interference.

The team agreed that a frustum fairing may slightly alleviate the structural contact problem, but would not by itself sufficiently reduce main parachute damage. Concept 5, one of the alternative recommended concepts, includes a frustum fairing as do concepts 13 and 18.

Concept 18: Individual Rigid Containers

This concept replaces each current deployment bag with a rigid deployment container with integral fairing. The three containers are joined to form an assembly which would replace the current MPSS.

Pros: Eliminates contact with bipod struts. Eliminates need for aft bay instafoam.

Cons: Chutes still deployed from rigid container. Improvements uncertain. New GSE required.

The team agreed that this concept would not sufficiently reduce main parachute damage because the three containers form an internal structure similar to the current isogrid.

Concept 19: Jettison Nozzle Extension at Apogee

The SRB nozzle extension is presently jettisoned during the main parachute phase of recovery just before water impact. Separating the extension at apogee would significantly reduce the severity of the deployment conditions for the drogue and main parachutes. This reduction occurs because of an increase in SRB tail-first aerodynamic drag without the extension.

47

Pros: Easy to implement. Milder deployment conditions. Eliminates nozzle extension break-up which threatens drogue parachute (potential loss of SRB).

Cons: Exposes interior of aft skirt to much more severe environment. Affects reuse of thrust vector control system components.

The team agreed that, from a recovery system standpoint, it is an excellent idea to jettison the extension at apogee. In fact, it has been done on two earlier flights. The problem, however, is the severe damage inside the aft skirt on these two flights. MSFC management has determined that from an overall standpoint, the high cost of this damage outweighs any parachute advantages.

Concept 20: Bridle-Deployed Soft Pack on Dome

In this concept, the parachutes are mounted on the forward dome of the SRB forward skirt and are deployed by a bridle attached to the frustum.

Pros: Eliminates damage due to structural contact. Not sensitive to frustum dynamics.

Cons: Possible beef-up of forward skirt. Extensive redesign. Requires drop tests. Very high bridle loads; main chutes get snatched violently off dome. Requires new GSE.

Problems associated with bridle loads led to development of concept 21.

Concept 21: Energy Absorber-Deployed Soft Pack on Dome

This concept is similar to concept 20 except that the parachutes are deployed by an energy absorbing bridle.

Pros: Eliminates damage due to structural contact. Not sensitive to frustum dynamics.

Cons: Possible beef-up of forward skirt. Extensive redesign. Requires drop tests. Requires new GSE.

The team concluded that this concept is worthwhile, but not worth the cost. It was essentially combined with concept 4 to become concept 4A, an alternative recommended concept. In concept 4A, suspending the parachutes in the frustum with energy absorbers removes the disadvantages associated with mounting the parachutes on the dome.

48

APPENDIX B

MAIN PARACHUTE DAMAGE HISTORY AND CAUSE ASSESSMENT

One task of the main parachute damage reduction team (MPDRT) was to review the history of parachute damage. In performing this task, the team compiled a summary of significant damage to the main parachutes and reevaluated the damage sources (section B.1). In addition, the team compiled a large amount of SRB flight data and parachute loads data (section B.2). A correlation analysis was then performed to determine if certain flight conditions contribute to main parachute damage (sections B.3 and B.4). Data in this appendix include the first 29 shuttle flights, through STS-30R. With minimal exceptions, data were obtained from the following sources: Martin Marietta Corporation postflight parachute reports; MSFC STS flight evaluation reports; and data presentations and memos. These sources are listed in the bibliography (section B.5).

The team obtained the data necessary to thoroughly review significant main parachute damage and damage causes. However, many of the SRB flight data and parachute loads data required for correlation analyses do not exist, or, in a few cases, could not be readily obtained. The amount of missing data can be seen in examining the figures associated with section B.2.

This appendix represents the first time all of the above data have been compiled and assembled in one document. It would be beneficial to the space shuttle program to keep this data base current.

B.1 Main Parachute Damage

A numbering system exists for main parachute ribbons which can be used to locate parachute damage. The skirt band at the bottom of the canopy is defined as horizontal ribbon No. 1, and each successive horizontal ribbon is numbered consecutively. The vent band is horizontal ribbon No. 264 for the small (115-ft diameter) main parachutes, and No. 304 for the current large (136-ft diameter) main parachutes. After inflation problems occurred on the first few flights with the large mains, 13 horizontal ribbons were added above the vent band to form a vent cap to reduce the effective vent area. The uppermost of the 13 horizontal ribbons (No. 317) is called the vent cap band. The first flight with this vent modification was STS-51F in July 1985.

An orderly system is used to define main parachute gore numbers, as shown in figure B-1 for the large mains. The small mains only have 96 gores, compared to 160 for the large mains, but the basic gore numbering system for each is similar in that for the deployed parachute the highest numbered gore is the furthest outboard. The main parachute position numbering system for a flight set of six chutes is also shown in figure B-1, and is the same for small or large parachutes.

A much more detailed damage record has been kept for the large main parachutes than for the small main parachutes. The detail of the large main parachute damage reports permits the damage to be compared to a critical flaw size. Critical flaw size indicates the approximate number of consecutively broken ribbons in a single gore that will cause propagation of the damage along the gore. The critical flaw size changes in different areas of the parachute. For the large mains, in the lightly loaded lower region which includes the skirt band through horizontal ribbon No. 100, the critical flaw size is 30 ribbons. For the moderately loaded region, horizontal ribbons 101 through 190, the critical flaw size is 22 ribbons. The critical flaw size is 16 ribbons for the region of horizontal ribbons 191 through 235, and
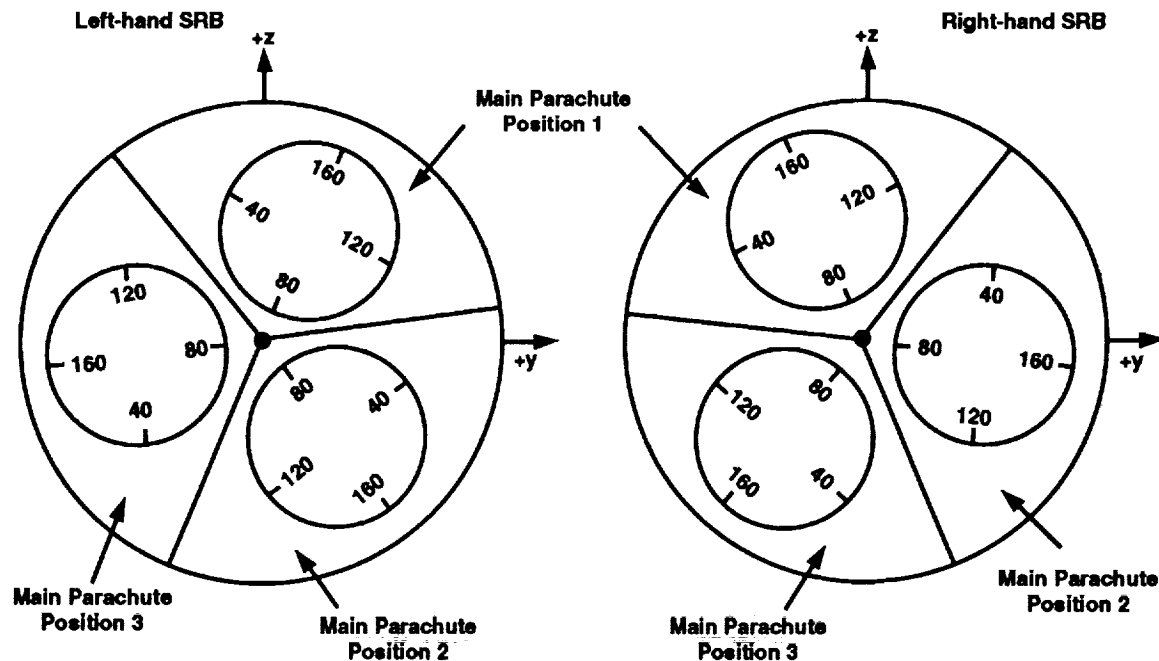
Note: (1) View looking up into SRB frustrums (shown greatly oversized).

(2) Gore numbers are indicated around circumference of deployed parachutes.

Figure B-1. Gore numbering system for large main parachutes.

12 ribbons for the highest loaded region, which includes horizontal ribbons 236 through the vent band (horizontal ribbon 304). These critical flaw size data apply only to the large mains without ripstops.

Critical flaw size is also a function of total parachute load. The above values are given for a nominally loaded parachute. If a given parachute has a higher than nominal total load, the critical flaw size is smaller for each region of the parachute. Conversely, if the total load is lower than nominal, the critical flaw size is larger. For the large mains, if the number of consecutively broken ribbons is defined as "near-critical flaw size" or greater, the damage is considered significant.

For the small mains, the damage was generally reported in terms of the total number of broken ribbons. The locations of the broken ribbons were not identified unless a "large" number of broken ribbons occurred in conjunction with vent band damage. If any small main parachute sustained this level of damage or greater, the damage is considered significant.

The following main parachute damage history is divided into two sections: one for the small main parachutes and one for the large main parachutes. Only significant damage that occurred during flight is included; no retrieval damage is described. A condensed tabulation of the 14 incidences of significant main parachute damage is presented in figure B-2. As a result of the team's reevaluation of damage sources, three of the original diagnoses have been changed: STS-1, STS-9, and STS-51B.

50

STS Mission	Damaged Chute	Gore With Most Damage	Number of Torn Ribbons in Gore	Cause of Damage
STS-1	LH #3	#45	43	Contact with MPSS
STS-3	RH #2	#3	250	Float entanglement
STS-9	LH #3	#57	251	Contact with MPSS
STS-11	LH #3	#39	257	Vent dynamics caused by MPSS contact
STS-13	RH #2	#47	241	Contact with MPSS
STS-13	LH #2	#18	262	Contact with MPSS
STS-51D	LH #3	#80	15	Chute-to-chute contact
STS-51B	LH #3	#59	240	Vent entanglement
STS-51G	LH #3	#87	132	Vent rebounding
STS-51F	RH #3	#103	317	Contact with MPSS (Note: Propagation of initial tear throughout entire gore was caused by reefing anomaly)
STS-61C	LH #3	#74	14	Unknown
STS-26R	RH #3	#121	18	Contact with MPSS
STS-29	RH #2	#155	23	Contact with MPSS
STS-30R	LH #2	#93	315	Vent entanglement

Figure B-2. Summary of significant main parachute damage.

B.1.1 Significant Small Main Parachute Damage History

STS-1   Damage to LH main parachute No. 3 consisted of a 43-ribbon tear at gore 45 up to, but not including, the vent band, which was damaged.

The tear was originally attributed to parachute contact with a nut cap in the lower part of the frustum, or possibly a flailing retrieval line. However, upon reevaluation, the team determined that this damage was caused by contact with the MPSS, most likely the isogrid.

STS-3   Damage to the RH main parachute No. 2 consisted of: a 250-ribbon tear in gore 3 (horizontal ribbons 14 through 263); a tear in gore No. 2 consisting of 34 ribbons just below the vent band; a break in the vent band at radial No. 3 between gores 2 and 3; broken vent line No. 51 (continuation of vent line 3).

Damage to the canopy is the result of entanglement of the float on main chute No. 2 with the float on main chute No. 1. Float entanglement resulted from float dynamic motions aggravated by the 30-degree tilt angle of the frustum during main chute deployment.

STS-9   Gore 57 on the LH main chute No. 3 was damaged. The vent band (horizontal 264) and all horizontal ribbons down through No. 14 were torn. On the adjacent gore, No. 58, the 77 horizontal ribbons nearest the vent band were also torn, although the vent band was not.

This damage was originally attributed to abrasion of the horizontal ribbons against the floats or deployment bag. However, the team determined that this damage was caused by contact with the MPSS, most likely the isogrid.

STS-11   On LH main parachute No. 3, gore 39 split from horizontal 8 through 264, the vent band. Friction burns were prevalent from horizontal 237 through the vent band and on vent lines.

This damage is attributed to vent dynamics during deployment that resulted in high-speed fabric-to-fabric contact between the vent and other upper portions of the same canopy, or between adjacent canopies. Vent dynamic behavior is considered to be caused by contact with the MPSS.

STS-13   On RH main chute No. 2, gore 47 was torn from ribbon 24 through 264.

On LH main chute No. 2, all horizontal ribbons in gore 18 except the skirt and vent bands were torn.

The damage on both these parachutes is attributed to the canopy being dragged across the isogrid or bipod struts during deployment.

B.1.2 Significant Large Main Parachute Damage History

STS-51D   Gore 80 on LH main chute No. 3 sustained 15 broken horizontal ribbons, from 207 through 220 and 222. This damage is considered a near-critical flaw size in this area of the canopy.

The damage is attributed to the vent area of LH chute No. 2 striking chute No. 3 during deployment.

STS-51B   Damage to LH chute No. 3 included horizontal ribbons torn from No. 65 through the vent band (No. 304) in gore 59, and horizontals 12 through 303 in gore 61. No horizontals were torn in gore 60.

Though the evidence was inconclusive, the damage was originally attributed to retrieval. However, upon reexamination by the team, the evidence supports an in-flight damage scenario. This evidence includes vent line burning and vent band stitch failures, suggesting vent entanglement like the STS-30R failure.

STS-51G   Damage to LH main chute No. 3 consisted of 132 torn horizontal ribbons, from No. 173 through the vent band in gore 87. There was also extensive burning and abrasion damage along a line intersecting gore 87 near horizontal ribbon 248.

This damage was self-inflicted and was attributed to vent rebounding. The evidence obtained from a photo aircraft indicates that the vent whipped over during deployment and contacted the outside of the canopy. This initial contact damage was centered at ribbon 248 in gore 87, and propagated along the gore.

STS-51F   The initial deployment damage to RH chute No. 3 was a tear in gore 103. The SRB onboard film indicates this tear consisted of about 10 to 15 consecutive horizontal ribbons located near ribbon 270. (Critical flaw size is 12 ribbons in this area of the canopy.) Subsequent damage to this chute resulted in it being nearly ripped apart. Gore 103 was completely split, and the split continued across the vent and down gore 33 almost to the skirt band. There was also a large amount of burn damage, more than any previous large main chute.

The cause of the initial tear and burn damage was contact with the MPSS that resulted from a large frustum tilt angle during deployment. All indications are that this initial tear would not have propagated under normal conditions. However, on this parachute, the first-stage and second-stage reefing lines were routed through one of the first stage cutters. The parachute attempted to inflate to full open at first stage disreef, causing the initial tear to propagate into a complete canopy failure. Because of the initial tear, the chute failed at a fairly low load of 153,000 lb.

STS-61C   In gore 74 of LH main chute No. 3, a near-critical flaw size of 14 consecutive broken ribbons occurred (233 through 246).

It is not clear what caused this damage. There is no witness paint, and only very little burn damage associated with this tear. It is in an area of high incidence of damage, adjacent to the MPSS, but there is no strong evidence that the parachute contacted the MPSS.

STS-26R   Damage consisted of a near-critical flaw size of 18 consecutive torn ribbons (131 through 148) in gore 121 of RH chute No. 3.

All indications, including pink witness paint, are that this was bipod strut damage.

STS-29   Damage to RH chute No. 2 consisted of 23 consecutive ribbons torn (121 through 143) in gore 155.

All indications, including pink witness paint, are that this was bipod strut damage.

STS-30R   Damage to LH main chute No. 2 consisted of a split in gore 93 from horizontal 3 through the vent cap band (No. 317). The adjacent gore, No. 94, was torn from horizontal ribbon 269 through the vent band (No. 304). The vent cap area was also heavily damaged.

The damage is attributed to vent entanglement caused by lack of support of the main parachute vent cap combined with a large frustum tilt angle of 25°. At deployment, the vent area had fallen inside the circle of the vent band. During the violent whipping action, entanglement of the vent lines ensued. The vent was drawn together between gores 1 and 30 and made smaller, causing the vent lines to be too long to react radial loads over the top of the parachute. With this vent band foreshortening, the large radial loads were reacted in hoop stress in the upper horizontal ribbons, causing parachute failure.

B.2 SRB and Parachute Data

This section presents tabular listings of the SRB flight data and parachute loads data compiled by the team to investigate correlations with main parachute damage. As mentioned previously, the data were obtained primarily from the reports, data presentations, and memos listed in the bibliography.

B.2.1 Data Measurement Methods

In the course of the shuttle program, several different data measurement methods have been used to determine the behavior of SRB's during reentry and the performance of the recovery system. These methods are discussed below.

B.2.1.1 Radar Tracking Ships

Two radar tracking ships, the *Vandenberg* and the *Redstone*, were used at various times early in the program. When properly equipped, each ship could provide tracking with both radar and high-quality motion picture cameras. A complete set of trajectory parameters, including angle of attack, could often be obtained for a significant portion of the SRB reentry and parachute phases. The *Vandenberg*, which was used only on the first five flights, normally had the equipment to track both of the SRB's with radars and cameras. The *Redstone* was not as well equipped. On either ship, the radars and cameras would occasionally lose target or would track the wrong SRB, but the tracking data were very useful in evaluating SRB reentry and recovery. Each ship also had an "Omegasond" system that could be carried aloft by balloon to obtain atmospheric measurements.

B.2.1.2 Development Flight Instrumentation

Development flight instrumentation (DFI) has been used on board the SRB's several times to provide data for ascent, reentry, and recovery. The DFI package is tailored for each flight to meet specific requirements. Typical recovery-related data measured by DFI include event times, parachute loads, SRB accelerations, and baroswitch plenum chamber pressure.

B.2.1.3 Photo Aircraft and SRB Onboard Cameras

One or two photo aircraft were available for the SRB's on almost every daytime shuttle launch through 1990. The aircraft were a WC-130, which carried a Starcast system, and a P-3, which carried a Cast Glance system. Each system had several motion picture cameras, and the aircraft were positioned to photograph the parachutes. Data from these camera systems were of great importance to the program; however, cloud cover sometimes limited photographic coverage.

SRB onboard motion picture cameras were first used on the second flight with large main chutes, and have been used often since. Because the cameras are located on the forward dome of the SRB forward skirt, only the main chutes can be photographed. Much valuable data have been derived from these cameras, and the data were especially useful in diagnosing the STS-30R failure.

B.2.1.4 Land-Based Radars

Beginning with STS-5, land-based radar has been used on each flight to track the SRB's during reentry. Normally, two radar sites are used, one for each SRB. Land-based radars cannot provide any information about the parachutes because the SRB's have descended below the horizon before the start of the parachute sequence. However, land-based radars typically provide good tracking of the SRB's for approximately 3 minutes after separation. The apogee altitude can be derived from the tracking data, and often the magnitude of the maximum dynamic pressure (Qmax) during reentry can be approximated.

B.2.1.5 Trajectory Reconstruction

Trajectory reconstruction can sometimes be used to determine a desired parameter for which no direct measurement was made during flight. The technique is valid even if available flight data are limited to such items as event times, photographic coverage, and observations from personnel on the retrieval ships. The inputs to the parachute dynamics computer simulation are incremented until the simulation results match the flight data. The simulated value of the desired parameter can then be used as an estimate for that parameter.

B.2.2 Availability of Data Measurement Methods

Figure B-3 presents a summary of the data measurement methods available for each shuttle flight. Flights are identified by a sequential flight number, STS mission designation, and launch date. For each flight, the presence of a tracking ship (either the *Vandenberg* or *Redstone*), the Cast Glance and Starcast photo aircraft, and SRB onboard cameras is indicated, as well as whether meteorological data at the impact were measured. In addition to the shuttle flight identification, each SRB in a flight set is identified. For each SRB, the presence of DFI, and drogue and main chute load cells in particular, is indicated. Next, tracking ship and photographic coverage for each SRB are indicated, and general comments on the quality and usability of the film are provided. No indication is given for land-based radars because they are now used on all flights.

B.2.3 SRB Trajectory Parameters

SRB trajectory parameters are presented in figure B-4. For each SRB, the parameters listed are: SRB separation time and altitude; apogee time and altitude; Qmax during reentry and the time and altitude at which it occurred; water impact time; and water impact vertical and horizontal velocities. Time is given in seconds relative to lift-off. Velocity is given in feet per second (ft/s), altitude in feet (ft), and dynamic pressure in pounds per square foot (lb/ft^2). Values for horizontal water impact velocity are often based on the wind speed.

Only one apogee altitude value is listed for each flight. Based on experience, the assumption is made that both SRB's on each flight have identical apogees. Only one reentry Qmax value is listed for each flight, even though small differences between Qmax values for the LH and RH SRB's have been observed. For this study, it was considered adequate to use one Qmax value for both SRB's on each flight. As a general rule, Qmax occurs at an altitude of between 40,000 and 50,000 ft.

Flight Number	STS	Launch Date	Tracking Ship	Cast Glance	Star-cast	SRB On-board	Met. Data	SRB	DFI	Drogue Loads	Main Loads	Tracking Ship Radar	Tracking Ship Film	Cast Glance	Star-cast	SRB On-board	Comments
1	1	04/12/81	Vand.	N	Y	N	Y	A07 (L)	Y	Y	Y	N	Y		Y		Good Starcast coverage
								A08 (R)	Y	Y	Y	Y	Y		N		
2	2	11/12/81	Vand.	N	Y	N	Y	A09 (L)	Y	Y	Y	Y	Y		Y		Frustum sep. from Starcast
								A10 (R)	Y	Y	Y	Y	Y		Y		
3	3	03/22/82	Vand.	N	N	N	Y	A11 (L)	Y	Y	Y	N	N				Frustum sep., main deploy
								A12 (R)	Y	Y	Y	Y	Y				
4	4	06/27/82	Vand.	N	N	N	Y	A13 (L)	Y	Y	Y	Y	Y				Lost in clouds
								A14 (R)	Y	Y	Y	Y	Y				
5	5	11/11/82	Vand.	Y	Y	N	Y	A15 (L)	Y	Y	Y	Y	Y	Y	?		Main deploy from ship
								A16 (R)	Y	Y	Y	N	N	Y	?		
6	6	04/04/83	Reds.	Y	Y	N	Y	A17 (L)	Y	Y	Y	Y	Y	Y	Y		Good coverage
								A18 (R)	Y	Y	Y	N	N	Y	N		
7	7	06/18/83	N	Y	Y	N	N	BI007L	Some	N	N			Y	Y		Good coverage
								BI007R	Some	N	N				Y		
8	8	08/30/83	Reds.	Y	N	N	Y	BI008L	Some	Y	Y	Y					Night launch
								BI008R	Some	Y	Y	N					
9	9	11/28/83	N	Y	Y	N	N	BI009L	Some	Y	Y			Y			Frustum sep. in clouds
								BI011R	N	N	N			Y	Y		
10	11	02/03/84	Reds.	Y	Y	N	Y	BI010L	Some	N	N	Y	N	Y	Y		Good Cast Glance coverage
								BI010R	Some	N	N	N	Y	Y	?		
11	13	04/06/84	N	Y	Y	N	N	BI012L	N	N	N				Y		Drogue deploy: RH, Frustum sep.: LH, RH
								BI012R	N	N	N			Y	Y		
12	41D	08/30/84	Reds.	Y	N	N	Y	BI011L	N	N	N	N	N	N			Events obscured by clouds
								BI009R	Some	Y	Y	Y	Y	Y			
13	41G	10/05/84	N	Y	N	N	N	BI013L	N	N	N			Y			Good coverage of RH
								BI013R	N	N	N			Y			
14	51A	11/08/84	N	Y	N	Y	N	BI014L	Some	N	Y			Y		Y	Frustum sep. obscured by clouds
								BI014R	Some	N	Y			Y		Y	
15	51C	01/24/85	N	Y	N	N	N	BI015L	N	N	N			Y			Good coverage
								BI015R	N	N	N			Y			

Figure B-3. Summary of SRB and parachute data measurement methods.

Flight Number	STS	Launch Date	Tracking Ship	Cast Glance	Star-cast	SRB On-board	Met Data	SRB	DFI	Drogue Loads	Main Loads	Tracking Ship Radar	Tracking Ship Film	Cast Glance	Star-cast	SRB On-board	Comments
16	51D	04/12/85	N	Y	N	N	N	BI018L	N	N	N			Y			Film quality poor; video O.K.
								BI018R	N	N	N						
17	51B	04/29/85	N	Y	N	N	N	BI016L	N	N	N			Y			Events obscured by clouds
								BI016R	N	N	N			Y			
18	51G	06/17/85	N	Y	N	N	N	BI019L	N	N	N			Y			Events obscured by clouds
								BI019R	N	N	N			Y			
19	51F	07/29/85	Reds.	Y	N	Y	Y	BI017L	Some	N	Y		Y	Y		Y	Video for RH
								BI017R	Some	N	Y		N	Y		Y	
20	51I	08/27/85	N	Y	N	Y	N	BI020L	N	N	N			Y		Y	Frustum sep.: LH; poor conditions
								BI020R	N	N	N			Y		Y	
21	51J	10/03/85	N	Y	N	Y	N	BI021L	N	N	N			Y		Y	
								BI021R	N	N	N			Y		Y	
22	61A	10/30/85	N	Y	N	Y	N	BI022L	N	N	N			Y		Y	
								BI022R	N	N	N			Y		Y	
23	61B	11/26/85	N	N	N	Y	N	BI023L	N	N	N						Night launch
								BI023R	N	N	N						
24	61C	01/12/86	N	Y	N	N	N	BI024L	N	N	N			Y		Y	Coverage through frustum sep.
								BI024R	N	N	N			Y		Y	
25	51L	01/28/86	N	Y	N	N	N	BI026L	N	N	N						
								BI026R	N	N	N						
26	26R	09/29/88	N	Y	Y	Y	N	BI029L	Y	Y	Y			?	?	Y	
								BI029R	Y	Y	Y			?	?	Y	
27	27R	12/02/88	N	Y	Y	Y	N	BI030L	Y	Y	Y			Y	?	Y	
								BI030R	Y	Y	Y			Y	Y	Y	
28	29	03/13/89	N	Y	Y	Y	N	BI031L	Y	N	N			Y	?	Y	Coverage of LH
								BI031R	Y	N	N			?	?	Y	
29	30R	05/04/89	N	Y	N	Y	N	BI027L	N	N	N			Y		Y	
								BI027R	N	N	N			N		Y	

Figure B-3. Summary of SRB and parachute data measurement methods (continued).

57

Flight Number	STS	SRB	SRB Sep. Time (s)	SRB Sep. Alt. (ft)	Apogee Time (s)	Apogee Alt. (ft)	Qmax Time (s)	Qmax Alt. (ft)	Qmax (lb/ft²)	Impact Time (s)	Impact Vert. Vel. (ft/s)	Impact Horiz. Vel. (ft/s)
1	1	A07 (L)	131.8	173,300	215.0	275,000	341	45,000	2,050	424.92	92.70	
		A08 (R)								428.01	91.60	
2	2	A09 (L)	130.0	167,902	207.0	257,000	331	45,000	2,150	411.52		31.20
		A10 (R)								414.27		31.50
3	3	A11 (L)	127.9	160,025	204.0	247,000	325	45,000	1,700	404.26	88.60	28.80
		A12 (R)								401.25	109.00	34.00
4	4	A13 (L)	130.0	154,886	199.0	226,000	314		1,500	386.30	637.00	
		A14 (R)								379.00	612.00	
5	5	A15 (L)	129.2	154,734	197.0	225,000	312		1,500	404.27	89.20	30.10
		A16 (R)								401.60	89.00	
6	6	A17 (L)	129.5	151,129	195.0	220,000	312		1,400	400.89	88.20	15.30
		A18 (R)								395.64	89.00	
7	7	BI007L	126.3	151,559	194.0	220,000			1,400	410.55	89.20	4.70
		BI007R								408.20	89.10	4.80
8	8	BI008L	124.4	152,257	190.0	219,000	306		1,500	391.50		19.90
		BI008R								395.47		
9	9	BI009L	126.4	162,989	198.0	242,000	320		2,100	388.94	89.30	25.60
		BI011R									89.00	
10	11	BI010L	128.0	150,595	192.0	210,000	305		1,615	384.75	109.20	35.00
		BI010R								385.91	101.30	36.00
11	13	BI012L	125.7	171,947	206.0	268,000			2,600	407.00	89.00	
		BI012R								405.60	109.00	
12	41D	BI011L	124.6	162,728	201.0	253,000	324		1,800	413.27	89.00	12.80
		BI009R									77.60	
13	41G	BI013L	124.2	157,076	195.0	234,000	313		1,700	396.70	89.00	
		BI013R								405.70	89.00	
14	51A	BI014L	125.8		196.0	231,000	313		1,700	410.52	75.00	34.00
		BI014R								398.28	75.00	34.00
15	51C	BI015L	127.8		198.0	231,000	315		1,800	395.00	89.00	
		BI015R								406.90	89.00	

Figure B-4. SRB trajectory parameters.

58

Flight Number	STS	SRB	SRB Sep. Time (s)	SRB Sep. Alt. (ft)	Apogee Time (s)	Apogee Alt. (ft)	Qmax Time (s)	Qmax Alt. (ft)	Qmax (lb/ft²)	Impact Time (s)	Impact Vert. Vel. (ft/s)	Impact Horiz. Vel. (ft/s)
16	51D	BI018L BI018R	126.9		195.0	224,000	311		1,600	405.00 404.50	75.00 75.00	
17	51B	BI016L BI016R	127.4		196.0	234,000	315		1,600		88.00 88.00	
18	51G	BI019L BI019R	124.7		205.0	258,000	327		1,750	401.92 419.08	91.00 75.00	
19	51F	BI017L BI017R	125.1		193.0	228,000	309		1,400	406.03 399.42	74.00 93.80	10.50
20	51I	BI020L BI020R	121.1		193.0	234,000	310		1,500	411.00 413.40	75.00	
21	51J	BI021L BI021R	124.6		194.0	233,700	313		1,500	417.00 417.00		
22	61A	BI022L BI022R	124.9		198.0	241,800	318		1,750	416.60 411.56		
23	61B	BI023L BI023R	123.6		189.0	211,300	300		1,300			
24	61C	BI024L BI024R	128.4		194.0	218,000			1,500	395.00 410.00	75.00 75.00	34.00 34.00
25	51L	BI026L BI026R										
26	26R	BI029L BI029R	124.9	153,500	196.5	232,200	315	43,000	1,800	414.97 412.46	75.00 75.00	20.00 20.00
27	27R	BI030L BI030R	126.3	154,500	194.5	226,500	310	44,000	1,700	396.46 400.45	75.00 75.00	34.00 34.00
28	29	BI031L BI031R	126.0	151,500	196.0	226,000	313	44,000	1,500	406.41 407.92	75.00 75.00	25.00 25.00
29	30R	BI027L BI027R	125.1	155,650	195.0	230,600	315	41,000	1,700	386.45 406.89	91.00 74.00	14.00 14.00

Figure B-4. SRB trajectory parameters (continued).

B.2.4 Nose Cap Separation Data

Figure B-5 displays the following data for each SRB: time (relative to lift-off) and altitude (ft) at which nose cap separation occurs; SRB angle of attack, alpha (in degrees); SRB roll angle (though this parameter was not available); SRB velocity (ft/s) and dynamic pressure (lb/ft^2); and drogue parachute stripping velocity (ft/s).

B.2.5 Frustum Separation Data

Figure B-6 shows the frustum separation conditions. These parameters are defined like those presented in figure B-5 for nose cap separation. Additional information consists of drogue hang time and frustum tilt angle (degrees). Drogue hang time is the elapsed time in seconds between nose cap separation and frustum separation. Frustum tilt angle is the angle between the frustum centerline and parachute canopy centerlines at line stretch. High frustum tilt angles cause parachute contact with the isogrid. Measurement of the tilt angle requires photo aircraft film coverage such that the plane of the tilt angle is nearly parallel to the plane of the camera lens. The few values presented in figure B-6 are approximate.

It should be noted that the unreasonably low (16.00 seconds) drogue hang time originally published for the LH SRB on STS-13 has been corrected by obtaining a better estimate of the nose cap separation time.

B.2.6 SRB Weight and CG Data

The weight and longitudinal CG location at SRB separation are shown in figure B-7. The weight is given in pounds (lb), and the CG location is specified by SRB station number (inches).

B.2.7 Drogue and Main Parachute Loads Data

Figure B-8 shows parachute peak load values (in thousands of pounds) for only those flights with load cells. The predicted nominal and dispersed parachute peak loads are given for comparison to the measured loads for each SRB. The main parachute position numbers (1, 2, and 3) are identified. Drogue and main chute loads are listed for each deployment stage such that the first, second, and third peak loads correspond to initial inflation, first disreef, and second disreef, respectively. STS-27R was the last flight with parachute load cells.

B.3 Main Parachute Damage Correlation With Flight Data

The team investigated data correlations to determine if main parachute deployment damage is related to certain flight parameters. Although this appendix includes the first 29 shuttle flights, the SRB's on two of those flights, STS-4 and STS-51L, were not recovered by parachute. The sample size for this correlation study is therefore 27 flights (54 SRB's). Of these 54 SRB's, 25 had small mains and 29 had large mains. The odd numbers are caused by the fact that STS-41D had large mains on only the RH SRB. Significant deployment damage occurred on 6 of the 25 SRB's recovered with small mains, and on 8 of the 29 SRB's recovered with large mains.

Because some of the flight data are not available, as mentioned earlier, many interesting suspected correlations could not be investigated. For instance, flight history shows that there has never been significant damage to main parachute No. 1 on either the LH or RH SRB. This would seem to indicate a correlation with SRB angular orientation, but no analysis can be done because of a scarcity of data.

Figure B-9 shows the correlation between SRB weight at separation and main chute damage. Weight data are available for all of the 54 SRB's in this study. The darkened symbols represent those SRB's with significantly damaged main chutes. Although the damage is fairly evenly scattered throughout the upper four-fifths of the weight range, no significant damage occurred on any of the 10 SRB's weighing less than 179,500 lb, implying a weak correlation.

Figures B-10 and B-11 present the correlation between SRB longitudinal CG location at separation and main chute damage. CG data are available for all of the 54 SRB's. The ranked values of SRB CG station in figure B-11 are given in descending order (high station numbers represent aft CG locations). It can be seen in figure B-11 that the parachute damage probability increases for an aft CG location. Of the 14 SRB's on which significant damage occurred, 9 had CG's in the top half of the ranking, and 6 had CG's in the top quarter of the ranking. This trend is considered a moderate correlation.

The correlation between apogee altitude and main chute damage is shown in figures B-12 and B-13. The two SRB's on each flight are assumed to have identical apogees for this study, and apogee data exist for all 27 flights. Although the occurrence of main parachute damage is distributed throughout the range of apogees in figure B-13, the top quarter of the ranking has a higher probability of damage than any of the other quarters. In fact, damage occurred on the three flights with the highest apogees. Overall, main parachute damage is considered to have a weak correlation with apogee altitude.

Figure B-14 shows the correlation between reentry Qmax and main chute damage. Data exist for all 27 flights. For this study, the two SRB's on each flight are assumed to have identical Qmax values. There is a definite increase in damage probability between the four flights with the lowest Qmax values and the four flights with the highest values, implying a weak correlation.

Figure B-15 shows the correlation between drogue hang time and main chute damage. Hang time data exist for 44 of the 54 SRB's, and indicates a weak correlation with parachute damage. No significant damage occurred on any of the eight SRB's with hang times greater than 24 s, while the two SRB's with the shortest hang times incurred damage. It appears that longer hang times allow SRB oscillations to damp out as much as possible before the main chutes are deployed, thereby reducing the potential for main chute damage.

The correlation between frustum tilt angle and main chute damage is shown in figure B-16. Tilt angle data are available for only 13 SRB's. The data show that large tilt angles, as expected, cause a drastic increase in damage probability. However, because of the small sample size, no evaluation was made of the correlation.

The team investigated several multiple parameter damage correlations, the most interesting of which is presented in figure B-17. This figure shows the combined effect of dynamic pressure at nose cap separation and longitudinal CG location. These data are available for only 14 SRB's, 12 of which had small mains. The figure shows that the probability of main chute deployment damage increases when a rear CG location is combined with high dynamic pressure at nose cap separation. Because of the small sample size, however, no definite conclusions could be drawn.

Flight Number	STS	SRB	Nose Cap Sep. Time (s)	Alt at Nose Cap Sep. (ft)	Alpha at Nose Cap Sep. (deg.)	Roll at Nose Cap Sep. (deg.)	Vel at Nose Cap Sep. (ft/s)	Dynamic Pressure at Nose Cap Sep. (lb/ft²)	Drogue Stripping Vel (ft/s)
1	1	A07 (L)	369.00	15,880	112		495	177	196
		A08 (R)	371.34						
2	2	A09 (L)	352.70	16,341	145		565	222	235
		A10 (R)	356.15	15,772	113		480	163	188
3	3	A11 (L)	347.21	16,190	145		590	245	239
		A12 (R)	353.13	15,950	131		521	189	206
4	4	A13 (L)	347.79	16,489	133		498	175	196
		A14 (R)	345.98	14,741	113		556	215	211
5	5	A15 (L)	344.34	15,880	120		547	211	212
		A16 (R)	341.17						218
6	6	A17 (L)	342.23	16,062	131		527	197	205
		A18 (R)	336.77		150				236
7	7	BI007L	348.28	16,311	100		482	158	
		BI007R	348.44	15,702	106		542	206	
8	8	BI008L	334.23	15,464	105		560	222	213
		BI008R	338.55						
9	9	BI009L	340.71					225	
		BI011R							
10	11	BI010L	333.02	15,638	112		568	241	213
		BI010R	332.68						
11	13	BI012L	352.00						
		BI012R	357.80						
12	41D	BI011L	351.12	16,350			581	232	196
		BI009R							
13	41G	BI013L	336.70						
		BI013R	348.20						
14	51A	BI014L	347.64						
		BI014R	338.21						
15	51C	BI015L	339.10						
		BI015R	342.40						

Figure B-5. SRB nose cap separation data.

Flight Number	STS	SRB	Nose Cap Sep. Time (s)	Alt. at Nose Cap Sep. (ft)	Alpha at Nose Cap Sep. (deg.)	Roll at Nose Cap Sep. (deg.)	Vel. at Nose Cap Sep. (ft/s)	Dynamic Pressure at Nose Cap Sep. (lb/ft²)	Drogue Stripping Vel. (ft/s)
16	51D	BI018L BI018R	341.30						
17	51B	BI016L BI016R							
18	51G	BI019L BI019R	348.50 353.00						
19	51F	BI017L BI017R	337.18 338.36	16,590			599	253	
20	51I	BI020L BI020R							
21	51J	BI021L BI021R	346.50 346.40						
22	61A	BI022L BI022R	351.07 347.70						
23	61B	BI023L BI023R							
24	61C	BI024L BI024R	334.00 341.69						
25	51L	BI026L BI026R							
26	26R	BI029L BI029R	345.02 343.73						
27	27R	BI030L BI030R	337.57 339.27						
28	29	BI031L BI031R	343.42 343.18						
29	30R	BI027L BI027R	337.46						

Figure B-5. SRB nose cap separation data (continued).

Flight Number	STS	SRB	Frustum Sep. Time (s)	Alt at Frustum Sep. (ft)	Alpha at Frustum Sep. (deg.)	Roll at Frustum Sep. (deg.)	Vel at Frustum Sep. (ft/s)	Dynamic Pressure at Frustum Sep. (lb/ft²)	Drogue Hang Time (s)	Frustum Tilt Angle (deg.)	Main Stripping Vel. (ft/s)
1	1	A07 (L)	391.49	6,529	171		359	122	22.49	23.0	244
		A08 (R)	393.79						22.45		
2	2	A09 (L)	377.51	6,158			354	121	24.81	17.5	248
		A10 (R)	379.26	6,295			357	122	23.11		249
3	3	A11 (L)	369.25	6,544			360	123	22.04	31.0	252
		A12 (R)	375.75	6,458			359	109	22.62		251
4	4	A13 (L)	372.60	6,700			343	111	24.81		241
		A14 (R)	365.80	6,400			362	125	19.82		249
5	5	A15 (L)	366.45	6,520			352	120	22.11		246
		A16 (R)	362.88						21.71		
6	6	A17 (L)	363.68	6,647			361	124	21.45	12.0	243
		A18 (R)	357.93						21.16	3.0	
7	7	BI007L	373.93	6,447				117	25.65	8.0	
		BI007R	369.59	6,683				122	21.15	13.0	
8	8	BI008L	356.28	6,360				119	22.05		235
		BI008R	360.21						21.66		
9	9	BI009L	364.06	5,884			392	148	23.35		249
		BI011R									
10	11	BI010L	354.97	6,420			346	116	21.95	17.0	230
		BI010R	355.59						22.91	20.5	233
11	13	BI012L	374.40						22.40	11.8	
		BI012R	381.50						23.70	14.0	
12	41D	BI011L	374.27	6,685			352	117	23.15		243
		BI009R									
13	41G	BI013L	361.30						24.60		
		BI013R	373.00						24.80		
14	51A	BI014L	371.16						23.52		229
		BI014R	359.62						21.41		238
15	51C	BI015L	359.30						20.20		
		BI015R	366.90						24.50		

Figure B-6. SRB frustum separation data.

Flight Number	STS	SRB	Frustum Sep. Time (s)	Alt at Frustum Sep. (ft)	Alpha at Frustum Sep. (deg.)	Roll at Frustum Sep. (deg.)	Vel at Frustum Sep. (ft/s)	Dynamic Pressure at Frustum Sep. (lb/ft²)	Drogue Hang Time (s)	Frustum Tilt Angle (deg.)	Main Stripping Vel. (ft/s)
16	51D	BI018L BI018R	363.40								
17	51B	BI016L BI016R	368.00						22.10		235
18	51G	BI019L BI019R	367.90 376.80						19.40 23.80		
19	51F	BI017L BI017R	358.49 359.61	6,840			360	121	21.31 21.25	22.0	
20	51I	BI020L BI020R	358.90								
21	51J	BI021L BI021R	369.00 367.60						22.50 21.20		
22	61A	BI022L BI022R	374.13 372.99						23.06 25.29		
23	61B	BI023L BI023R									
24	61C	BI024L BI024R	354.30 366.60						20.30 24.91		
25	51L	BI026L BI026R									
26	26R	BI029L BI029R	370.14 366.42						25.12 22.69		
27	27R	BI030L BI030R	359.28 360.29						21.71 21.02		
28	29	BI031L BI031R	364.22 363.64						20.80 20.46		
29	30R	BI027L BI027R	356.73						19.27	25.0	

Figure B-6. SRB frustum separation data (continued).

Flight Number	STS	SRB	Weight at SRB Sep. (lb)	CG Station at SRB Sep. (inches)
1	1	A07 (L) A08 (R)	182,022.0 182,738.0	1,257.61 1,254.85
2	2	A09 (L) A10 (R)	181,590.0 181,814.0	1,258.97 1,256.77
3	3	A11 (L) A12 (R)	182,537.0 182,225.0	1,258.21 1,257.06
4	4	A13 (L) A14 (R)	182,937.0 182,651.0	1,259.15 1,261.35
5	5	A15 (L) A16 (R)	183,299.0 182,906.0	1,260.86 1,261.04
6	6	A17 (L) A18 (R)	179,315.0 179,621.0	1,258.43 1,259.34
7	7	BI007L BI007R	178,177.0 177,803.0	1,262.46 1,261.59
8	8	BI008L BI008R	179,183.0 179,050.0	1,265.82 1,264.56
9	9	BI009L BI011R	182,763.0 182,365.0	1,266.20 1,269.40
10	11	BI010L BI010R	180,675.0 180,729.0	1,267.96 1,267.52
11	13	BI012L BI012R	179,723.0 179,660.0	1,272.17 1,270.83
12	41D	BI011L BI009R	178,833.0 180,776.0	1,267.05 1,257.73
13	41G	BI013L BI013R	178,688.0 179,182.0	1,266.29 1,267.98
14	51A	BI014L BI014R	181,984.0 181,506.0	1,258.58 1,259.64
15	51C	BI015L BI015R	179,014.0 178,574.0	1,268.22 1,269.73

Figure B-7. SRB weight and longitudinal CG location at SRB separation.

Flight Number	STS	SRB	Weight at SRB Sep. (lb)	CG Station at SRB Sep. (inches)
16	51D	BI018L BI018R	179,709.0 179,720.0	1,259.67 1,260.31
17	51B	BI016L BI016R	179,890.0 179,978.0	1,260.28 1,260.32
18	51G	BI019L BI019R	181,448.0 181,623.0	1,264.33 1,263.86
19	51F	BI017L BI017R	182,532.0 182,488.0	1,262.26 1,261.68
20	51I	BI020L BI020R	180,197.0 180,183.0	1,260.98 1,260.77
21	51J	BI021L BI021R	180,647.0 180,761.0	1,261.25 1,261.33
22	61A	BI022L BI022R	180,712.0 180,698.0	1,261.55 1,260.51
23	61B	BI023L BI023R	180,172.0 180,574.0	1,260.86 1,261.08
24	61C	BI024L BI024R	180,300.0 180,243.0	1,260.59 1,260.70
25	51L	BI026L BI026R		
26	26R	BI029L BI029R	188,343.0 188,407.0	1,264.83 1,264.46
27	27R	BI030L BI030R	188,905.0 188,597.0	1,264.55 1,264.31
28	29	BI031L BI031R	189,207.0 189,171.0	1,263.75 1,266.04
29	30R	BI027L BI027R	187,240.0 188,168.0	1,267.28 1,268.74

Figure B-7. SRB weight and longitudinal CG location at SRB separation (continued).

STS	Peak	Drogue Parachute Peak Loads Predicted Min	Nom	Max	Measured Left	Right	Main Parachute Peak Loads Predicted Min	Nom	Max	Measured Left 1	2	3	Right 1	2	3
1	1	140.1	175.9	259.2	188	145	91.4	114.1	135.3	107	113	81	88	68	106
	2	203.3	237.3	276.3	251	219	101.9	141.5	179.9	118	158	140	154	137	155
	3	210.4	240.7	280.3	275	256	78.6	124.0	160.5	122	118	116	142	125	104
2	1	124.5	155.0	209.9	222.1	141.8	71.8	94.5	116.5	92	95	98	98	105	105
	2	206.8	239.8	277.3	260.9	234.8	107.8	147.5	197.7	144	150	125	134	118	165
	3	245.9	280.6	319.1	301.7	259.9	98.8	144.2	184.0	116	138	104	123	122	124
3	1	117.1	160.2	294.2	274.4	160.2	75.4	98.1	120.1	102.2	98.3	85.3	90.4	110.7	109.8
	2	190.9	234.4	303.3	281.2	245.2	106.7	146.4	196.6	104.2	159.4	143.7	181.4	*	233.2
	3	231.2	272.2	328.1	306.7	292.5	96.5	141.9	181.7	97.6	135.5	115.1	180.2	*	193.3
5	1	109.0	156.1	273.6	181.4	145.0	75.7	98.5	113.9	124.8	104.3	102.1	100.0	113.4	121.8
	2	198.2	235.4	187.1	255.6	238.8	97.8	137.5	184.8	139.2	137.7	136.3	149.8	123.7	124.3
	3	235.0	272.6	322.8	288.6	277.1	96.1	141.5	179.9	122.1	123.1	115.9	113.7	112.8	132.0
6	1	116.9	155.1	272.6	190.6	242.7	92.7	115.4	130.8	110.4	103.0	109.9	87.7	96.1	133.0
	2	196.2	231.7	283.4	252.5	282.1	86.8	126.5	173.8	132.7	137.6	129.8	129.8	125.6	158.4
	3	229.7	267.2	317.4	298.9	313.5	91.8	137.2	175.6	124.3	103.9	111.2	117.7	99.2	122.6
8	1	112.9	168.7	284.5	147.6	129.8	83.7	111.0	135.6	116.5	96.4	121.5	120.1	92.1	119.1
	2	199.6	246.4	315.2	246.7	238.0	92.9	132.9	180.2	144.0	146.3	130.7	148.1	147.1	145.2
	3	231.2	273.3	326.1	269.9	304.5	93.2	138.6	177.0	119.4	124.5	122.7	124.6	119.0	124.8
9	1	108.6	180.4	287.5	191.2	-	98.2	125.5	150.7	140.9	123.8	90.8	-	-	-
	2	183.2	250.2	319.0	265.4		95.9	135.9	183.2	170.3	136.9	101.9			
	3	(Occurred after frustum sep.)					77.3	122.7	161.1	139.0	114.8	110.1			
41D	1	106.4	171.7	264.8	-	153.8	86.6	126.2	158.4	-	-	-	73.5	76.0	129.1
	2	192.8	244.4	290.5		233.6	97.9	119.0	178.5				105.2	105.3	236.4
	3	226.2	269.0	315.5		254.7	78.1	125.9	171.3				123.5	135.5	93.4
51A	1	107.2	172.5	265.6	-	-	49.9	126.8	185.1	82.3	123.9	103.6	109.5	77.8	124.1
	2	194.6	246.2	292.3			93.8	154.0	305.5	80.1	197.3	129.9	167.9	**	189.5
	3	228.8	271.6	318.1			72.0	141.2	203.5	105.4	109.0	125.5	173.4	61.2	190.8
51F	1	107.2	172.5	265.6	-	-	97.6	139.7	169.1	120.5	123.7	121.9	110.6	131.8	101.3
	2	194.6	246.2	292.3			114.2	168.7	207.5	106.9	116.1	147.2	89.0	135.6	152.6
	3	228.8	271.6	318.1			118.9	159.8	204.8	113.1	119.1	127.6	152.4	168.0	*
26R	1	140.7	168.0	230.7	145.4	178.4	91.3	123.3	168.6	114.6	130.8	138.9	142.7	154.5	105.8
	2	228.9	265.1	308.3	217.0	253.4	79.6	115.4	166.8	118.1	115.5	124.6	136.1	133.1	116.4
	3	236.5	273.3	314.5	262.4	302.6	83.2	125.4	194.1	83.3	137.4	101.9	135.0	106.7	103.4
27R	1	140.7	168.0	230.7	182.5	180.0	91.3	123.3	168.6	101.2	98.5	105.4	103.5	122.0	130.3
	2	228.9	265.1	308.3	244.4	230.8	79.6	115.4	166.8	178.8	58.1	119.5	101.0	114.6	138.1
	3	236.5	273.3	314.5	276.3	250.4	83.2	125.4	194.1	106.4	128.9	123.2	72.4	131.0	115.8

- = Not Measured; * = Failed After Previous Peak; ** = No Definite Peak

Figure B-8. Predicted and measured peak loads for drogue and main parachutes (all loads in thousands of pounds).
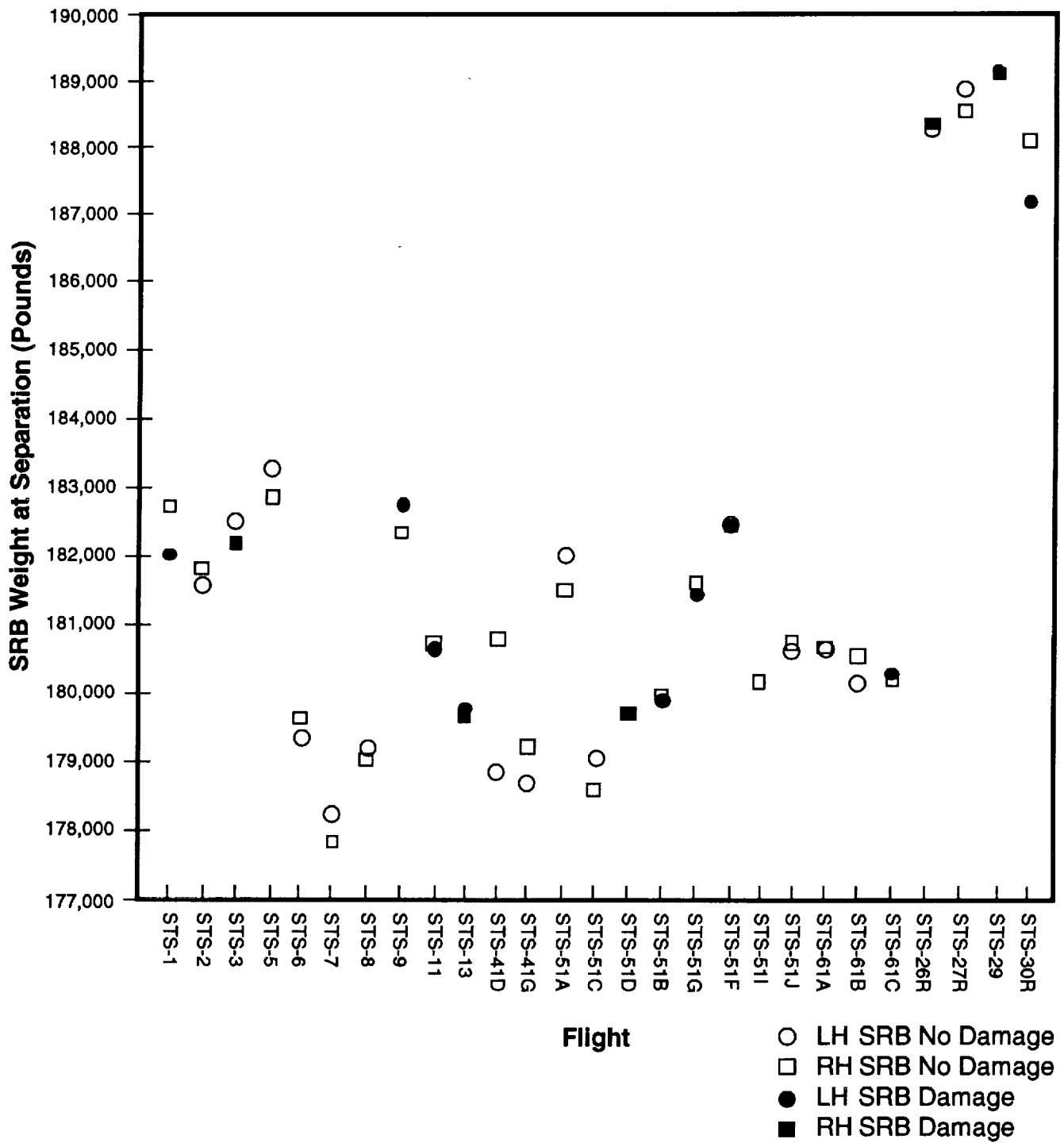
Figure B-9. Correlation between SRB weight at separation and main parachute damage.
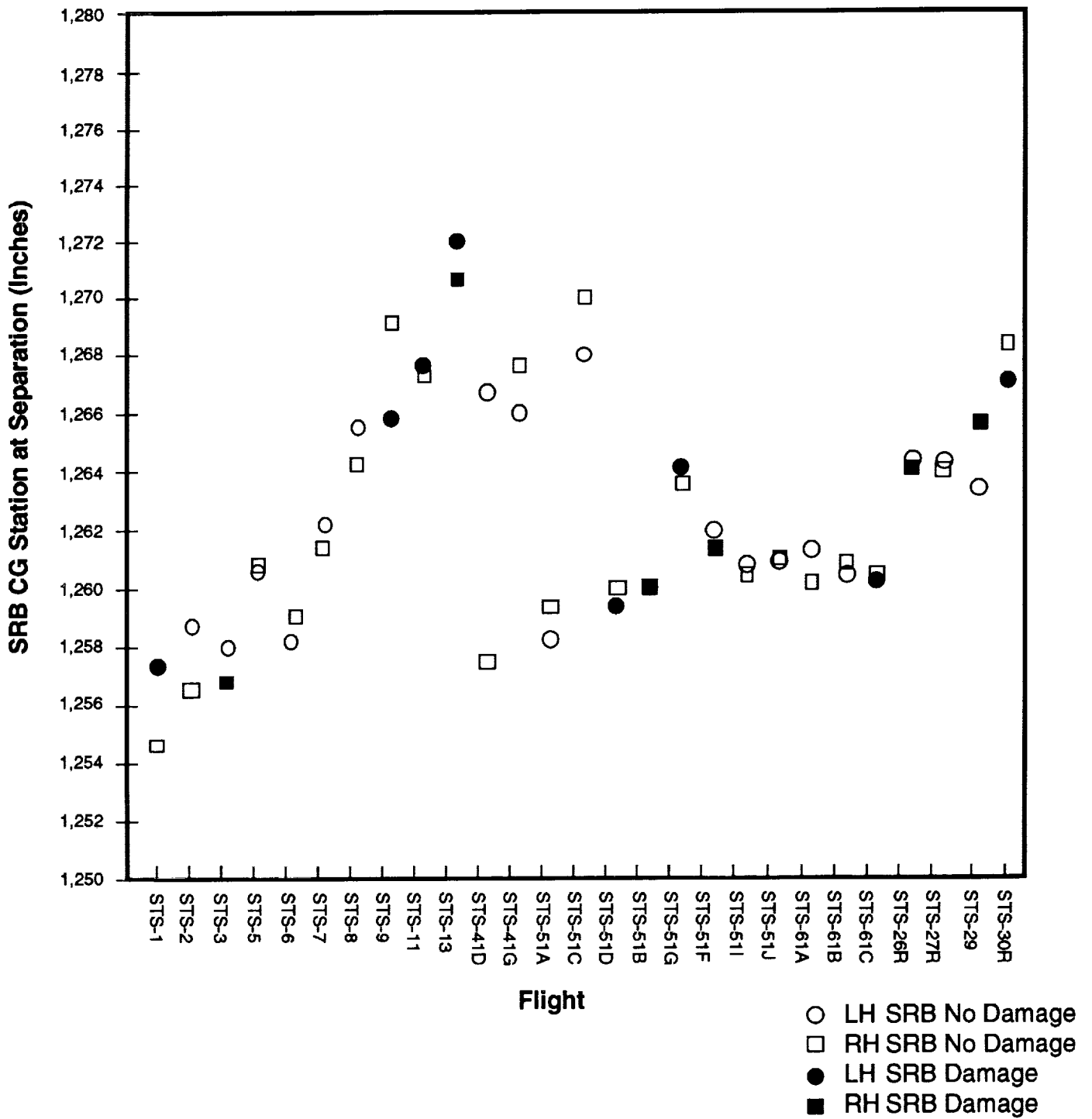
Figure B-10. Correlation between SRB longitudinal CG location and main parachute damage.

Ranking	Flight	SRB	CG Station (Inches)	Parachute Damage
1	STS-13	Left	1,272.17	Damage
2	STS-13	Right	1,270.83	Damage
3	STS-51C	Right	1,269.73	
4	STS-9	Right	1,269.40	
5	STS-30R	Right	1,268.74	
6	STS-51C	Left	1,268.22	
7	STS-41G	Right	1,267.98	
8	STS-11	Left	1,267.96	Damage
9	STS-11	Right	1,267.52	
10	STS-30R	Left	1,267.28	Damage
11	STS-41D	Left	1,267.05	
12	STS-41G	Left	1,266.29	
13	STS-9	Left	1,266.20	Damage
14	STS-29	Right	1,266.04	Damage
15	STS-8	Left	1,265.82	
16	STS-26R	Left	1,264.83	
17	STS-8	Right	1,264.56	
18	STS-27R	Left	1,264.55	
19	STS-26R	Right	1,264.46	Damage
20	STS-51G	Left	1,264.33	Damage
21	STS-27R	Right	1,264.31	
22	STS-51G	Right	1,263.86	
23	STS-29	Left	1,263.75	
24	STS-7	Left	1,262.46	
25	STS-51F	Left	1,262.26	
26	STS-51F	Right	1,261.68	Damage
27	STS-7	Right	1,261.59	
28	STS-61A	Left	1,261.55	
29	STS-51J	Right	1,261.33	
30	STS-51J	Left	1,261.25	
31	STS-61B	Right	1,261.08	
32	STS-5	Right	1,261.04	
33	STS-51I	Left	1,260.98	
34	STS-61B	Left	1,260.86	
35	STS-5	Left	1,260.86	
36	STS-51I	Right	1,260.77	
37	STS-61C	Right	1,260.70	
38	STS-61C	Left	1,260.59	Damage
39	STS-61A	Right	1,260.51	
40	STS-51B	Right	1,260.32	
41	STS-51D	Right	1,260.31	
42	STS-51B	Left	1,260.28	Damage
43	STS-51D	Left	1,259.67	Damage
44	STS-51A	Right	1,259.64	
45	STS-6	Right	1,259.34	
46	STS-2	Left	1,258.97	
47	STS-51A	Left	1,258.58	
48	STS-6	Left	1,258.43	
49	STS-3	Left	1,258.21	
50	STS-41D	Right	1,257.73	
51	STS-1	Left	1,257.61	Damage
52	STS-3	Right	1,257.06	Damage
53	STS-2	Right	1,256.77	
54	STS-1	Right	1,254.85	

Figure B-11. Correlation between SRB longitudinal CG location and main parachute damage (ranked values).
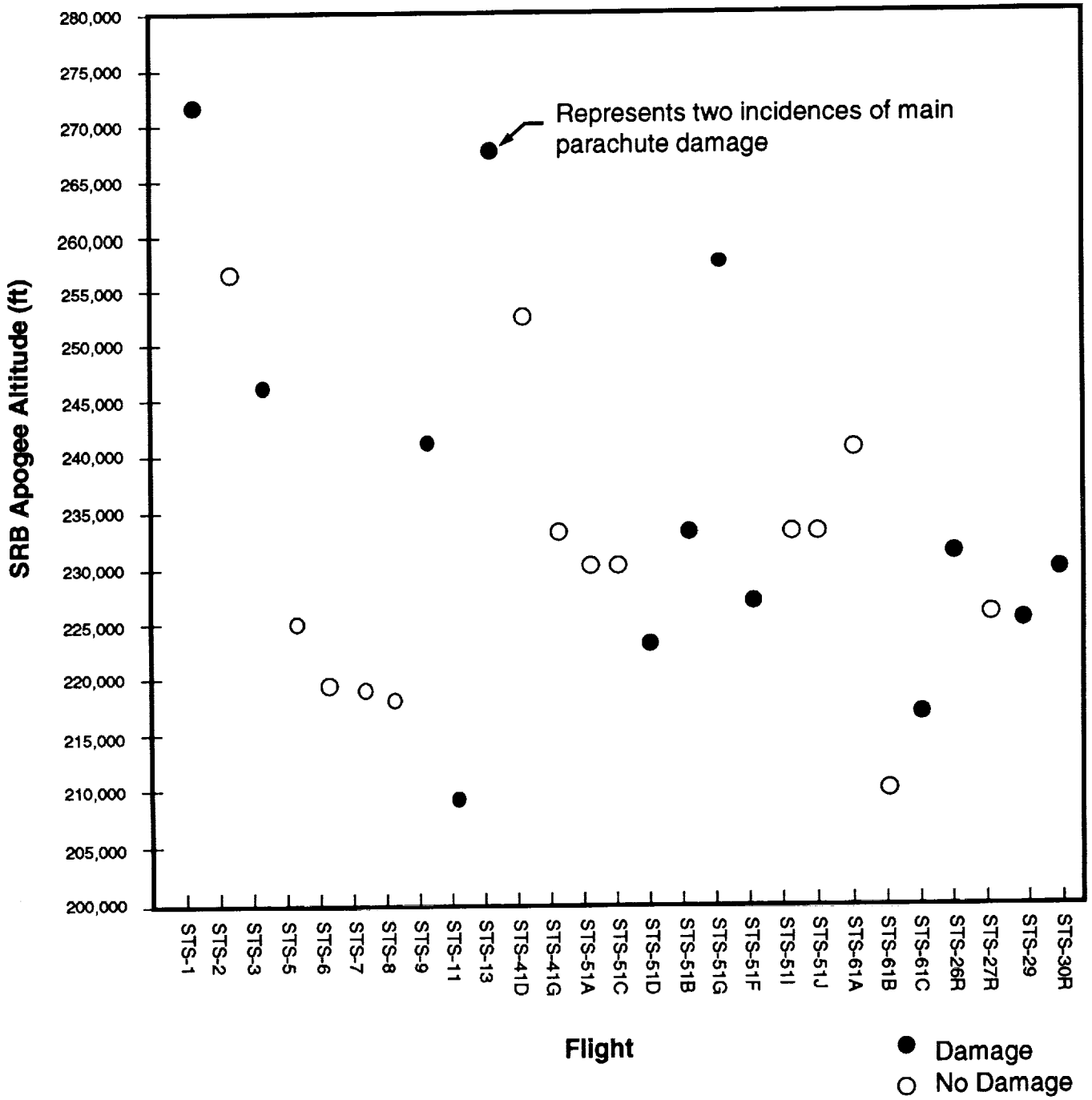
Figure B-12. Correlation between SRB apogee altitude and main parachute damage.

Ranking	Flight	Apogee (ft)	Parachute Damage
1	STS-1	275,000	Damage
2	STS-13	268,000	Damage on both SRB's
3	STS-51G	258,000	Damage
4	STS-2	257,000	
5	STS-41D	253,000	
6	STS-3	247,000	Damage
7	STS-9	242,000	Damage
8	STS-61A	241,800	
9	STS-41G	234,000	
10	STS-51B	234,000	Damage
11	STS-51I	234,000	
12	STS-51J	233,700	
13	STS-26R	232,800	Damage
14	STS-51A	231,000	
15	STS-51C	231,000	
16	STS-30R	230,700	Damage
17	STS-51F	228,000	Damage
18	STS-27R	226,500	
19	STS-29	226,000	Damage
20	STS-5	225,000	
21	STS-51D	224,000	Damage
22	STS-6	220,000	
23	STS-7	220,000	
24	STS-8	219,000	
25	STS-61C	218,000	Damage
26	STS-61B	211,300	
27	STS-11	210,000	Damage

Figure B-13. Correlation between SRB apogee altitude and main parachute damage (ranked values).

73
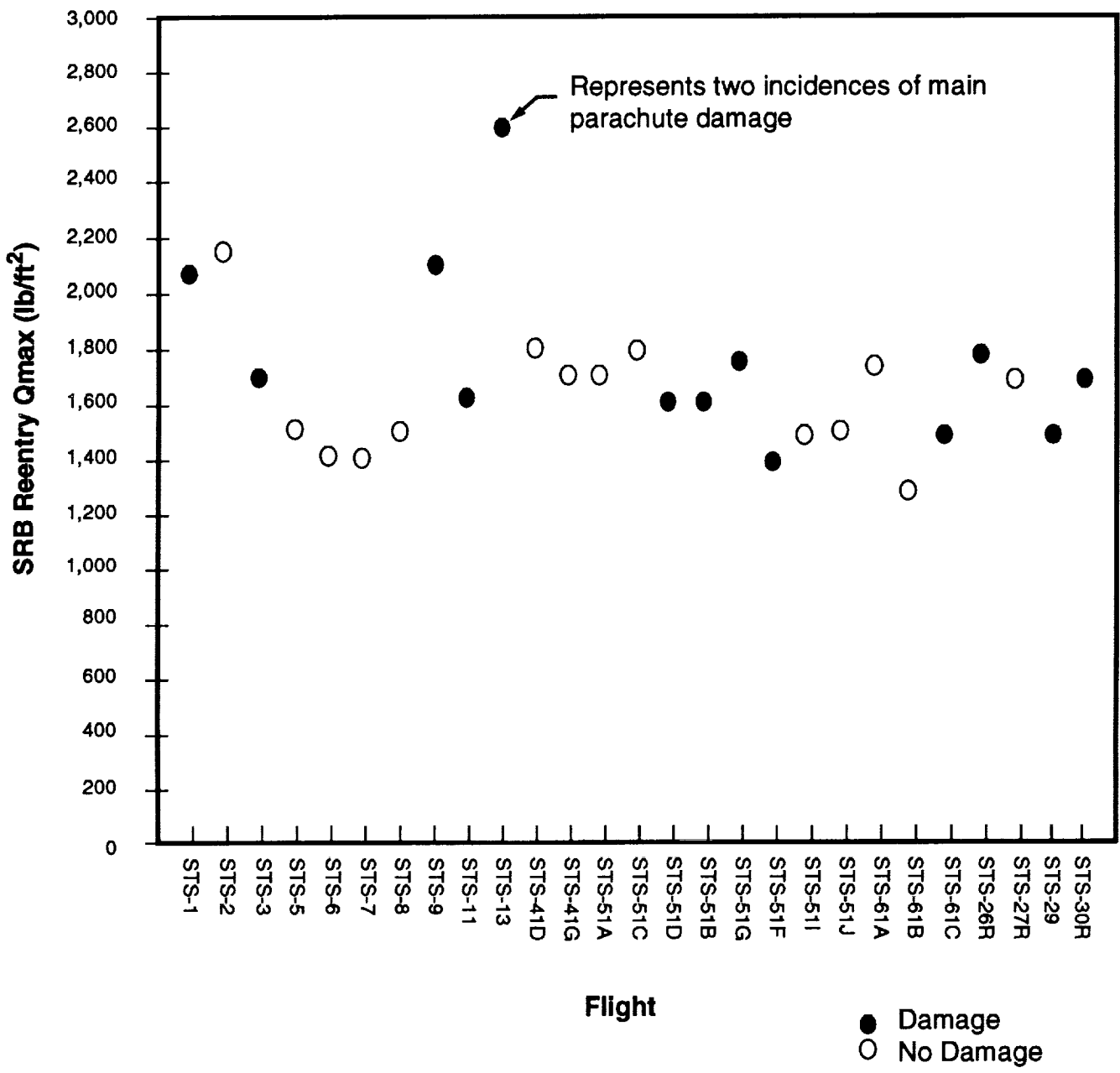
Figure B-14. Correlation between SRB reentry Qmax and main parachute damage.
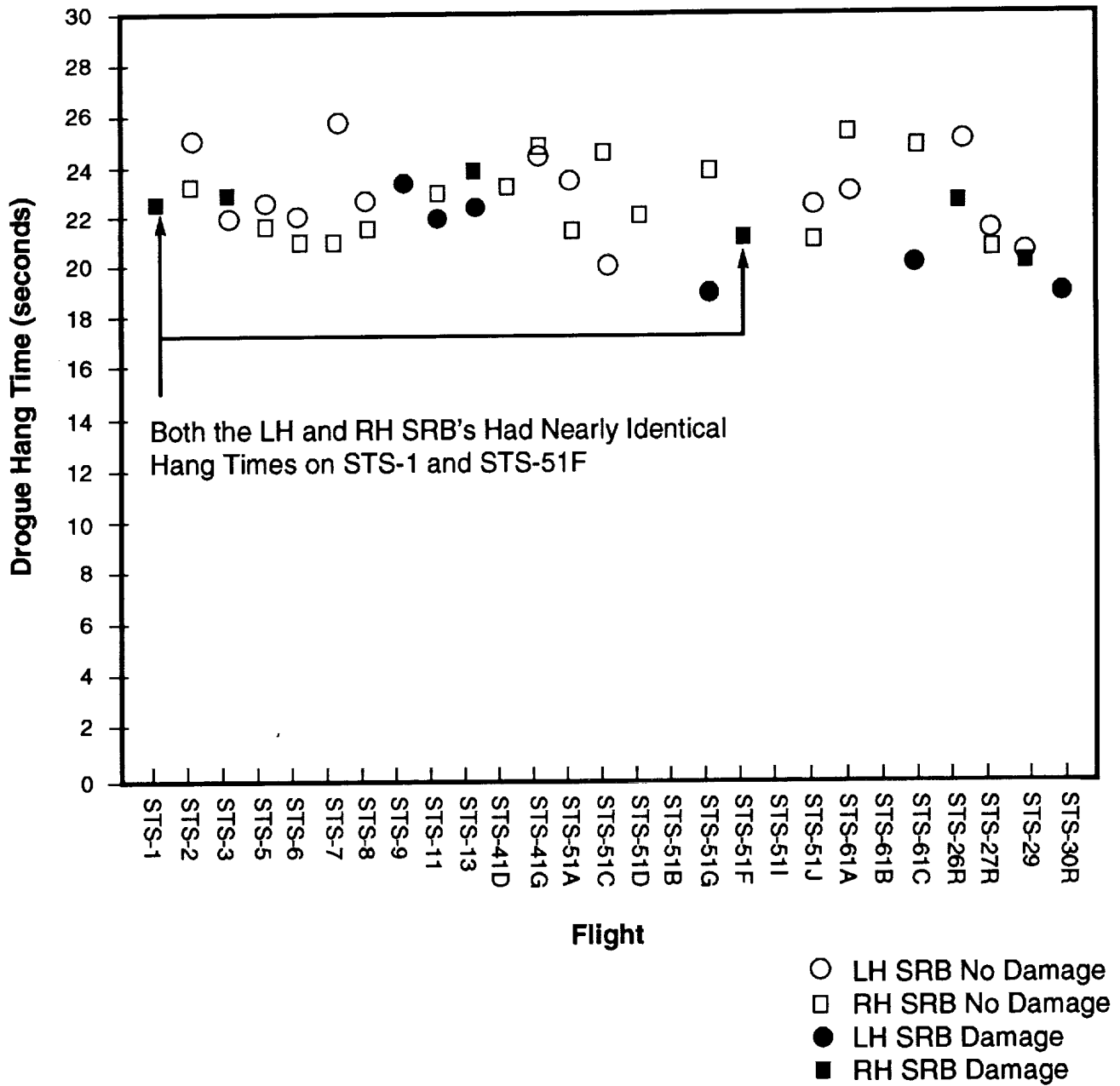
Figure B-15. Correlation between SRB drogue hang time and main parachute damage.
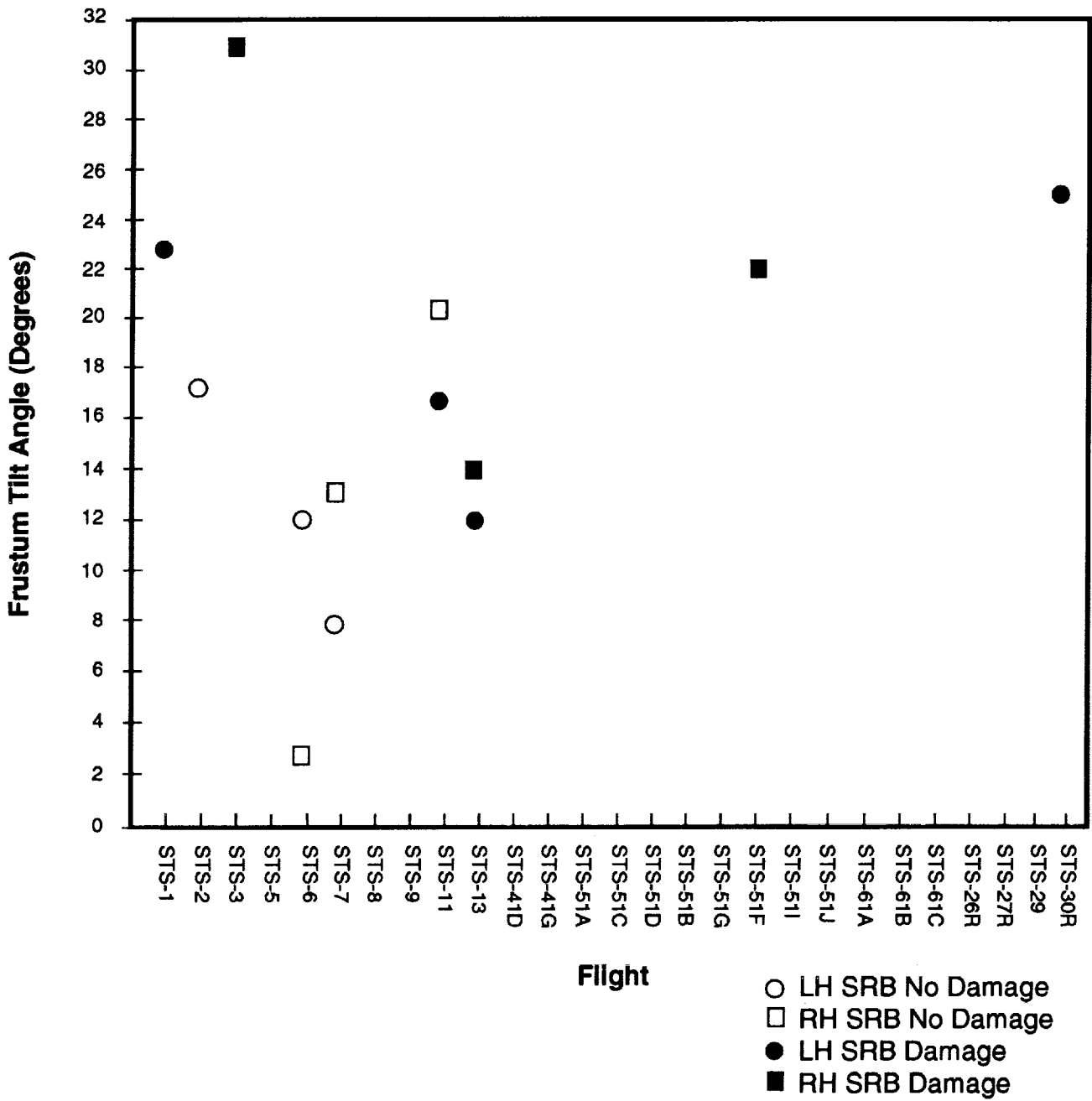
Figure B-16. Correlation between SRB frustum tilt angle and main parachute damage.
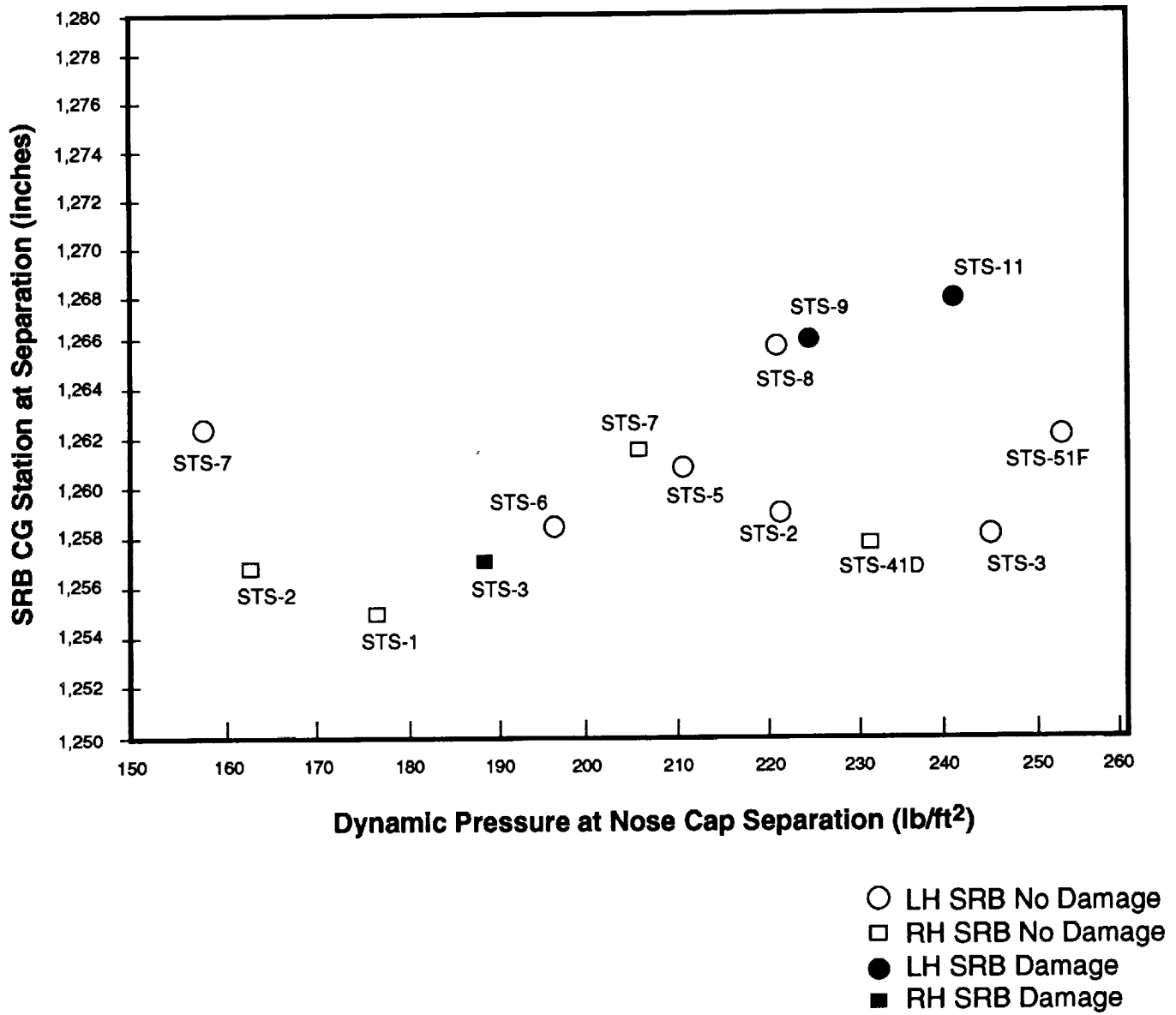
Figure B-17. Correlation between main parachute damage and the combined effect of dynamic pressure at nose cap separation and SRB longitudinal CG location.

B.4 Damage Correlation Summary

The team accomplished its objective of finding cause-and-effect relationships between flight parameters and significant main chute damage. Although not enough data exist to conduct rigorous correlation studies, the results are still considered valid. Moderate and weak correlations were observed that relate an increase in significant main parachute deployment damage to the following five parameter changes:

1. Increase in SRB weight

2. Rearward shift in SRB CG location

3. Increase in SRB apogee altitude

4. Increase in SRB reentry Qmax

5. Decrease in drogue hang time.

It has been known since the early years of the shuttle program that these parameter changes, along with others, are generally detrimental to SRB recovery. The damage correlations identified in this study confirm the importance of these parameters. The effects of these parameters should be taken into account when future changes are considered for the SRB or recovery system.

B.5 Bibliography

This section lists the primary sources used in compiling the main parachute damage history, parachute loads data, and SRB flight data provided in appendix B.

B.5.1 Martin Marietta Corporation Postflight Reports

1. "STS-1 Postflight Analysis and Report." Contract Report SRB-DSS-TM-12-1, Martin Marietta Corporation, Denver, CO, October 1981.

2. "STS-2 Postflight Analysis and Report." Contract Report SRB-DSS-TM-12-2, Martin Marietta Corporation, Denver, CO, March 1982.

3. "STS-3 Postflight Analysis and Report." Contract Report SRB-DSS-TM-12-3, Martin Marietta Corporation, Denver, CO, August 1982.

4. "STS-4 Postflight Analysis and Report." Contract Report SRB-DSS-TM-12-4, Martin Marietta Corporation, Denver, CO, December 1982.

5. "STS-5 Postflight Analysis and Report." Contract Report SRB-DSS-TM-12-5, Martin Marietta Corporation, Denver, CO, March 1983.

6. "STS-6 Postflight Analysis and Report." Contract Report SRB-DSS-TM-12-6, Martin Marietta Corporation, Denver, CO, August 1983.

7. "STS-7 Postflight Analysis and Report." Contract Report SRB-DSS-TM-12-7, Martin Marietta Corporation, Denver, CO, October 1983.

8. "STS-8 Postflight Analysis and Report." Contract Report SRB-DSS-TM-12-8, Martin Marietta Corporation, Denver, CO, December 1983.

9. "STS-9 Postflight Analysis and Report." Contract Report SRB-DSS-TM-12-9, Martin Marietta Corporation, Denver, CO, March 1984.

10. "Mission 41B (STS-11) Postflight Analysis and Report." Contract Report SRB-DSS-TM-12-10, Martin Marietta Corporation, Denver, CO, May 1984.

11. "Mission 41C (STS-13) Postflight Analysis and Report." Contract Report SRB-DSS-TM-12-11, Martin Marietta Corporation, Denver, CO, July 1984.

12. "Mission 41D (STS-14) Postflight Analysis and Report." Contract Report SRB-DSS-TM-12-12, Martin Marietta Corporation, Denver, CO, January 1985.

13. "Mission 41G (STS-17) Postflight Analysis and Report." Contract Report SRB-DSS-TM-12-13, Martin Marietta Corporation, Denver, CO, December 1984.

14. "Mission 51A (STS-19) Postflight Analysis and Report." Contract Report SRB-DSS-TM-12-14, Martin Marietta Corporation, Denver, CO, February 1985.

15. "Mission 51C (STS-20) Postflight Analysis and Report." Contract Report SRB-DSS-TM-2-1, Martin Marietta Corporation, Denver, CO, March 1985.

16. "Mission 51D (STS-23) Postflight Analysis and Report." Contract Report SRB-DSS-TM-2-2, Martin Marietta Corporation, Denver, CO, May 1985.

17. "Mission 51B (STS-24) Postflight Analysis and Report." Contract Report SRB-DSS-TM-2-3, Martin Marietta Corporation, Denver, CO, June 1985.

18. "Mission 51G (STS-25) Postflight Analysis and Report." Contract Report SRB-DSS-TM-2-4, Martin Marietta Corporation, Denver, CO, September 1985.

19. "Mission 51F (STS-26) Postflight Analysis and Report." Contract Report SRB-DSS-TM-2-5, Martin Marietta Corporation, Denver, CO, November 1985.

20. "Mission 51I Postflight Analysis and Report." Contract Report SRB-DSS-TM-2-6, Martin Marietta Corporation, Denver, CO, November 1985.

21. "Mission 51J Postflight Analysis and Report." Contract Report SRB-DSS-TM-2-7, Martin Marietta Corporation, Denver, CO, November 1985.

22. "Mission 61A Postflight Analysis and Report." Contract Report SRB-DSS-TM-2-8, Martin Marietta Corporation, Denver, CO, December 1985.

23. "Mission 61B Postflight Analysis and Report." Contract Report SRB-DSS-TM-2-9, Martin Marietta Corporation, Denver, CO, January 1986.

24. "Mission 61C Postflight Analysis and Report." Contract Report SRB-DSS-TM-2-10, Martin Marietta Corporation, Denver, CO, February 1986.

## B.5.2 MSFC Flight Evaluation Reports

1. "Space Shuttle STS-1 Final Flight Evaluation Report—Volume 1." MSFC-RPT-1030, Marshall Space Flight Center, AL, July 22, 1981.

2. "Space Shuttle STS-2 Final Flight Evaluation Report—Volume 1." MSFC-RPT-1031, Marshall Space Flight Center, AL, March 2, 1982.

3. "Space Shuttle STS-3 Final Flight Evaluation Report—Volume 1." MSFC-RPT-1032, Marshall Space Flight Center, AL, June 10, 1982.

4. "Space Shuttle STS-4 Final Flight Evaluation Report—Volume 1." MSFC-RPT-1033, Marshall Space Flight Center, AL, September 22, 1982.

5. "Space Shuttle STS-5 Final Flight Evaluation Report." MSFC-RPT-1034, Marshall Space Flight Center, AL, no date.

80

6. "Space Shuttle STS-6 Final Flight Evaluation Report." MSFC-RPT-1035, Marshall Space Flight Center, AL, June 8, 1983.

7. "Space Shuttle STS-7 Final Flight Evaluation Report." MSFC-RPT-1036, Marshall Space Flight Center, AL, August 10, 1983.

8. "Space Shuttle STS-8 Final Flight Evaluation Report." MSFC-RPT-1037, Marshall Space Flight Center, AL, October 21, 1983.

9. "Space Shuttle STS-9 Final Flight Evaluation Report—Shuttle Projects." MSFC-RPT-1038, Marshall Space Flight Center, AL, January 20, 1984.

10. "Space Shuttle STS-11 Final Flight Evaluation Report—Shuttle Projects." MSFC-RPT-1039, Marshall Space Flight Center, AL, March 21, 1984.

11. "Space Shuttle STS-41C Final Flight Evaluation Report—Shuttle Projects." MSFC-RPT-1040, Marshall Space Flight Center, AL, May 14, 1984.

12. "Space Shuttle STS-41D Final Flight Evaluation Report—Shuttle Projects." MSFC-RPT-1041, Marshall Space Flight Center, AL, September 18, 1984.

13. "Space Shuttle STS-41G Final Flight Evaluation Report—Shuttle Projects." MSFC-RPT-1042, Marshall Space Flight Center, AL, October 22, 1984.

14. "Space Shuttle STS-51A Final Flight Evaluation Report—Shuttle Projects." MSFC-RPT-1043, Marshall Space Flight Center, AL, November 26, 1984.

15. "Space Shuttle STS-51C Flight Evaluation Report—Shuttle Projects." MSFC-RPT-1044, Marshall Space Flight Center, AL, February 14, 1985.

16. "Space Shuttle STS-51D Flight Evaluation Report—Shuttle Projects." MSFC-RPT-1045, Marshall Space Flight Center, AL, April 26, 1985.

17. "Space Shuttle STS-51B Flight Evaluation Report—Shuttle Projects." MSFC-RPT-1046, Marshall Space Flight Center, AL, May 13, 1985.

18. "Space Shuttle STS-51G Final Flight Evaluation Report—Shuttle Projects." MSFC-RPT-1221, Marshall Space Flight Center, AL, July 1, 1985.

19. "Space Shuttle STS-51F Flight Evaluation Report—Shuttle Projects." MSFC-RPT-1222, Marshall Space Flight Center, AL, August 13, 1985.

20. "Space Shuttle STS-51I Flight Evaluation Report—Shuttle Projects." MSFC-RPT-1223, Marshall Space Flight Center, AL, September 10, 1985.

21. "Space Shuttle STS-51J Flight Evaluation Report—Shuttle Projects." MSFC-RPT-1224, Marshall Space Flight Center, AL, October 17, 1985.

22. "Space Shuttle STS-61A Flight Evaluation Report—Shuttle Projects." MSFC-RPT-1225, Marshall Space Flight Center, AL, November 13, 1985.

23. "Space Shuttle STS-61B Flight Evaluation Report—Shuttle Projects." MSFC-RPT-1226, Marshall Space Flight Center, AL, December 10, 1985.

24. "Space Shuttle STS-61C Flight Evaluation Report—Shuttle Projects." MSFC-RPT-1227, Marshall Space Flight Center, AL, January 27, 1986.

25. "Space Shuttle STS-26R Flight Evaluation Report—Shuttle Projects." MSFC-RPT-1573, Marshall Space Flight Center, AL, December 22, 1988.

26. "Space Shuttle STS-27R Flight Evaluation Report—Shuttle Projects." MSFC-RPT-1574, Marshall Space Flight Center, AL, March 24, 1989.

27. "Space Shuttle STS-29 Flight Evaluation Report—Shuttle Projects." MSFC-RPT-1575, Marshall Space Flight Center, AL, May 30, 1989.

28. "Space Shuttle STS-30R Flight Evaluation Report—Shuttle Projects." MSFC-RPT-1576, Marshall Space Flight Center, AL, July 25, 1989.

B.5.3 Presentations and Memos

1. Runkle, R., and Henson, K.: "STS-3 Main Parachute Failure." NASA TM-82490, Marshall Space Flight Center, June 1982.

2. Reinartz, S.R.: "SRB Deceleration System Review Team Presentation to Dr. Lucas." NASA Internal Presentation, Marshall Space Flight Center, AL, May 29, 1984.

3. "Update of Main Chute Failure and Corrective Action History." Presentation to NASA-MSFC, Martin Marietta Corporation, Denver, CO, December 11, 1985.

4. Wolf, D.F.: "Failure Investigation Report for STS-30 Main Parachute S/N 8045." Memorandum to NASA-MSFC, Sandia National Laboratories, Albuquerque, NM, June 12, 1989.

5. McFadden, P.G.: "Summarization of Large Main (136 ft) Parachute Damage and Failures." Memorandum to NASA-MSFC, United Technologies/USBI Co., Huntsville, AL, October 13, 1989.
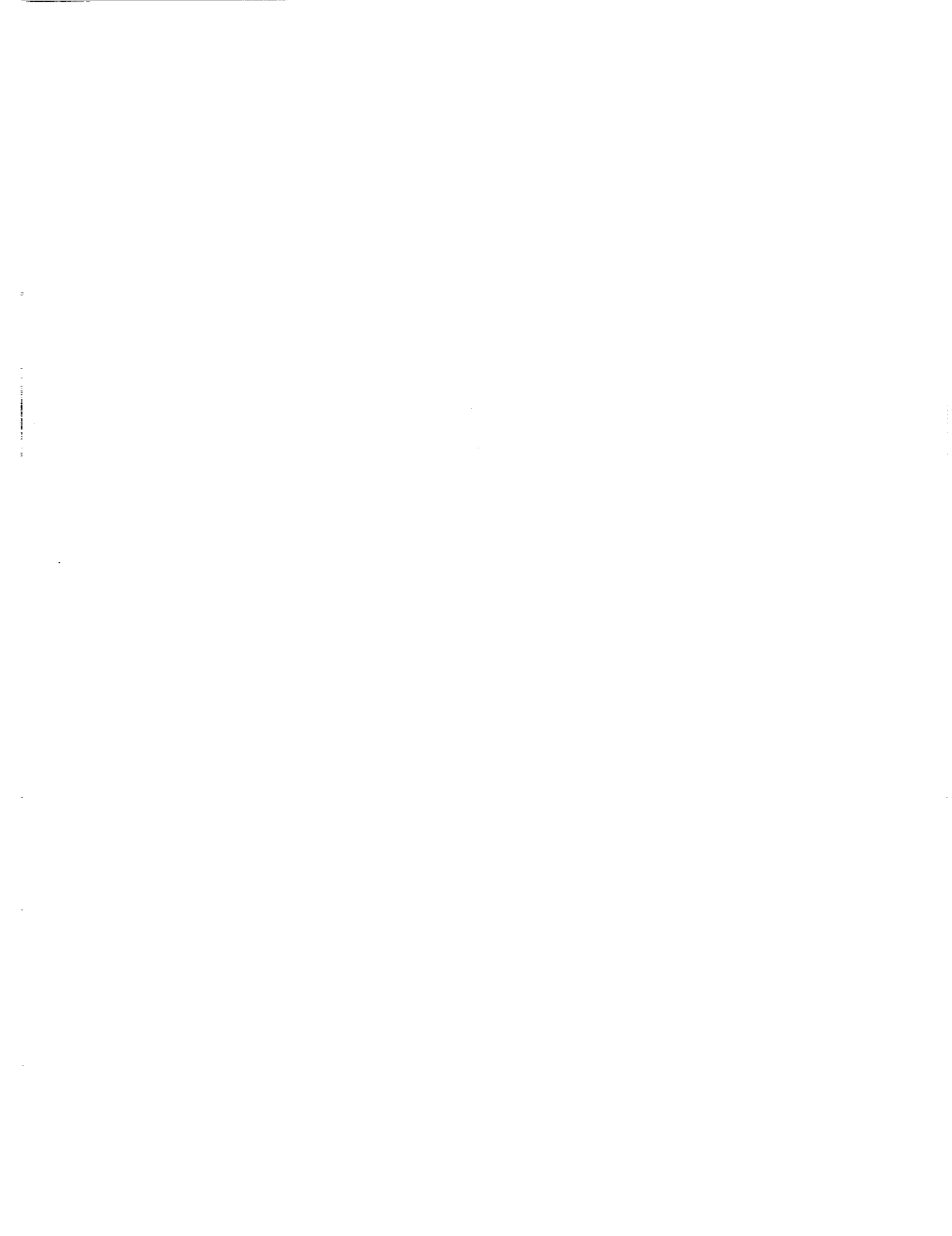
REPORT DOCUMENTATION PAGE

Public reporting burden for this collection of information is estimated to average 1 hour per response, including the time for reviewing instructions, searching existing data sources, gathering and maintaining the data needed, and completing and reviewing the collection of information. Send comments regarding this burden estimate or any other aspect of this collection of information, including suggestions for reducing this burden, to Washington Headquarters Services, Directorate for Information Operations and Reports, 1215 Jefferson Davis Highway, Suite 1204, Arlington, VA 22202-4302, and to the Office of Management and Budget, Paperwork Reduction Project (0704-0188), Washington, DC 20503

1. AGENCY USE ONLY (Leave blank)	2. REPORT DATE	3. REPORT TYPE AND DATES COVERED
	January 1993	Technical Memorandum

4. TITLE AND SUBTITLE

Space Shuttle Solid Rocket Booster Main Parachute
Damage Reduction Team Report

5. FUNDING NUMBERS

6. AUTHOR(S)

G. Watts

7. PERFORMING ORGANIZATION NAME(S) AND ADDRESS(ES)

George C. Marshall Space Flight Center
Marshall Space Flight Center, Alabama 35812

8. PERFORMING ORGANIZATION REPORT NUMBER

M–706

9. SPONSORING / MONITORING AGENCY NAME(S) AND ADDRESS(ES)

National Aeronautics and Space Administration
Washington, DC 20546

10. SPONSORING / MONITORING AGENCY REPORT NUMBER

NASA TM–4437

11. SUPPLEMENTARY NOTES

Prepared by Structures and Dynamics Laboratory, Science and Engineering Directorate.

12a. DISTRIBUTION / AVAILABILITY STATEMENT

Unclassified—Unlimited

Subject Category: 15

12b. DISTRIBUTION CODE

13. ABSTRACT (Maximum 200 words)

This report gives the findings of the space shuttle solid rocket booster main parachute damage reduction team. The purpose of the team was to investigate the causes of main parachute deployment damage and to recommend methods to eliminate or substantially reduce the damage. The team concluded that the two primary causes of significant damage during deployment are vent entanglement and contact of the parachutes with the main parachute support structure. As an inexpensive but effective step towards damage reduction, the team recommends modification of the parachute packing procedure to eliminate vent entanglement. As the most effective design change, the team recommends a pilot chute-deployed soft-pack system. Alternative concepts are also recommended that provide a major reduction in damage at a total cost lower than the pilot chute-deployed soft pack.

14. SUBJECT TERMS

SRB, Main Parachute, Recovery System, Drogue Parachute, Pilot Chute

15. NUMBER OF PAGES

96

16. PRICE CODE

A05

17. SECURITY CLASSIFICATION OF REPORT	18. SECURITY CLASSIFICATION OF THIS PAGE	19. SECURITY CLASSIFICATION OF ABSTRACT	20. LIMITATION OF ABSTRACT
Unclassified	Unclassified	Unclassified	Unlimited